Department of Cellular and Molecular Physiology

Institute of Translational Medicine

University of Liverpool

Metabolic Reprogramming in Gastric Cancer

Thesis submitted in accordance with the requirements of the University of Liverpool for the degree of Doctor in Philosophy

Emily Elizabeth Heald Linnane

Supervisors: Prof. Chris Sanderson and Prof. Andrea Varro

February 2015

Abstract

Globally, gastric cancer claims around 800,000 lives per year. As many patients present at an advanced stage of disease, prognosis remains poor for most patients, with five-year survival rates of less than 30%. As many patients show only limited short-term benefits from current therapeutic regimes, there is a clear need for improved understanding of the molecular mechanisms that drive the development and spread of gastric cancer. In this context, the role of the tumour microenvironment in cancer development and the potential for new forms of therapeutic intervention has become a field of increasing interest in many areas of cancer research. It is now well established that the development and progression of gastric tumours is facilitated by reciprocal communication between cancer cells, and cells within the surrounding tissue. In this study we focus our investigation on the mechanisms and consequences of paracrine communication between gastric cancer cells and different populations of stromal myofibroblasts, which are prevalent within the cancer microenvironment and form a significant proportion of many solid tumours.

Previous studies show that myofibroblasts derived from gastric tumours (CAMs) have inherently different profiles of gene expression, compared to patient matched adjacent tissue myofibroblasts (ATMs), or normal tissue myofibroblasts (NTMs). Given these differences, we were interested to know if specific myofibroblast populations respond differently to signals from cancer cells; or conversely, if they exhibit differential ability to facilitate pro-tumourogenic changes in gastric cancer cells. Using a combination of

bioinformatics and experimental techniques we demonstrate that CAM-conditioned media induces distinct changes in the gene expression profiles and metabolic activity of AGS gastric cancer cells. Significantly, these changes were not observed following exposure to conditioned media derived from either ATM or NTM cells. Conversely, CAM cells were found to have higher levels of GLUT1 and MCT4 expression with a corresponding reduction in mitochondrial activity compared to NTM cell lines. Finally, initial analysis of CAM imposed changes in AGS gene-expression suggests changes may reflect patient prognosis or stage of tumour development, implying future potential for patient stratification. In conclusion, data from this study shows that activated CAMs are robustly programmed by cancer cells to facilitate optimal conditions for tumour growth. Therefore, further analysis of this system may provide much needed options for improved therapeutic intervention and precision medicine.

Acknowledgements
First and foremost I would like to thank my supervisor, Professor Chris Sanderson, for all your help and scientific guidance throughout this PhD project. You have been a great mentor to me, and I would like to thank you for all your patience, enthusiasm and support for the past three years. I would also like to thank Professor Varro and Professor Dockray for all your ideas, help and scientific direction throughout the past three years.

Thanks to the members of the Sanderson lab past and present; Rob and Kelly, for your help, support and friendship during the beginning of my PhD project. Amy, Bron, Jen, Jo and Hanna, for making the lab such a pleasant place to work in during the latter part of my project, and for all the fun times and nights out! I wish you all the best of luck with your projects and the future. Thanks also to Dave Peeney – we started our PhD around the same time and now we are both at the end of it, you have been a great friend to me, thank you for all the scientific discussions, help with lab work and laptops, and for providing many laughs and hilarity in the lab.

A special thanks to Dr Helen Smith; what I learnt from you in the first few months of this PhD project has been invaluable to me throughout the entirety of my work. I really appreciate all the hours you spent teaching me bioinformatics, R and especially the time you have given recently, helping with extra analyses of our data (all whilst working and with a new baby!) You have also been a fantastic friend and support to me during the PhD process, thank you.

To all my other friends who have put up with me during my write up- thank you! Dr Sarah Dryhurst, without your Skype pep-talks I honestly do not know what I would have done, thanks for always listening, for your advice, and for always being there for me when I needed a chat.

I would like to extend a massive heartfelt thank you to Dr Andrea Linford; you are an absolute star, especially for all your support over the past few months. Thank you for always believing in me, for providing your time and expertise during my write up period, and most of all, for always telling me the truth!!!

A big thank you to all my family, especially to my sister Rose, thank you for putting up with my moaning and for helping me see the light at the end of the tunnel. Thank you to my wonderful parents; to my dad, for all your support, and for reading through this thesis (and understanding it!) Mum, you are an absolute inspiration to me, and the reason why I have chosen this career. Without both your love and encouragement I would not have achieved as much as I have.

Finally, thanks to Daniel. I am so lucky to have you by my side, your love and support. Thanks for putting up with me through this write up- you have been my rock and I am so grateful for all you have done to help me. You have supported me in every way possible, helped me carry on when I felt like giving up, and you have made me smile every day.

List of abbreviations

AGS Angiosarcoma

ATM Adjacent Tissue Myofibroblast

ATP Adenosine Triphosphate

BSA Bovine Serum Albumin

CAGA cytotoxin-associated gene A

CAGB cytotoxin-associated gene B

CAIX carbonic anhydrase IX

CAM Cancer Associated Myofibroblast

DMEM Dulbecco's Modified Eagle's Medium

DNA Deoxyribonucleic acid

DPBS Dulbecco's Phosphate Buffered Saline

EDN1 Endothelin-1

FBS Foetal Bovine Serum

GLUT-1 Glucose Transporter 1

H.Pylori *Helicobactor pylori*

HNSCC Head and Neck Squameous Cell Carcinoma

MCT1 Monocarboxylate Transporter One

MCT4 Monocarboxylate Transporter Four

MSCs Mesenchymal Stem Cell

NTM Normal Tissue Myofibroblast

PBS Phosphate-buffered saline

RNA Ribonucleic acid

TGF-B Transforming Growth Factor Beta

TGF B ig-h3 Transforming growth factor-induced gene-h3

uPAR Urokinase Plasmingen Activator Receptor

VEGF Vascular endothelial growth factor

α-SMA Alpha- Smooth Muscle Actin

Contents

List of Tables

List of Figures

Appendices

List of supplementary files provided on CD:

Supplementary file I:

Gene Set Enrichment Analysis, 2.0

GeneVestigator Figures, 2.1, 2.2 and 2.3

Canonical Pathway Analysis, 2.4

Supplementary File II:

Seahorse XF Flux Analyser Data, 3.1, 3.2 and 3.3

AGS conditioning gene lists, 3.4

Chapter I

Introduction

1.0 Overview

The most fundamental property of living cell systems is the ability to consume and transform energy, a process termed “metabolism” originating from the Greek word “metabolismos,” meaning, “to change.” Cellular metabolism consists of many individual chemical reactions, which occur throughout metabolic pathways. These pathways exist in a delicate balance between anabolic (energy consuming) or catabolic (energy producing). Metabolic processes and pathways in cancer cells have been a subject of much interest since the observations of Otto Warburg and his contemporaries in the early 20th century (Warburg *et al.,* 1927 and Warburg 1956). Despite almost ninety years of research on this subject, there are still many unanswered questions regarding the role of metabolic change in cancers.

The field of cancer therapeutics has greatly progressed over the past decade; however, with increased incidence of chemotherapy resistance, and global increase in the prevalence of cancer, further understanding and new methods for therapeutic intervention are needed. Work presented in this thesis highlights the role of metabolism in gastric cancer and its tumour microenvironment, and the potential use as a therapeutic target in combatting this disease.

1.1 Gastric Cancer: An Overview

Cancers are a large family of multifactorial diseases, characterised by abnormal cell growth and often the ability to metastasise and spread to other parts of the body. There are many factors that contribute to the development and progression of cancer, including: genetics, environmental stress, diet and lifestyle choices. The progression of normal cells, which form a mass, to malignant cancer cells, is primarily due to accumulation of molecular changes in cells as a result of exposure to these genetic or environmental factors. There are two key papers by Hannahan and Weinburg, which have since become the *sine qua non* for cancer biologists**.** The 'Hallmarks of Cancer' were first published in 2000 and covered the main cellular capabilities that cells require when evolving from healthy cells to malignant tumours. More recently an updated and revised version of the paper was published, 'Hallmarks of Cancer: the Next Generation' (Hannahan and Weinburg., 2011) which reviewed the evidence supporting the importance of the tumour microenvironment and energy metabolism in the process of carcinogenesis. The relationship between tumour cells and the tumour microenvironment is closely linked to that of energy metabolism, however there is much conflict in the literature regarding the fundamentals of this relationship, this present thesis attempts to address these issues in using a gastric cancer model and primary gastric stromal cells.

Gastric cancer is currently the fifth most common cancer in the world, with just under one million new cases diagnosed in 2012 alone (Wcrf.org, 2014). Despite the continuing research and some improvements in cancer

therapeutics, treatment of gastric cancer remains problematic and the prognosis for most patients remains poor.

As with most cancers, early detection of gastric cancer correlates with good long-term survival rates for patients (Hohenberger *et al.,* 2009), however, due to non-specific symptoms and lack of routine screening, early diagnosis is rare and only 1 in 5 people survive the disease for five years or more after diagnosis (Cancer Research UK, 2014).

Late diagnosis inevitably results in patients requiring post or peri operative chemotherapy, or radiotherapy in combination with surgery, depending upon the localisation and spread of the tumour (Meyer and Wilke 2011*).* Unfortunately, for patients who present with advanced tumours, especially with spread to the lymph nodes and metastasis, there are limited treatment options available. Current strategies for treatment include using combinations of chemotherapy agents, mainly platinum and fluoropyrimidine based compounds, such as 5-fluorouracil (5-FU) and doxorubicin (Cunningham *et al.,* 2008, Tetzlaff *et al.,* 2008, and Van Cutsem *et al.,* 2009*).* Advances in identification of stage and sub-group specific biomarkers, will improve therapeutic prescription of drugs to patients most likely to show responses, thereby limiting unnecessary treatment or suffering in inappropriate patient cohorts.

HER2 overexpression has been identified in nearly 25% of gastric cancer patients and is associated with a poor prognosis (Kunz *et al.,* 2012 and Meyer and Wilke 2011). Combining monoclonal antibody treatment with traditional

chemotherapeutic agents in patients overexpressing HER2 using trastuzumab is a current treatment strategy in both gastric and breast carcinomas (Jørgensen 2010 and Bose *et al.,* 2013). With the use of these chemotherapeutic agents for palliative treatment of gastric cancer resulting in median survival times of only 9 to 11 months, increasing to 14 months in HER2 expressing patients treated with trastuzumab (Van Cutsem *et al.,* 2009) and the problem of resistance to chemotherapy, there is a substantial need to establish new and improved therapeutic strategies.

1.2 Epidemiology of Gastric Cancer

Histologically, there are two distinct variants of gastric carcinoma which have been identified: diffuse-type gastric cancer, sometimes known as signet ring carcinoma (Otsuji 1998 and Li *et al.,* 2007) which comprises of individual neoplastic cells that are infiltrating into the stomach wall tissue, but do not form glandular structures (Zhang *et al.,* 2010 and Kim *et al.,* 2004) and intestinal-type adenocarcinomas, which advance through a series of histological stages (gastric atrophy, followed by intestinal metaplasia, which in turn may lead to dysplasia) (Ming 1977, Dicken *et al.,* 2005 and Wroblewski *et al.,*2010). There have been various classifications of gastric cancer over the years but the Lauren classification, first introduced in 1965 is the most common and widely used today. This classification system is able to histologically distinguish, between gastric adenocarcinomas of diffuse origin (DGCA) and gastric adenocarcinomas intestinal (IGCA) subtypes (Vauhkonen *et al.,* 2006). The primary prognostic factors in gastric carcinoma are the size and location of the tumour, and if the patient has any accompanying diseases

(Meyer and Wilke 2011, Takahashi *et al.,* 2013 and Tetzlaff *et al.,* 2008). There are two main tumor sites of gastric adenocarcinoma, and these are classed as proximal and distal (Crew and Neugut, 2006). The majority of stomach cancers are attributed to environmental factors such as *Helicobacter pylori* (*H. Pylori),* gastritis, and lifestyle factors such as diet and smoking (Forman and Burley 2006 and Correa 2013). Indeed, occurrence of gastric cancer varies significantly between populations, with the highest number of cases occurring in East Asia (Leung *et al.,* 2008), indicating that both environmental and genetic factors may contribute to occurrence and progression of the disease. Other factors contributing to the progression of gastric cancer include over production of the gastric antral hormone, gastrin, which has been shown to alter a ranger of cellular processes including proliferation, apoptosis, migration and tissue remodelling (Burkitt *et al.,* 2009 and Dockray 2004).

1.2.1 *Helicobactor pylori*

H. pylori is a class I carcinogen, it was first isolated in 1982, during a study of 100 patients, all of which were undergoing gastroscopies (Warren and Marshall, 1984). The bacterial strain was identified in all patients presenting with gastric ulcers, chronic gastritis and intestinal ulcer; ultimately leading to the general use of antibiotics as a treatment for gastric ulcers (Warren and Marshall, 1984). Since the discovery of *H. pylori,* the bacterium has become the focus of countless gastric studies and is now known to be one of the most common infections in humans (Cave, 1997, Fuccio *et al.,* 2007 and Uemura *et al.,* 2001). *H. pylori* infection, specifically cytotoxin-associated gene A (CAGA)

positive strains are known to be potentially carcinogenic, as this strain is known to be associated with peptic ulceration with different strains of *H.pylori* being associated with different clinical outcomes [figure 1.1].

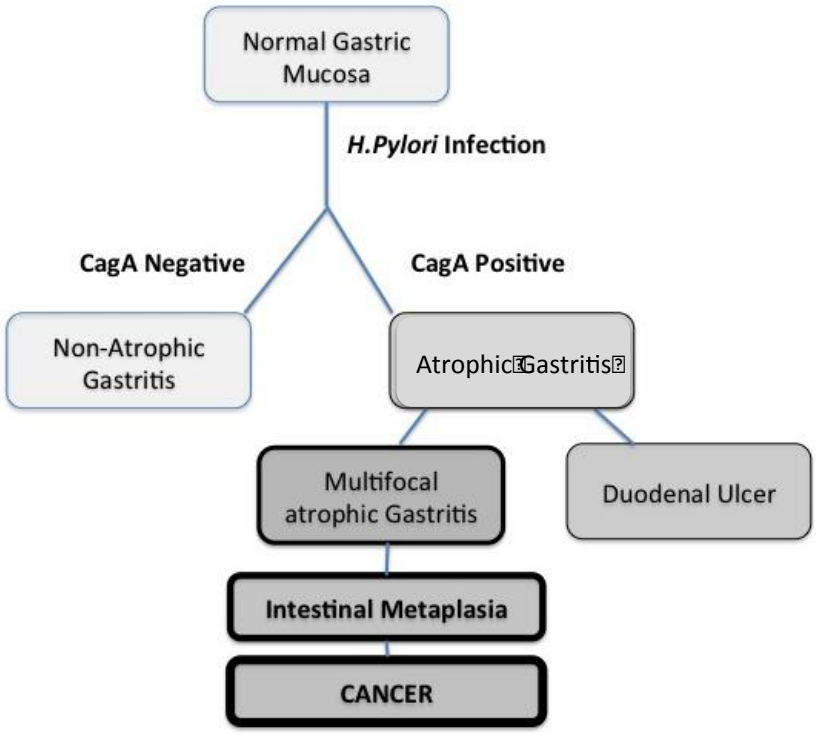

Figure 1. 1. Schematic adapted from Correa and Plazuelo (2012).
Clinical outcomes of infection with CagA positive and negative *H.Pylori* infections.

1.2.2 Diet and Gastric Cancer

Gastric cancer is a multifactorial disease, and the type of diet an individual consumes may have an important role to play in increased risk of the disease. Nitrate – rich foods such as processed meats, salted fish and pickled vegetables have all been reported to contribute to an increased risk of gastric carcinoma (Lee *et al.,* 1995 and Navarro Silvera 2008). The method of cooking

food may also be linked to increased risk, as frying or grilling foods produce greater quantities of heterocyclic amines (Jedrychowski *et al.,* 1993, Liu *et al.,* 2009 and Correa 1992). Equally, high dietary salt intake is also reported to be associated with a greater risk, as it may be linked to intestinal metaplasia and also could potentially increase the risk of infection with *H.pylori (*Correa 1992 and Tsugane *et al.,*1994*).*

1.2.3 Genetics and Gastric Cancer

Gastric cancer is a multifactorial disease, characterised by abnormal cell proliferation and the ability to metastasise to other tissues of the body. There are well-documented genetic changes in gastric cancer including up-regulation of NET1 (Bennett *et al.,* 2011), which is associated with increased proliferation, and invasion of gastric cells into the surrounding stroma. HERG was also identified as being involved in the progression of gastric cancer (Shao *et al.,* 2008), as it was found to be exclusively expressed in gastric cancer cells, it was also proposed to be a potential therapeutic target (Shao *et al.,*2008).

Genome-wide association studies can also be used to further understand and elucidate genetic factors that make people more susceptible to polygenic diseases and cancers. A genome-wide association study carried out on diffuse type gastric carcinoma identified a prostate stem cell antigen and the Mucin 1 (MUC1) genes, which were both associated with diffuse-type gastric cancer (Saeki *et al.,* 2013). Further investigation into genetic factors contributing to gastric cancer and the tumour microenvironment may provide additional

opportunities for identification of better prognostic biomarkers and new methods of therapeutic intervention

1.3 Targeting the Gastric Microenvironment

Understanding the complex relationship between different cells within the tumour stroma is vital in understanding the true mechanism of tumour development and drug resistance. As such, this is now an area of considerable interest for both patient stratification, and the identification of new targets for pharmacological inhibition. Indeed, many pharmaceutical companies and academic laboratories are focusing research on the development of new ways to inhibit tumour- associated stromal cells. Examples of these developments include; re-educating immune cells of the microenvironment through targets such as general control non-derepressible 2 (GCN2) (Yu *et al.,* 2007 and Ye *et al.,* 2010), targeting tumour associated macrophages (Mantovani *et al.,* 2006) and also blocking the paracrine communication between myofibroblast cells and cancer cells through mechanisms such the wnt signalling pathway (Liu *et al.,* 2013 and Yauch *et al.,* 2008). Despite these recent developments, there is still much we do not know about cells of the tumour stroma or reciprocal mechanisms of communication within the cancer microenvironment.

1.4 Cells of the Gastric Stroma and The Tumour Microenvironment

The gastric stroma is comprised of a range of cells, many of which make up the connective, supportive framework of the functional epithelium cells. These include; fibroblasts, mesenchymal stem cells (MSCs), myofibroblast cells and

immune cells. The cancer microenvironment contains a dynamic mixture of these non-cancerous cells, both in and around the developing tumour, these stromal cells can transform to aid and support cancer cell growth (Albini and Sporn, 2007).

1.4.1 Fibroblast Cells

Fibroblast cells function as a part of normal connective tissue. They have a distinct morphology, with elongated cell bodies and extended cellular processes. They are slow dividing cells with reduced motility and whilst structurally similar to myofibroblast cells, they do not express α-SMA (Grotendorst *et al.,* 2004). During normal wound healing, they migrate to the site of injury, where they establish a collagen rich extra-cellular matrix (ECM) (Gabbiani *et al.,* 1971).

The literature often refers to myofibroblast cells as 'fibroblast' cells however it is important to note the distinction between the two cell subtypes. Fibroblast cells are a pre-cursor to myofibroblast cells (or 'active' fibroblasts) differentiating into myofibroblast cells upon exposure to inflammatory or oncogenic signalling (Tomasek *et al.,* 2002).

1.4.2 Mesenchymel Stem Cells

Mesenchymel stem cells (MSCs) are multipotent adult cells that have been shown to differentiate into a range of connective tissue cell subsets, including myofibroblasts (Haniffa *et al.,* 2009). They are characterised by the expression of markers such as CD105, CD29 and CD90, which are associated with the stroma, and the absence of expression of haemotopoetic cells

markers (Lee *et al.,* 2013). Literature on the role of MSCs is conflicting with reports showing they have the potential to exhibit both positive and negative effects on tumour growth (Martin *et al.,* 2010, Prockop and Youn., 2012, Al Jumah and Abumaree., 2012 and Anton *et al.,* 2012). However, as they are thought to home to the site of developing tumours there is significant interest in the use of programmed MSCs to inhibit tumour development.

1.4.3 Myofibroblast Cells

1.4.3.1 The Origin of The Myofibroblast Cell

During the late 1970s, extensive studies were performed into the composition of granulation tissue, leading to the identification of myofibroblasts which were found to be fundamental to the process of wound healing (Gabbiani *et al.*, 1971,). After further investigation it became apparent that myofibroblasts not only play a key role in wound healing, but also within the stroma of some neoplasms (Sobral *et al.,* 2011, Tsujino *et al.,* 2007 and Ishii *et al.,* 2003). Despite the cells morphology, immunohistochemistry (Shimasaki *et al.,* 2007) and biochemistry being more fully elucidated following their discovery, there is still much that is unclear about these cells.

It is reported that myofibroblasts are derived from normal fibroblasts, which are activated when inflammation or injury occurs, often being stimulated by transforming growth factor (TGF)-β and endothelin-1 (EDN1) (Phan *et al.,* 2003). Current opinion is that fibroblasts firstly become protomyofibroblasts, expressing both beta and gamma cytoplasmic actins before finally

transforming to active myofibroblasts, which express smooth muscle actin fibres (Micallef *et al.,* 2012). It is known that urokinase plasminogen activator receptor (uPAR), which is an extracellular protease system involved in cell migration, the modelling of the extracellular matrix and growth factor activation is present on the surface of fibroblasts (Bernstein *et al.,* 2007)**.** This receptor is reported to regulate cell transition from fibroblasts to myofibroblasts. Studies show that down-regulation of uPAR is necessary for the differentiation of fibroblasts into active myofibroblasts. Thus, loss of uPAR can be used as a marker for some myofibroblast populations (Bernstein *et al.,* 2007)**.**

As the origin of tissue myofibroblasts appears to be heterogeneous, it is highly likely that not all myofibroblast cells will display identical properties (Chauhan *et al.,* 2003). There is further evidence to suggest that other cells can become "active" and display myofibroblast-like characteristics these include pericytes, MSCs (Kosinski *et al.,* 2010) and fibrocytes (Mitcallef *et al.,* 2012). Also, it is possible that the origin of myofibroblasts may depend on the site of damage; for example, in pathological situations within the liver, myofibroblast-like cells expressing α-SMA are thought to be derived from both hepatic stellate cells and local liver fibroblasts (Yin *et al.,* 2013).

1.4.3.2 Identifying Myofibroblast Cells

Aside from α-SMA, myofibroblast cells also express other muscle cell markers, such as myosin and desmin, they can also be characterised by expression of vimentin and reduced CAV-1 expression. They share a similar phenotype with

smooth muscle cells in the expression of actin microfilament bundles. This is why the most common myofibroblast marker is alpha-smooth muscle actin (α-SMA) (Hinz *et al.,* 2003 and Hinz *et al.,* 2001). Although both myofibroblasts and smooth muscle cell types express smooth muscle actin at high levels, these cells have distinctive morphologies and gene expression profiles (Gan *et al.,* 2007). Significantly, the functional properties of myofibroblasts vary according to the initial cause or process of activation, such as tissue inflammation or proximity to a developing tumour.

In light of these observations it is clear that myofibroblasts do not have simple unifying properties, their functional profiles and degree of activity is clearly influenced by the form and extent of niche-specific paracrine conditioning. As such, the mechanism and consequences of myofibroblast conditioning must be carefully defined in different tumours, at different stages of development and different tissue locations in order to define tumour specific signatures and unify mechanisms of cancer reprogramming.

1.4.3.3 Myofibroblasts in Cancer

The role of myofibroblasts in cancer is currently inconclusive but presence of α-SMA myofibroblasts has been used as a marker of poor prognosis (Fuyuhiro *et al.,* 2011). Information relating to the role of myofibroblasts in tumour development varies considerably between tumour types. Recruitment and activation of myofibroblasts is known to correlate with tumour invasion, but not in the initiation of tumour formation (De-Assis *et al.,* 2012). It is well known that in prostate cancer the tumour microenvironment plays a role in

tumour progression and metastasis (Barron *et al.,* 2012, Giannoni *et al.,* 2013, Shaw *et al.,* 2009,Giannoni *et al.,* 2010). Studies have been carried out to elucidate the mechanisms behind the relationship between the stromal cells and prostate cancer progression. A study by Shaw et al (2009) examines the role of paracrine signalling between the tumour and it's microenvironment via the sonic hedgehog pathway. Another, more recent study found that preventing differentiation of prostate myofibroblast cells by using DHA, reduced epithelial to mesenchymel transition and tumour invasion (Bianchini *et al.,* 2012). These studies indicate that the ability to influence myofibroblast function may provide an effective means of indirectly regulating the proliferation and migration of the cancer cells.

Studies in breast cancer again indicate that the presence of myofibroblasts often correlates with increased invasiveness and poor prognosis (Surowiak *et al.,* 2006 and Yamashita *et al.,* 2012*).* One study by (Yazhou *et al.,* 2004) showed that loss of Hematopoietic progenitor cell antigen CD34 expression and increased expression of α-SMA was associated with carcinomas and not with normal breast tissue containing CD34 expressing fibroblast cells. CD34 is linked to stem cell phenotypes and is associated with Another study by Surowiak *et al* (2006), reported a consistent positive correlation between the prevalence of myofibroblasts in the tumour stroma and expression of a marker of proliferation (Ki67) and the proto-oncogene HER-2 in breast cancer cells. In lung adenocarcinoma, positive staining of active myofibroblast cells was associated with lymph node metastasis, high stage, high grade, vascular invasion and a reduced survival times (Zhu *et al.,* 2007.) However, there is

conflicting evidence to the role of myofibroblast cells in lung cancer, as Matsubara *et al* (2009) reported that sub-epithelial myofibroblasts identified by α-SMA expression in lung adenocarcinoma was a histological indicator of excellent prognosis in the patients they tested (Matsubara *et al.,* 2009). These varying reports on the role of myofibroblasts in cancer progression need to be further elucidated for a greater range of tumour types.

1.4.3.4 Myofibroblasts in gastric cancer

The role of the myofibroblast cell in gastric cancer is not very well documented; studies in scirrhous gastric cancer patients show that an increase in myofibroblast cells is correlated with a worse prognosis (Fuyuhiro *et al.,* 2011). Also studies in mouse models of gastric cancer have shown that tumour associated myofibroblasts express VEGFA which contributes to the promotion of angiogenesis (Guo *et al.,* 2008). Work carried out in the laboratory of Professor A. Varro showed that gastric cancer associated myofibroblasts (CAMs) caused increased cancer cell migration and proliferation when compared to adjacent tissue myofibroblasts (ATMs) and normal tissue myofibroblasts (NTMs) (Holmberg *et al.,* 2012). Also a comparative proteomic analysis of myofibroblast secretomes revealed a decrease in extracellular matrix adaptor protein like transforming growth factor-induced gene-h3 (TGFβig-h3) in the CAM secretome. This decrease was correlated with lymph node metastasis, worse prognosis and shorter patient survival (Holmberg *et al.,* 2012). It is therefore vital to further elucidate the role of the gastric CAMs in cancer progression and patient prognosis.

1.5 Signalling in the Gastric Cancer Environment

Complex methods of cross-talk have been identified between cancer cells and cells in the tumour microenvironment, [figure 1.2]. Whilst the process itself is well documented, the molecular mechanisms that control these processes are not fully understood, and may vary according to the type of malignancy, the stage of tumour development and the dynamic composition of the surrounding tissue.

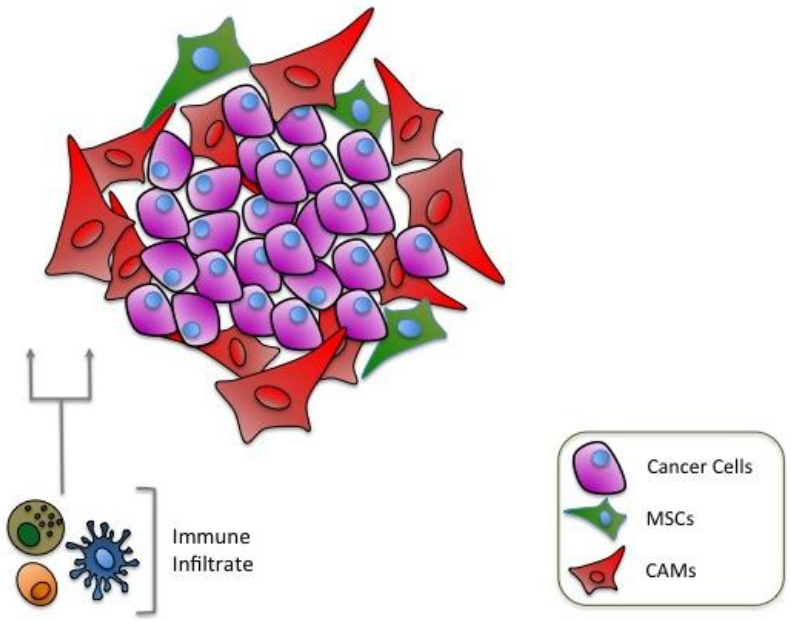

Figure 1. 2. Schematic showing cellular cross-talk in the tumour microenvironment.
The cancer microenvironment contains a dynamic mixture of cancerous cells and non-cancerous cells, both in and around the developing tumour including myofibroblast cells (CAMs) which act to recruit immune cells (TAMs), stem cells (MSCs) and form an environment supporting tumour growth.

Research in breast cancer models suggest that metastasis and chemo-resistance are driven by molecular changes in both tumour cells and the surrounding stroma, (Acharyya *et al.,* 2012), with up-regulation of TNF-α in stromal cells conferring chemo-resistance in the cancer cells (Acharyya *et al.,* 2012). Cancer associated fibroblasts (CAFs) via TGF-beta signalling have shown to confer a more aggressive and metastatic phenotype due to induction of epithelial to mesenchmel transition in breast cancer cells (Yu *et al.,* 2014). Up regulation of growth factors secreted by stromal cells (Turner *et a*l., 2010), deregulation of endothelin-1 (Hinsley *et al*., 2012) and changes in hedgehog ligand and Wnt signalling (Yauch *et al*., 2008) are all examples of paracrine communication which enhance tumourigenesis. The dependency of cancer cells on the tumour microenvironment is well established, however, the molecular process that facilitates functional reprogramming in cancer or stromal cells has yet to be defined. In particular, which processes are transient reversible responses to external factors, or the consequences of longer term epigenetic programming, remain important unanswered questions.

1.5.1 Transcription Factors

Transcription factors are proteins that bind to specific DNA sequences in the promoter regions of target genes, thereby driving gene expression. Transcription factors are known to be key factors in cancer initiation and progression (Darnell 2002, Thorne *et al.,* 2009 and Libermann 2006). For example, up-regulation of STAT-3 has a key role in many cancers including; metastasis in prostate cancer (Abdulghani *et al.,* 2008), drug resistance in gastric cancer (Huang *et al.,* 2011) and proliferation in ovarian and breast

cancers (Burke *et al.,* 2001). Also, up-regulation of the SP family of transcription factors has been implicated in tumour development (Kong *et al.,* 2010 and Chuang *et al.,* 2009), as they are reported to have a role in cell-cycle progression and cell differentiation. In addition, acting in conjunction with Akt they also play an important role in regulating tumour cell metabolism, (Archer 2009).

More recently, the differential regulation of transcription factors in cancer stromal cells has also become an area of increased interest. Indeed, there is a growing body of evidence to show that regulation of transcription networks in stromal cells directly leads to the proliferation and migration of cancer cells (Hatiboglu *et al.,* 2011 and Kim *et al.,* 2011). In particular, the role of NRF2 and NF-κB in hypoxia and the microenvironment is a vital process in the development and progression of tumour cells (Satoh *et al.,* 2002).

Dysregulation of transcription factors is thought to be a key factor in the instigation and development of gastric tumours, based on studies performed in gastric cell lines (Kang *et al.,* 2011, Almedia *et al.,* 2003, and Huang *et al.,* 2011), however currently there are no reports regarding the effects of paracrine communication on transcriptional regulation in the gastric cancer microenvironment. Transcriptional analysis of co-culture, or conditioned media microarray studies from tumour – stroma interactions would provide deeper insight and understanding behind the molecular mechanisms driving cancer progression in the tumour stroma.

1.5.2 Epithelial to Mesenchymal Transition

Epithelial to mesenchymal transition (EMT) is the process whereby epithelial cells lose their polarity and convert to a migratory mesenchymal phenotype (Jiang *et al.,* 2011). EMT is critical for appropriate embryonic development, it also occurs during fibrosis, wound healing, tissue regeneration, organ fibrosis, cancer progression and metastasis, as well as diseases of chronic inflammation such as inflammatory bowel disease (Powell *et al.,* 2011). Cancer cells utilise EMT to facilitate invasion of cells into surrounding tissues, crossing endothelial barriers and entering circulation; thus enabling metastasis to other organs in the body (Jiang *et al.,* 2011). There is much evidence supporting the concept of hypoxia-associated factors inducing EMT through transcriptional regulation (Kang and Massagué.. 2004). It has been established that the most common and important inducers of EMT are transcription factors that suppress E-cadherin expression, such as TWIST and SNAIL (Kang and Massagué., 2004). There have also been reports that EMT is induced by inflammatory chemokines and cytokines (Shirakihara *et al.,* 2011). TGF-β has been shown to have both pro and anti-tumour effects. It is associated in EMT in late-stage tumours, by enhancing production of growth factors that encourage migration and production of matrix molecules (Heldin *et al.,* 2012). TGF-β has also been shown to alter normal epithelial cells in the tumour microenvironment, promoting EMT and encouraging invasion of cancer cells into surrounding tissue (Shirakihara *et al.,* 2011). The cytokine tumour necrosis factor alpha (TNF α) has also been reported to induce EMT

in human HCT116 cells, showing to promote invasion and metastasis of colorectal cancer cells (Wang *et al.,* 2013).

1.5.4 Hypoxia

Hypoxia results when regions of the body are deprived of oxygen. It is well established that hypoxia is a critical factor in the regulation of wound healing, due to increasing blood supply to the damaged area, restoring homeostasis to the site of injury (Trabold *et al.,* 2003). One of the many ways that cells adapt to a shortage of oxygen is production of angiogenic factors (Rofstad and Danielsen 1999, Shweiki *et al.*, 1992 and Tamura *et al.,* 2009), in order to increase local blood supply. Despite hypoxia being important in wound healing (Oberringer *et al.,* 2008), in carcinogenesis, sustained hypoxia can have severe implications on both the metabolism and migratory abilities of cells. Indeed, hypoxia plays a critical role in tumour development and progression (Tamura *et al.,* 2009, Hong *et al.,* 2005 and Lee 2009). The effects of hypoxia are mediated by a number of signalling molecules, such as the family of hypoxia inducible factors (HIFs) and their downstream effectors (Papandreou *et al.,* 2006 and Du *et al.,* 2011). Transcription factor, nuclear factor-erythroid 2 (NRF2) is also a key component in the cellular response to oxidative stress, and is linked to increased levels of angiogenic factors and HIF1-α expression (Kim *et al.,* 2011). Blocking NRF2 was shown to supress tumour angiogenesis in colon cancer through inhibiting HIF1-α (Kim *et al.,* 2011).

HIF1 is a heterodimeric basic helix-loop-helix structure consisting of the alpha subunit (HIF1-α) and the aryl hydrocarbon receptor nuclear translocator

which is the beta subunit HIF-β (Ke and Costa 2006). In normoxia HIF is usually down-regulated by the ubiquitin-proteosome pathway, however in hypoxic conditions, degradation of HIF is prevented by prolyl-hydroxylases that act to stablise the α-subunit of HIF1-α, enabling it to translocate to the nucleus and form a heterodimer with HIF-β (Jiang *et al,,* 2010). When in the nucleus, HIF drives expression of a multitude of genes relating to cell survival and hypoxia, enabling the cell to adapt to a lack of oxygen, by switching metabolism to glycolysis from mitochondrial respiration (Lu *et al.,* 2002). In solid tumours it is well established that there are many regions of hypoxia due to the rapid growth of cancer cells, and poor vasculature. There have been various studies that show activation of HIF leads to increased cancer cell invasion (Koh *et al.,* 2011, Manalo *et al.,* 2005, Branco-Price *et al.,* 2012, Li *et al.,* 2009, Semenza 2011 and Maxwell 2005). HIF expression is strongly associated with the regulation of angiogenic factors such as vascular endothelial growth factors (VEGF) (Cao *et al.,* 2009, Pugh and Ratcliff 2003 and Park *et al.,* 2007). Indeed, loss of HIF-1 expression was linked to profound inhibition of blood vessel growth in solid tumours, due to decreased VEGF expression (Tang *et al.,* 2004). Up–regulation of hypoxia-associated factors has also been linked to enhanced EMT (Misra *et al.,* 2012) and there is a strong link between Akt mediated signal transduction (Elstrom *et al.,*2004) active HIF-1α, and expression of enzymes involved in glycolysis (Koukourakis *et al.,*2006). Breast cancer models have shown that hypoxia can induce a metabolic phenotype, in which cells up-regulate HIF1-α, glucose transporter 1 (GLUT-1) and carbonic anhydrase IX (CAIX), which confers resistance to the resulting decrease in extracellular pH (Chen *et al.,*2010). The regulation of

metabolic transporter channels has also been linked with hypoxia, as HIF1-α induces up regulation of the monocarboxylate transporter 4 (MCT4), which facilitates the increased lactic acid produced during hypoxia to be promptly removed from the cell (Ullah *et al.,* 2006).

1.5.5 Cytokines

Cytokines are small soluble secreted proteins that act as messengers between cells, especially cells of the immune system (Borish and Steinke, 2003). They can be released into the circulation to act on cellular receptors to initiate a downstream response cascade (Jiang *et al,.* 2013). The role of cytokines in cancer is varied, and depending on the cells of the tumor microenvironment, cytokines can initiate either a pro-tumour (Jiang *et al,.* 2013) or anti-tumour response (Banchereau *et al.,* 2012). Indeed TGF-β is well documented to have an ambiguous role in cancer progression as it has been shown to display both tumour-suppressing and -enhancing effects (Buck *et al.,* 2006 and Ranganathan *et al.,* 2007).

In most cases of chronic inflammation, cytokines act to induce cellular transformation and initiate malignancy (Landskrone *et al.,* 2014). For example in cases such as multiple myeloma and other B cell malignancies, cytokine CCL5 produced by stromal cells, leads to the up-regulation of immunoglobulin secretion by B cells and increased expression of IL-6 via activation of GLI2 (Elsawa *et al.,* 2011). Factors such as IL-6 are reported to be implicated in migration and the invasive properties of tumour cells.

(Ashizawa *et al.,* 2005). The immune system is known to play a key role in detecting and destroying cancer cells in the body. Indeed, immunotherapy is showing great promise for treatment of several forms of cancer (Mellman *et al.,* 2011, Palucka and Banchereau, 2012 and Lesterhuis *et al.,* 2011). However, the adaptability of cancer cells means that in some cases tumours evolve to overcome detection by the immune system. Tumour cells can down-regulate expression of self-antigens and can produce specific cytokines and chemokines which act to desensitise immune cells causing immune cell anergy (Ben-Baruch *et al.,* 2006 and Stewart and Smyth, 2011).

1.6 .Metabolism and Cancer

The word 'metabolism' is derived from the Greek word "Metabolismos" and means "to change". In the early 20th century, Otto Warburg pioneered studies in respiration and metabolism, particularly in relation to cancer cell metabolism (Warburg *et al.,* 1924 and Warburg 1956). Hans Kreb worked as research assistant to Warburg, and later in his career pioneered work, in the field of metabolism, which lead to the discovery of the fundamentals in cellular metabolic processes; the urea cycle and the citric acid cycle (Krebs, 1937, Krebs *et al.,* 1938 and Krebs 1938). These key discoveries form the basis and understanding of most cellular metabolic processes today.

1.6.1 The Warburg Effect

As discussed above, Otto Warburg pioneered studies of cancer cell in the 1920s that, demonstrating that even under aerobic conditions, tumour tissues metabolise glucose to lactate at a considerably increased rate compared to

normal tissues, a phenomenon termed the Warburg effect (Warburg *et al.,* 1927). Since this discovery there have been numerous studies acknowledging the switch of cancer cells to a more glycolytic phenotype (Schulze *et al.,* 2011, Salminen *et al.,* 2010 and Cai *et al.,* 2010). However, what causes alterations in these metabolic processes in cancers is still relatively unknown. Indeed, changes in cancer cell metabolism have been linked to changes in the expression of oncogenes (Muñoz-Pinedo *et al.,* 2012), disruption of circadian rhythm (Sahar *et al.,* 2009) and also loss of tumour suppressor function (Lyssiotis *et al.,* 2012).

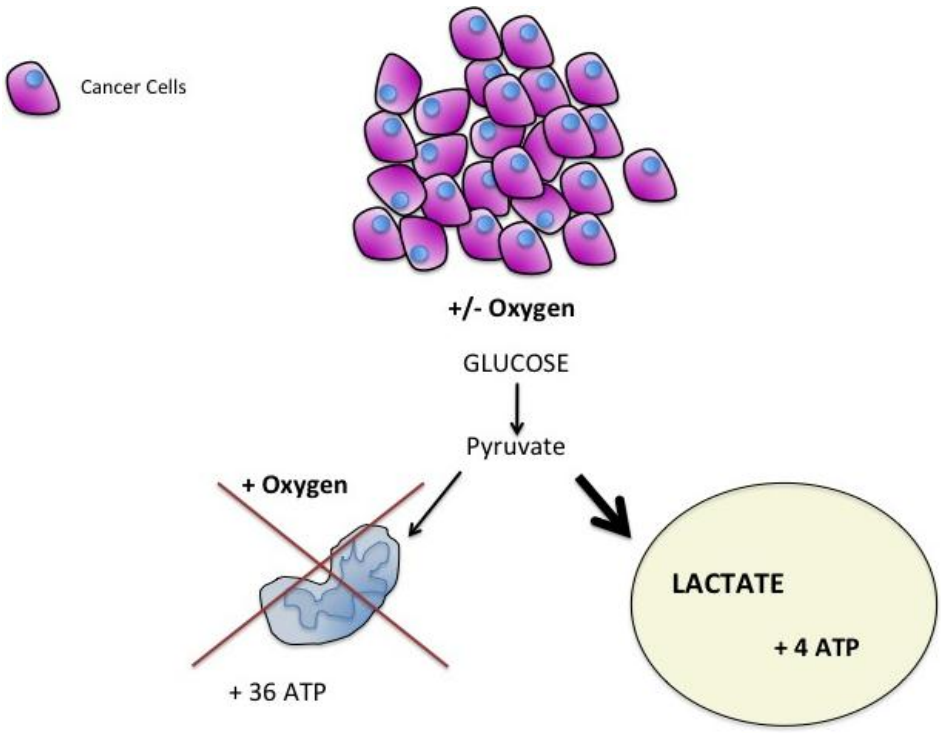

Figure 1. 3. Schematic to illustrate the Warburg type effect.
Cancer cells switch from oxidative phosphorylation to glycolysis, a less energy efficient way of respiration.

The question of why cancer cells would switch to glycolysis, a less efficient way of energy production, is something which has puzzled many scientists. Warburg postulated that the switch to glycolysis was due to defective mitochondrial function in these cells (Warburg *et al.,* 1927). More recently these metabolic changes have been further elucidated and in some cancer models it is reported that cells still maintain mitochondrial function but preferentially utilise glycolysis for ATP production (Futin *et al.,* 2006 and Koppenol *et al.,* 2011) however the reasons for this still remain unclear.

1.6.2 The Reverse Warburg Effect

More recently, there have been studies identifying the importance of metabolic changes in stromal cells, which then support the growth of cancer cells (Pavlides et al 2009, Bonuccelli *et al.,* 2010 and Sotgia *et al.,* 2012). The reverse Warburg model suggests that tumour cells actively utilise their mitochondria and receive high-energy metabolites from surrounding stromal cells, which in turn have switched to glycolysis [figure 1.4]. Understanding the mechanisms behind changes in metabolism in both the tumour and its microenvironment is vital for progression and development of improved therapeutic strategies and identification of biomarkers for new approaches to precision medicine.

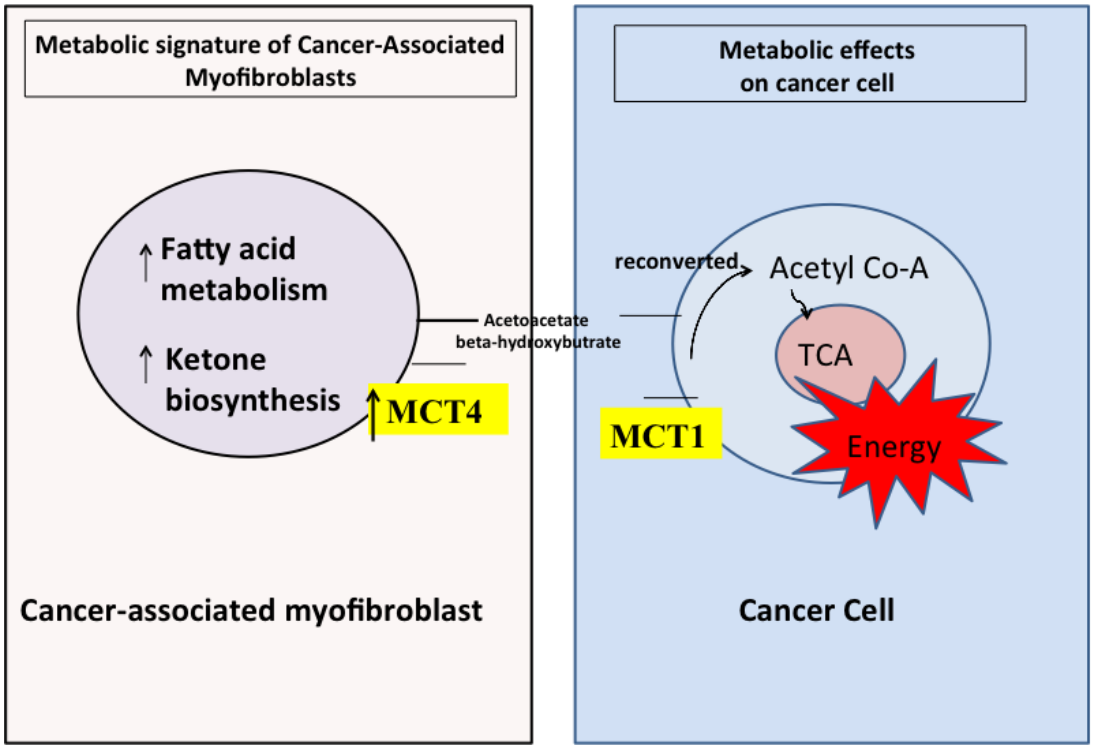

Figure 1. 4. Schematic to illustrate a reverse Warburg type effect.
Cancer cells utilise high energy metabolites for oxidative phosphorylation which have been received from stromal cells, using glycolysis for respiration.

There is increasing evidence for the important role of the tumour microenvironment in the regulation of energy metabolism in carcinogenesis, indeed these changes are now considered a hallmark of cancer (Hannahan and Weinburg., 2011). However, as there is much conflict in the literature regarding the fundamentals of this relationship, this thesis attempts to address these issues in the context of gastric cancer model and primary gastric stromal cells.

1.8 Hypotheses, Aims and Objectives

The primary purpose of this work was to characterise functional changes induced by communication between gastric myofibroblasts and AGS gastric cancer cells.

To address this issue we aimed:

1. To test the hypothesis that there would be differences in AGS cell gene expression profiles after conditioning with CAM or ATM media compared to control media.

2. To establish the inherent and reciprocally induced metabolic profiles of gastric cancer epithelial cells and primary gastric cancer associated myofibroblasts

3. To determine the effects of cancer co-culture on re-programming of normal tissue myofibroblast cells (NTMs)

Chapter II

Gene Expression Profiling Of Gastric Cancer Cells

2.0 Introduction

Historically, a selection of primary myofibroblast cell lines were isolated from a cohort of 12 patients with gastric cancer or 8 tissue donors with no history of gastric cancer (Varro laboratory). These cell lines included Cancer Associated Myofibroblasts (CAMs), isolated from tissue immediately juxtaposed to gastric tumours and matched tissue Adjacent Tissue Myofibroblasts (ATMs), myofibroblasts isolated from tissue neighbouring the site of gastric tumours [figure 2.1]. In contrast, primary myofibroblasts isolated from patients with no history of cancer are defined as Normal Tissue Myofibroblasts (NTMs).

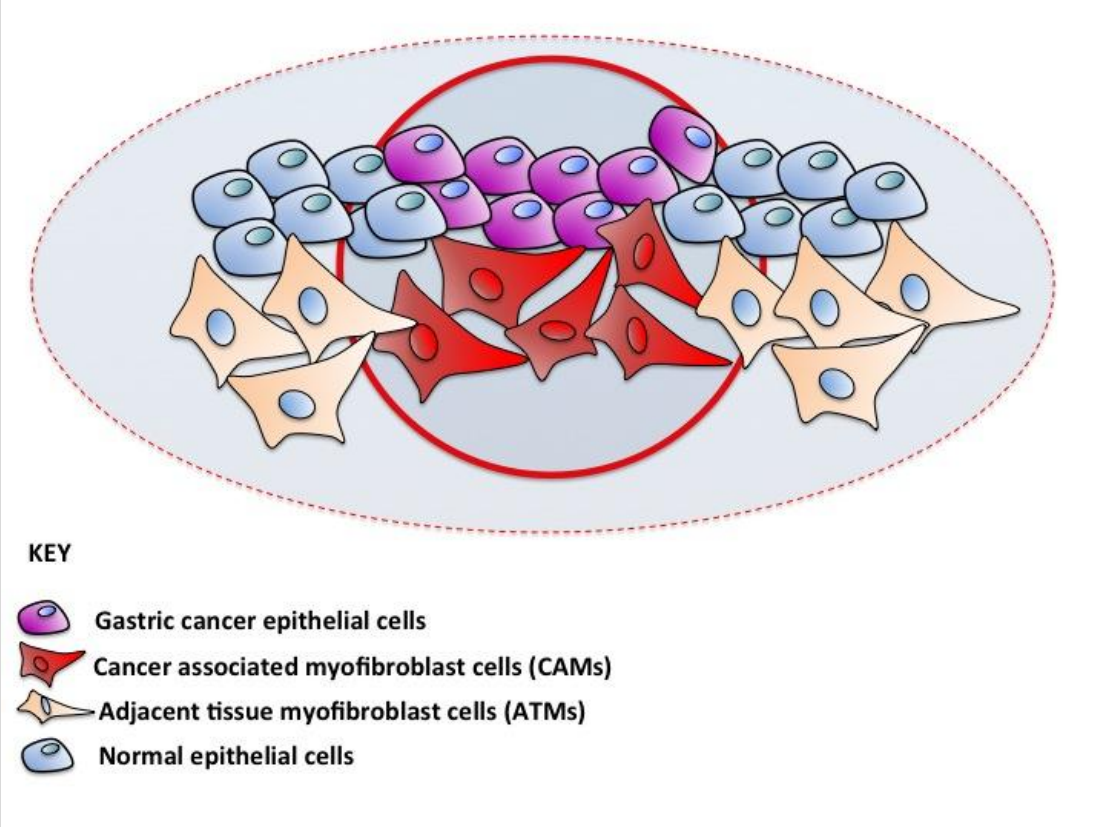

Figure 2. 1 Cells of the stroma.
Schematic showing distinction between matched cancer associated (CAM) and adjacent tissue (ATM) myofibroblasts and epithelial cancer cells.

Previous analysis of gene expression profiles of all patient primary gastric myofibroblast cell-lines showed that each form of myofibroblast (CAM, ATM and NTM) has distinct and characteristic global gene expression profiles (Jones *et al.,* unpublished data). In addition, statistical correlation analysis enabled CAMs derived from early and late stage tumours to be correctly clustered into prognostic groups based on trends in gene expression profiles.

In this study we aimed to further investigate the functional differences between these cell populations by performing comparative analysis of differential gene expression profiles that result from exposure to differentially conditioned media. Microarray analysis allows for a data driven approach to identify potential biomarkers or pathways for follow up analysis. In these studies, AGS cells were exposed to conditioned media, derived from five sets of primary CAM and ATM cells, for 24h before processing samples for global gene expression analysis (work carried out by the Varro Laboratory). The work carried out in this chapter aimed to determine any trends or potential targets of interest in AGS cells that were induced upon conditioning with primary myofibroblast cell media. It was hypothesised that there would be differential gene expression profiles between AGS cells conditioned with media from myofibroblast cells, compared to AGS cells grown in non-conditioned media.

2.1 Aims and Hypotheses

This chapter describes the analysis and interpretation of data from a series of conditioning microarray experiments, which were originally performed in the laboratory of Professor Andrea Varro, the collaborating laboratory in this study. The primary purpose of this chapter was to establish trends in gene expression profiles between AGS cells conditioned with primary gastric myofibroblast cell media. We wanted to test the hypotheses that trends in AGS gene expression profiles would vary between CAMs and ATM conditioning versus controls.

The aims this chapter were:

1. To confirm that the cells used in these studies retain previously defined markers and functional characteristics of CAM, ATM and NTM cells
2. To establish the quality of available microarray data and to assess cell-type specific trends in global gene expression profiles
3. To validate primary microarray data by targeted qPCR analysis
4. To confirm that gene expression profiles observed in primary microarray data are retained in primary myofibroblasts used in subsequent functional studies.
5. To generate potential targets of interest from bioinformatics analysis, which may contribute to, observed functional properties of different myofibroblast populations.

2.2 Chapter Specific Materials and Methods

Full details of materials and methods can be found in chapter VI.

2.2.1 Microarray Sample Selection and Data Processing

All microarray studies were performed on low passage (P4-P10) myofibroblast cell-lines [table 1]. In all conditioning experiments, the effects of AGS conditioned media were compared to corresponding molecular signatures and functional phenotypes observed in non-conditioned serum-free media. Details of patient data are shown in table 1.

Label	Sample	Sample Type	Array Sample Name
190 CAM	Sz190/1 P4	Cancer	AV 55. CEL
190 ATM	Sz190/2 P4	Adjacent	AV 56. CEL
192 CAM	Sz192/1 P5	Cancer	AV 82. CEL
192 ATM	Sz192/2 P5	Adjacent	AV 83. CEL
294 CAM	Sz294/1 P4	Cancer	AV 59. CEL
294 ATM	Sz294/2 P5	Adjacent 1	AV 60. CEL
305 CAM	Sz305/1 P5	Cancer	AV 84. CEL
305 ATM	Sz305/22 P5	Adjacent 1	AV 86. CEL
308 CAM	Sz308/1 P5	Cancer	AV 87. CEL
308 ATM	Sz308/22 P6	Adjacent	AV 88. CEL
CONTROL	N/A	N/A	AV 58. CEL
CONTROL	N/A	N/A	AV 57. CEL
CONTROL	N/A	N/A	AV 94. CEL

Table 1. Primary myofibroblast cell-lines used in AGS conditioning microarray studies.

Microarrays were carried out by the Varro laboratory and data was processed in Partek by Dr Jithesh Puthen (University of Liverpool). For grouped patient analysis an FDR cut of value of 0.25 was applied and ANOVA analysis was carried out, before gene lists were exported to excel for further analysis.

2.2.2 qPCR for Real Time Evaluation of Microarray Data

Primary CAM myofibroblast cell-lines 190, 294 and 305 were selected for qPCR validation of induced gene expression profiles, as these represent different survival/prognosis patient subgroups, identified by previous informatics analysis of unconditioned CAM gene expression profiles (Jones *et al.,* unpublished data). Gene specific qPCR primers were designed for differentially regulated gene changes within each microarray data set.

2.2.3 Proliferation and Migration Assays

Proliferation and migration profiles of cell lines used in this study have been previously defined (Holmberg *et al.*, 2012). To confirm the validity of data presented in our current study, comparative proliferation and migration assays were performed on a selection of low-passage (P4-P9) CAM cells 190, 308 294 and 305 which had also been used previously in microarray studies.

2.3 Results
2.3.1 Characterisation of primary myofibroblast cell lines

To confirm the cells were myofibroblast cell lines, cell phenotype, morphology, quantity and abundance were determined by the Varro Laboratory (Holmberg *et al.,* 2012) [figure 2.2]. To confirm isolated primary CAMs, ATMs and NTMs retained their characteristic morphology and function, each cell line was stained to confirm the presence of a spindle or stellate morphology and expression of the two canonical myofibroblast markers, vimentin and α-SMA (Holmberg *et al.* 2012) [Figure 2.3]. Collated data from these experiments confirms that when RNA was prepared from primary gastric myofibroblasts for microarray analysis, cell lines maintained all of the hallmarks that have been used to define this cell type in other tissues.

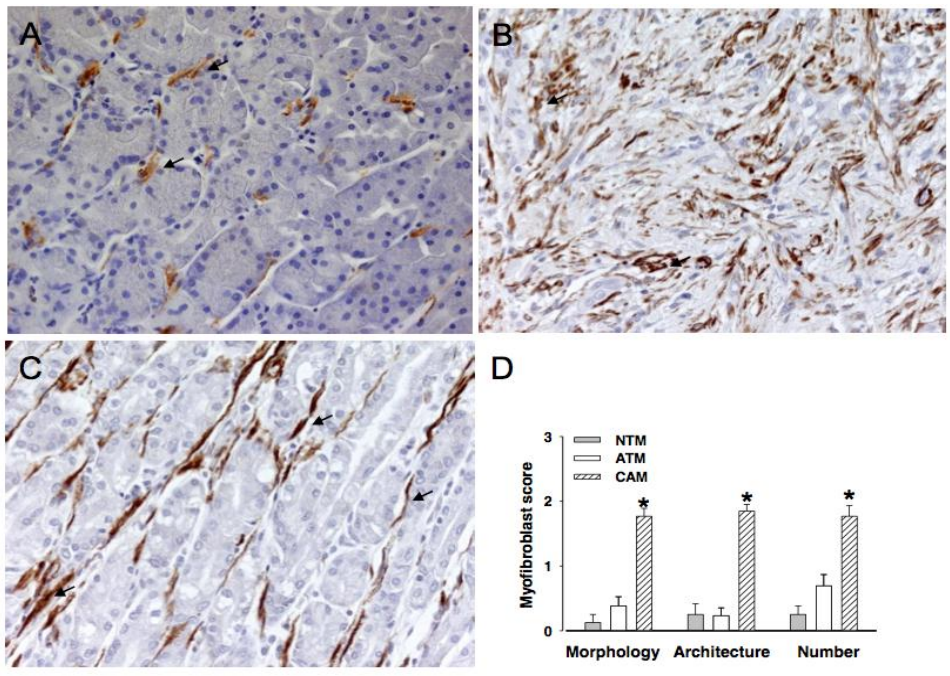

Figure 2. 2 Characterisation of myofibroblast cell types.
Representative images of tissues from which NTMs (A), CAMs (B) or ATMs (C) were isolated. Brown stain shows localization and relative abundance of myofibroblasts in each tissue. (D) Quantification of myofibroblast morphology, architecture and number in cancer, adjacent and normal tissues. Figure taken from Holmberg *et al.,* Carcinogenesis 33:1553 (2012).

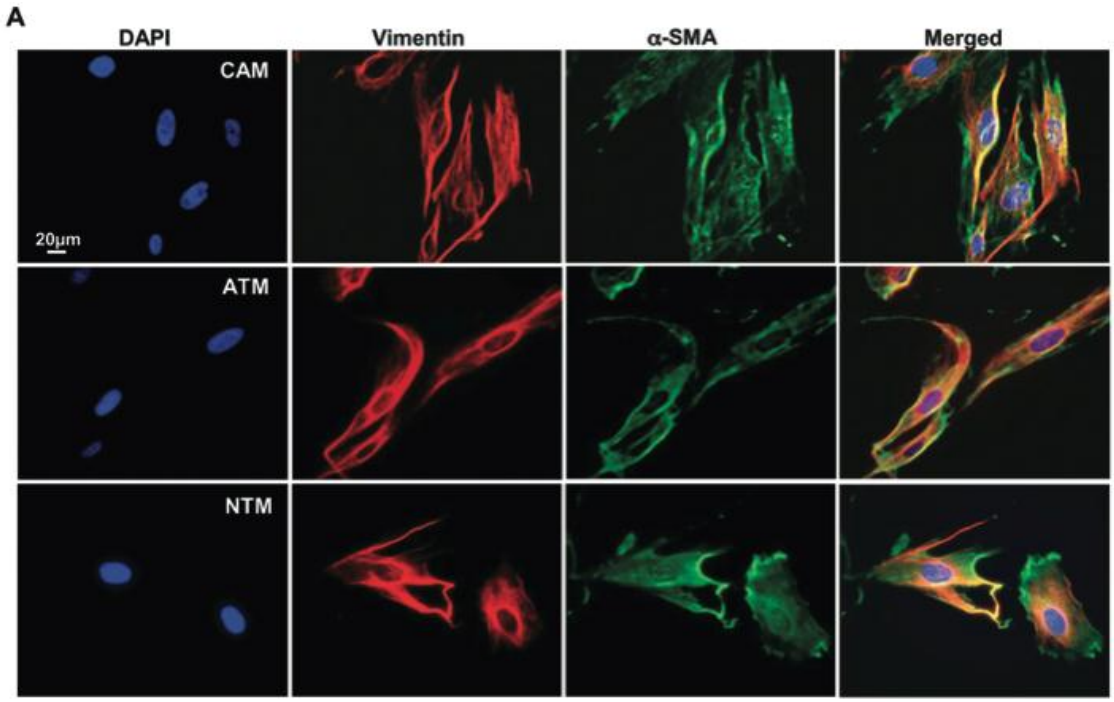

Figure 2. 3. Characterisation of myofibroblast cell types.
Immunofloruescnce to show strong coexpression of the myofibroblast markers vimentin and α -SMA in isolated primary human CAMs, ATMs and NTMs. Figure taken from Holmberg *et al.*, Carcinogenesis 33:1553 (2012).

2.3.2 Microarray Processing and Quality Analysis

The primary purpose of the microarray analysis was to allow for a data driven, exploratory approach, to identify potential candidates of interest for follow up analysis. In order to progress with the microarray data experiments, a series of quality control and normalisation steps were carried out. Firstly, the RNA extracted from AGS conditioned cells, passed quality (RQI) and purity thresholds and could therefore be used in subsequent microarray experiments (Varro Laboratory).

Affymetrix array chips allowed for normalisation locally, as each gene is

matched to 11 pairs of probes, which are evenly distributed throughout the chip to detect any noise within the genechip (as well as gene expression). Each chip also contains probes which measure non-specific binding of cRNA which also eliminates non-specific signals and enables the data to be normalised effectively. To ensure quality control between the 12 arrays, there is also a selection of normalisation probes on the gene chip, which have constant levels of expression, these are used to normalise signals across the multiple arrays.

An array quality metrics report (AQMR) can also be generated to look more closely at batch effects and to identify any potential outliers or skewing in the data sets. These reports were carried out on our microarray datasets by Dr Helen Jones (University of Manchester). Full details of AQMR generated for these microarrays can be found in the appendix [supplementary file IIII). Briefly, histograms showing density distribution of the microarrays were found to be highly comparable, showing consistent and comparable intensity ranges [Figure 2.4].

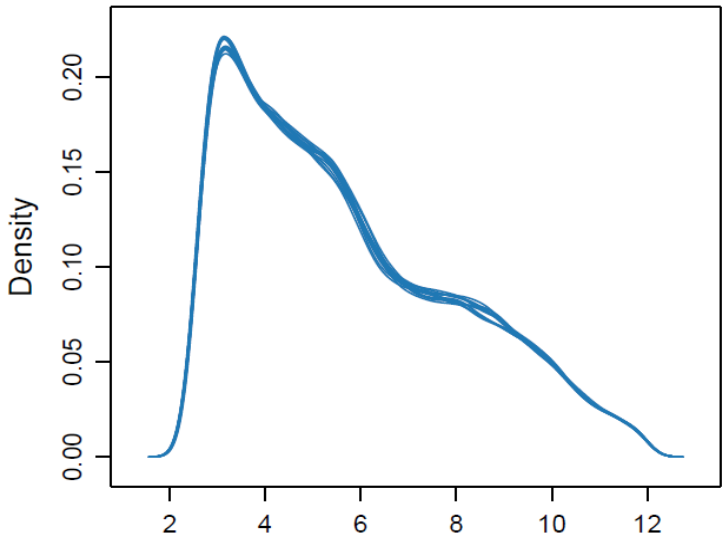

Figure 2. 4 Density estimates (smoothed histograms) of AGS conditioned microarray data.
Each array is indicated by a single blue line showing the density distributions between data from individual microarrays were found to be highly comparable.

Distance between arrays were plotted using a false colour heatmap [figure 2.5] to assess clustering of biologically related samples or experimental trends, which may indicate unwanted batch effects. Outlier detection was performed by looking for arrays for which the sum of the distances to all other arrays, $S_a = \Sigma_b \, d_{ab}$ was exceptionally large. Three such arrays were detected as outliers in this analysis, marked by an asterisk in figure 2.5.

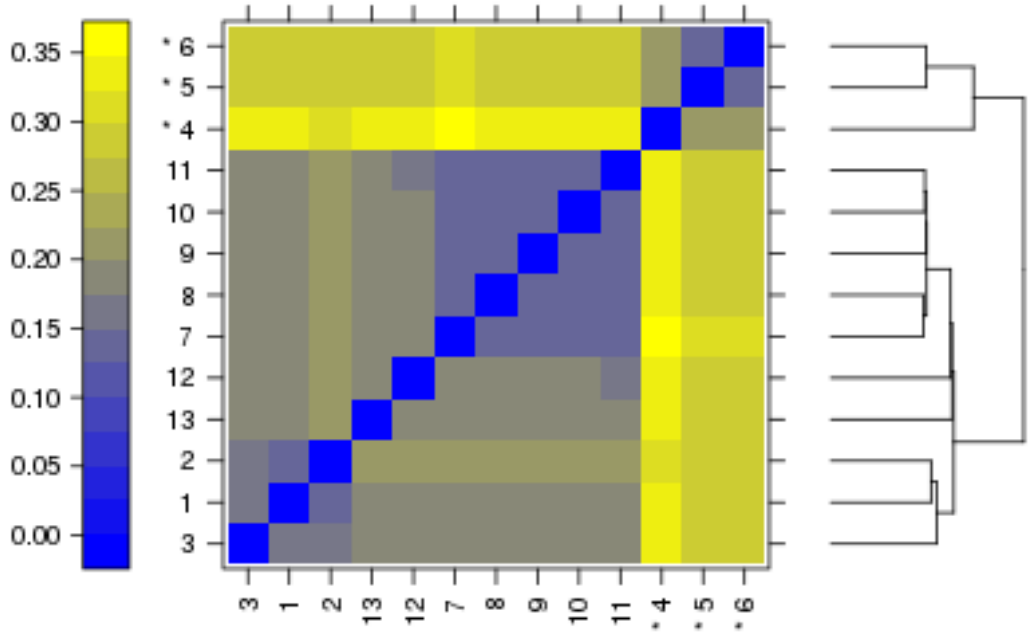

Figure 2. 5. False colour heat-map of arrays.
The plot shows variation between data from individual arrays by clustering of related trends. Outliers in this analysis are indicated by the asterisk (*).

As these three arrays were performed on the same day it is highly probable that this variation could be due to an experimental batch effect. To establish if the three identified outliers were due to batch effect, a principle component analysis was also carried out both before (work carried out by Dr Helen Jones) [figure 2.10] and then after batch correction, using Partek©. software (work carried out by Dr Jithesh Puthen) to generate a 3D model of the global gene expression data [figure 2.11]. Significantly, data from this analysis shows that batch correction does effectively remove deleterious effects of batch processing. Therefore, batch corrected microarray data was considered to be suitable for use in all subsequent gene expression and bioinformatics studies.

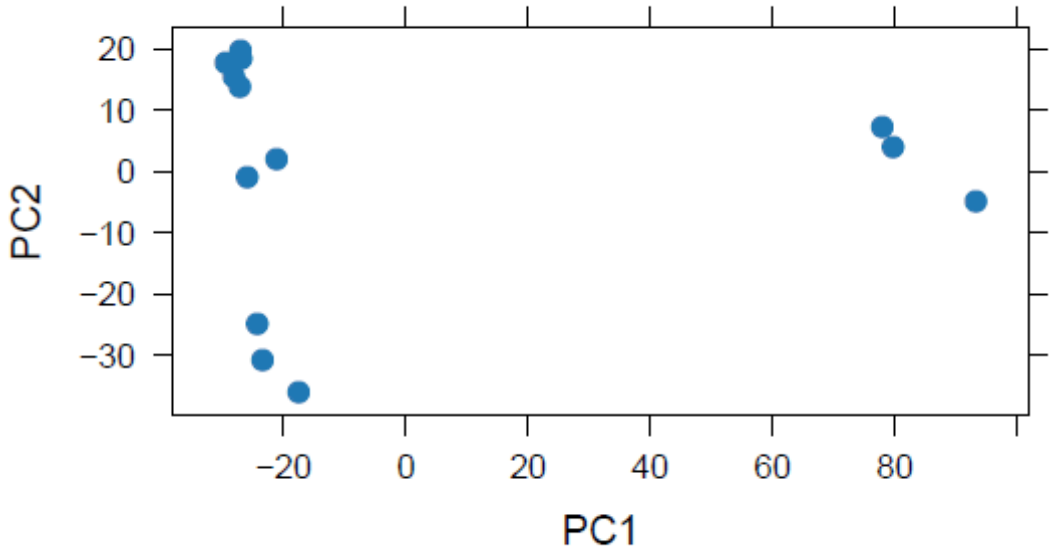

Figure 2. 6 Principle component analysis of microarray data.
The array quality metrics report plotted the PCA showing the global gene expression of the arrays both before batch correction.

.

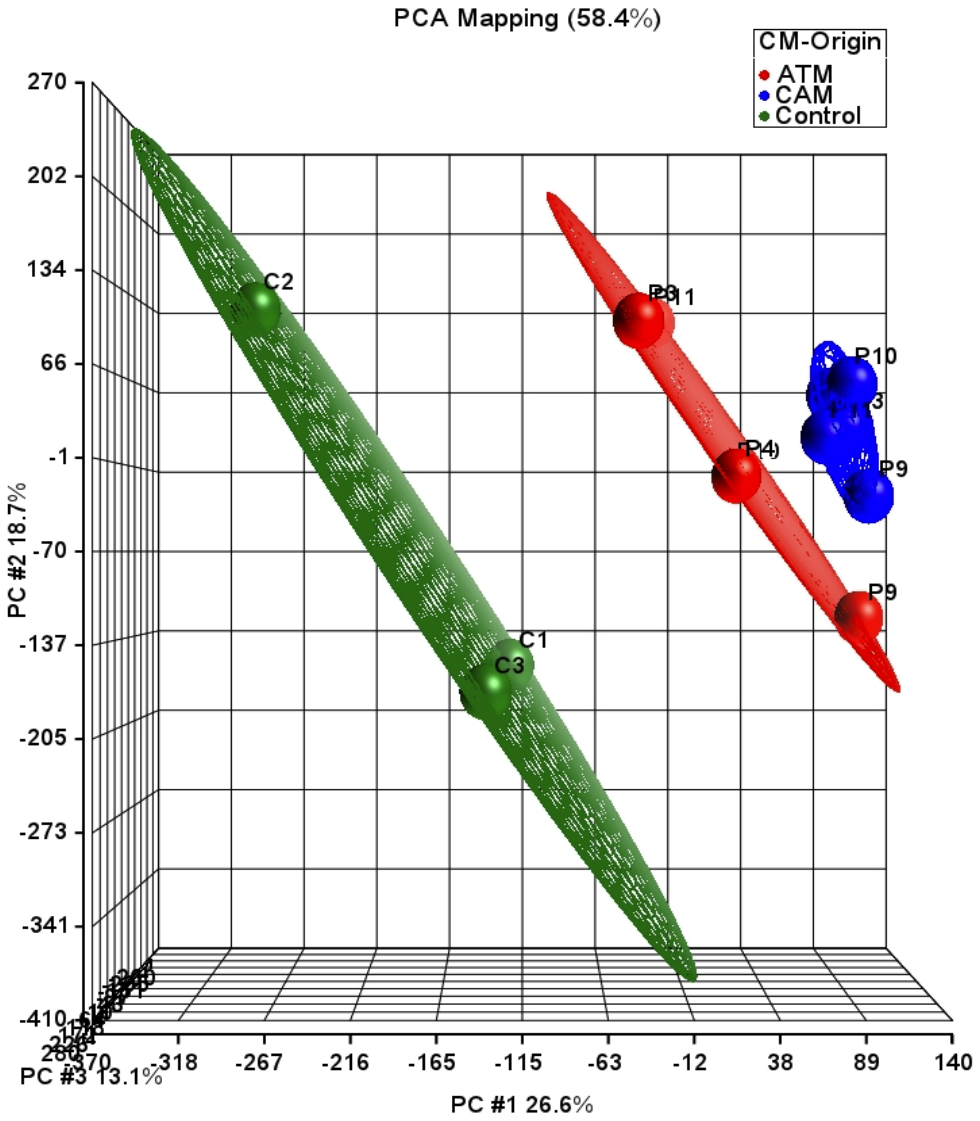

Figure 2. 7 Principle component analysis of global gene expression profiles of AGS conditioning microarray data using PARTEK©.
After RMA normalisation and batch correction data was plotted and global gene expression analysed by principle component analysis.

As stated previously, RNA quality was determined before the microarray was carried out, however RNA quality can also be evaluated on the raw data set after the microarray was carried out using the AQMR. Any arrays with a slope highly different from others arrays may indicate significant variation in RNA quality. Results shown in Figure 2.8 indicate that there was no significant difference between the mean intensities of the data; therefore we

can be confident that RNA the quality of RNA is consistent across all samples used in these studies.

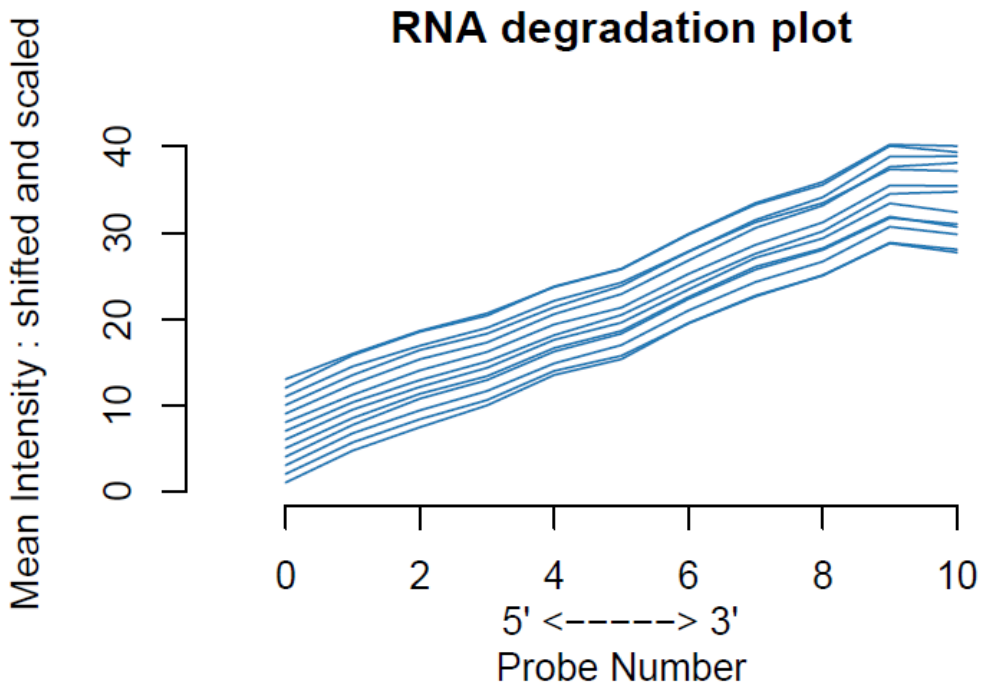

Figure 2. 5. Relative levels of RNA degradation across all microarray samples.
All values were calculated from the pre-processed data after background correction and quantile normalisation. Each array is represented by a single line.

2.3.3 Microarray Validation by qPCR

Following quality analysis of microarray data, a series of targeted qPCR studies were performed to validate observed variations in gene expression profiles; and to demonstrate that cell stocks used in subsequent functional studies maintain the ability to induce comparable changes in patterns of AGS gene expression as observed in the original conditioned media microarray studies. Therefore, targeted real time qPCR analysis was carried out on

cDNA derived from AGS cells treated with CAM conditioned media for 24h. In each case expression profiles were compared to AGS cells treated with unconditioned serum free media (consistent with conditions used in original microarray studies). Significantly, qPCR data from this analysis directly reflects differential trends in gene expression identified in primary microarray analysis across all cell lines tested [figure 2.9].

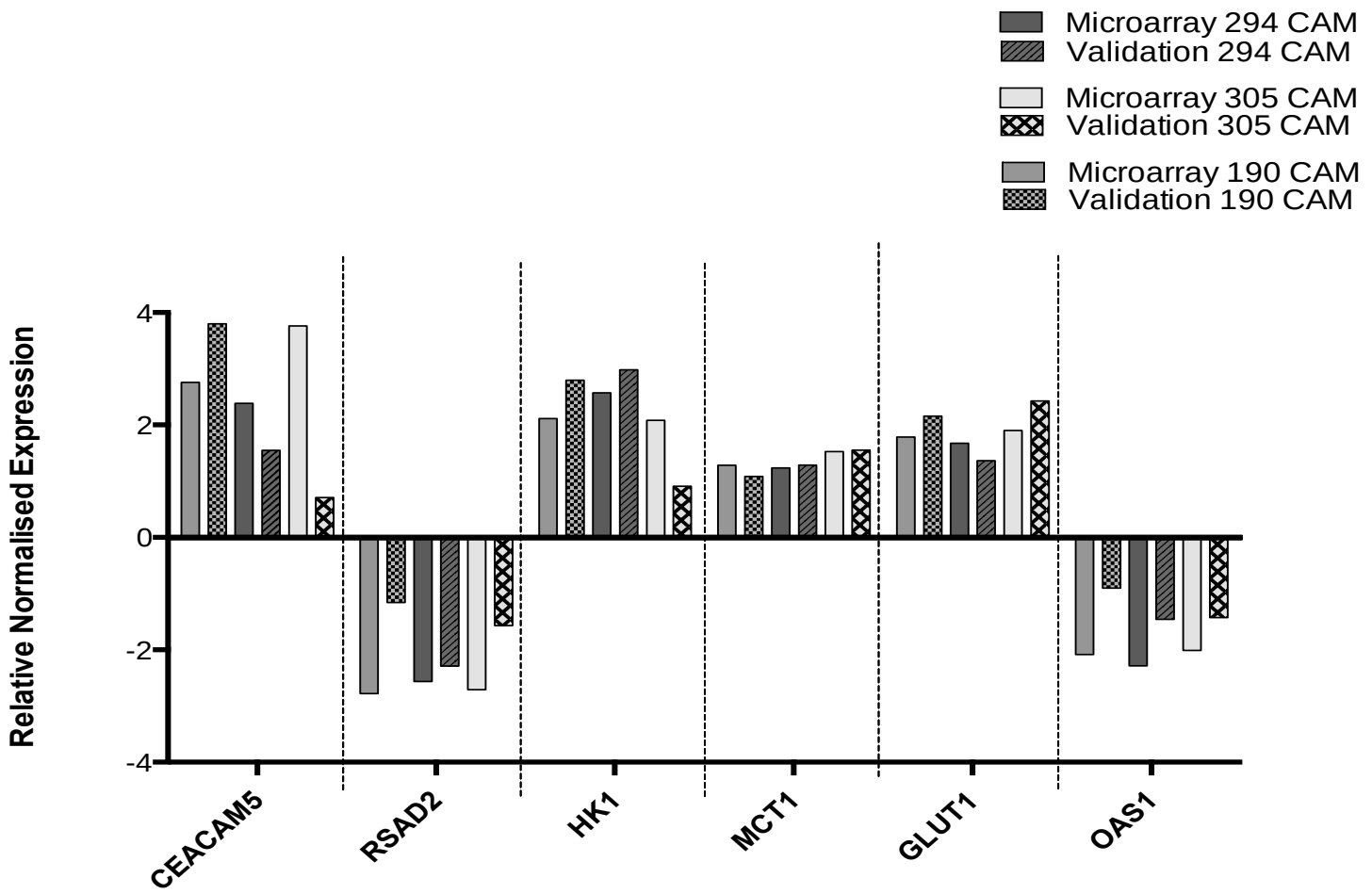

Figure 2. 6. qPCR validation of microarray gene targets from AGS treated with media from 294, 305 and 190 CAM. qPCR was carried in triplicate, all genes were normalised to beta-actin (housekeeping gene) and the serum free control.

2.3.4 Microarray Data Analysis

The purpose of the microarray data analysis was to generate potential interesting signatures, pathways or genes of interest to investigate further. Affymetrix arrays were normalised by Dr Jithesh Puthen using Robust Multi-array Average (RMA) and processed for batch correction (as previously described) using Partek statistical and visual data analysis software. Gene lists were generated for AGS treated with conditioned media for both CAM (n=5) and ATM (n=5) cell lines compared to controls [table 1] and also as individual patient data sets. As the purpose of this analysis was hypothesis generating, fold change cut offs of 1.6 were used to filter the data to allow for maximum number of significant genes to be used in bioinformatics analysis. Gene lists were analysed using Ingenuity software platform to identify statistical signatures and trends [figure 2.10]. Grouped analysis confers statistical significance within CAM and ATM conditioned subsets, whilst single patient analysis identifies patient specific trends within the data sets. Results were analysed using both approaches, to generate a thorough overview of the data set, to establish any differences between patient subgroups and to generate as much information as possible to from the microarray data sets.

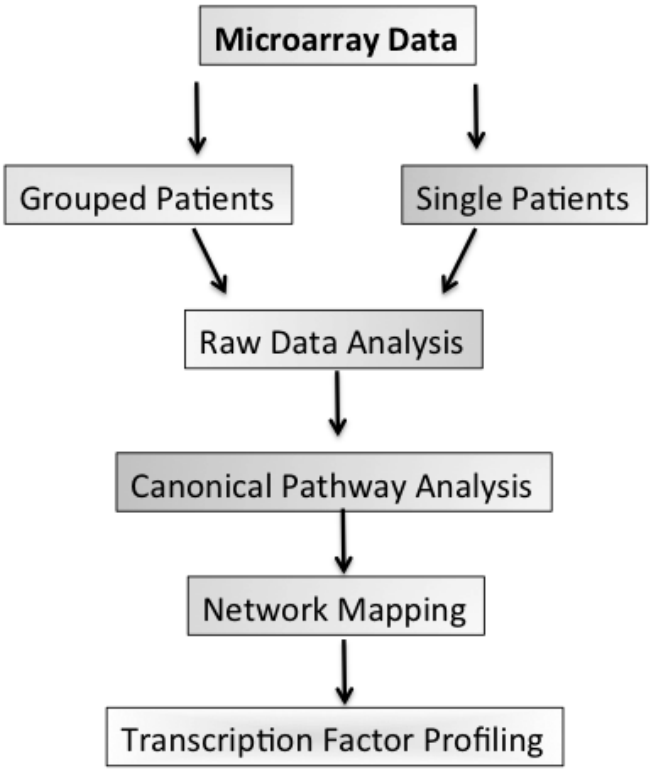

Figure 2. 10. Schematic showing sequential stages of microarray data analysis.
Gene lists were ranked and analysed, then up-loaded into Ingenuity software platform to identify statistical signatures and trends in pathways, networks and transcription factors for both grouped and single patient data

2.3.4.1 Raw Data Analysis- Grouped Patient Data

In order to investigate the hypothesis further, to determine if there were any differences in AGS gene expression following conditioning with primary myofibroblast cell media, raw gene-expression data analysis of microarray data was carried out. This analysis ranked genes according to fold change and p-value significance from the gene lists generated after initial processing (work carried out in Partek, by Dr Jithesh Puthen). As previously stated, the work in this chapter was hypothesis generating, and used to investigate any potential trends within the data, therefore a p-value cut off of less than 0.5 was applied to filter the data, and a fold change cut off of 1.6 was used as an arbitrary cut off for on all data sets. Three gene lists were generated for further analysis: (1) AGS conditioned with CAM media vs control media; (2) AGS conditioned with ATM media vs control and (3) AGS conditioned with CAM media vs ATM media. Both CAM vs control and ATM vs control datasets had 200 genes, which significantly changed within the dataset after applying stringent cut offs ($p<0.05$, fc>1,6,<-1.6) compared to only 73 in the CAM vs ATM comparison. This result suggests that CAMs and ATMs have the ability to induced similar changes in AGS gene expression profiles.

Table 2 shows the top ranking genes that are over expressed in CAM vs control dataset. Results show AGS treated with CAM conditioned media resulted in an up-regulation of cytoplasmic enzymes COQ3 and CYP1A1, kinase HK1 and enzyme CEACAM5 [table 2.]. Many of these differentially regulated genes have previously been reported to be associated with carcinogenesis; CEACAM5 expression has been correlated with worsened

prognosis of colon cancer, (Govindan *et al.*, 2009 and Zheng *et al.*, 2011) and also invasion and metastasis of cancer cells into surrounding tissue (Blumenthal *et al.*, 2005). IGFBP5 has also been associated with breast cancer progression and metastasis (Akkiprik *et al.,* 2009. Interestingly, the most prominent down-regulated gene signatures were mostly from interferon or interferon-related pathways, including IFNL2, OAS2, IFIT3 and IFI44L [table 3].

Symbol	Entrez Gene Name	p-value	Fold Change	Location	Type(s)
IGFBP5	insulin-like growth factor binding protein 5	2.11E-08	4.803	Extracellular Space	other
CEACAM5	carcinoembryonic antigen-related cell adhesion molecule 5	3.37E-04	2.758	Plasma Membrane	other
PGBD1	piggyBac transposable element derived 1	7.62E-04	2.612	Extracellular Space	enzyme
PRSS1	protease, serine, 1 (trypsin 1)	8.76E-04	2.435	Other	peptidase
CFI	complement factor I	4.70E-05	2.33	Extracellular Space	peptidase
COQ3	coenzyme Q3 methyltransferase	1.52E-02	2.32	Cytoplasm	enzyme
CYP1A1	cytochrome P450, family 1, subfamily A, polypeptide 1	3.52E-06	2.205	Cytoplasm	enzyme
AGK	acylglycerol kinase	1.40E-03	2.187	Cytoplasm	kinase
MDP1	magnesium-dependent phosphatase 1	3.07E-03	2.124	Other	phosphatase
HK1	hexokinase 1	2.07E-05	2.114	Cytoplasm	kinase

Table 2. Top ranking differentially up-regulated significant genes in CAM vs Control AGS conditioning data set. Data was ranked by fold change.

Symbol	Entrez Gene Name	p-value	Fold Change	Location	Type(s)
IFNL2	interferon, lambda 2	1.14E-02	-2.451	Extracellular Space	other
OAS2	2'-5'-oligoadenylate synthetase 2, 69/71kDa	1.60E-07	-2.464	Cytoplasm	enzyme
USP18	ubiquitin specific peptidase 18	1.38E-04	-2.465	Cytoplasm	peptidase
IFIT3	interferon-induced protein with tetratricopeptide repeats 3	1.59E-10	-2.506	Cytoplasm	other
IFI44L	interferon-induced protein 44-like	5.84E-05	-2.587	Other	other
PMCH	pro-melanin-concentrating hormone	8.15E-04	-3.01	Extracellular Space	other
RSAD2	radical S-adenosyl methionine domain containing 2	2.01E-07	-3.128	Cytoplasm	enzyme
ZNF114	zinc finger protein 114	3.43E-02	-3.267	Cytoplasm	other
MX2	myxovirus (influenza virus) resistance 2 (mouse)	2.28E-07	-3.488	Nucleus	enzyme

Table 3. Top ranking differentially down-regulated significant genes in CAM vs Control AGS conditioning data set. Data was ranked by fold change.

Similar gene changes were observed in ATM vs Control data set, showing signatures of up-regulated genes such as CEACAM5 and IGFBP5, and with down-regulation of interferons and interferon associated proteins [table 4]. This trend differed in the CAM vs ATM dataset, where a different array of differentially regulated genes were present [table 5], interestingly showing up regulation of TGF-B which is strongly associated with poor prognosis (Bhowmick *et al.,* 2004). DAAM2 was also up regulated, and is involved with the wnt signalling pathway in cancer, which may confer a more aggressive phenotype. Further analysis of these data sets by transcriptional profiling may identify up and down–stream effectors and potential 'hubs', which control pathway signalling. Therefore, pathway and network mapping of differentially regulated gene signatures will provide more insight into relevant signalling and metabolic pathways, molecular networks, and biological functions, as well as predicting the direction of downstream effects on biological processes within the cell.

Symbol	Entrez Gene Name	p-value	Fold Change	Location	Type(s)
IGFBP5	insulin-like growth factor binding protein 5	1.29 E-08	5.213	Extracellular Space	other
CEACAM5	carcinoembryonic antigen-related cell adhesion molecule 5	2.59E-04	2.858	Plasma Membrane	other
PRSS1	protease, serine, 1 (trypsin 1)	6.27E-04	2.540	Other	peptidase
HEG1	Heart development protein	7.25E-03	2.373	Plasma	other
COQ3	coenzyme Q3 methyltransferase	2.65E-02	2.113	Cytoplasm	enzyme
RSAD2	radical S-adenosyl methionine domain containing 2	4.67E-08	-3.778	Cytoplasm	enzyme
OAS2	2'-5'-oligoadenylate synthetase 2, 69/71kDa	3.94E-09	-3.764	Cytoplasm	enzyme
MX2	myxovirus (influenza virus) resistance 2 (mouse)	2.28E-07	-3.488	Nucleus	enzyme
IFIT3	interferon-induced protein with tetratricopeptide repeats 3	1.59E-10	-2.506	Cytoplasm	other
PMCH	pro-melanin-concentrating hormone	8.15E-04	-3.01	Extracellular Space	other

Table 4. Top ranking differentially up and down-regulated significant genes in ATM vs control AGS conditioning data set.
Data was ranked by fold change.

Symbol	Entrez Gene Name	p-value	Fold Change	Location	Type(s)
PPP1R14A	protein phosphatase 1, regulatory (inhibitor) subunit 14A	0.024	5.57	Cytoplasm	phosphatase
TGFB2	transforming growth factor, beta 2	0.025	5.33	Extracellular Space	growth factor
RGS5	regulator of G-protein signaling 5	0.042	4.94	Plasma Membrane	other
NDNF	neuron-derived neurotrophic factor	0.013	4.38	Extracellular Space	other
DAAM2	dishevelled associated activator of morphogenesis 2	0.014	4.13	Other	other
PRSS3	protease, serine, 3	0.033	-3.93	Extracellular Space	peptidase
HPSE	heparanase	0.041	-3.96	Plasma Membrane	enzyme
SDK1	sidekick cell adhesion molecule 1	0.047	-4.06	Plasma Membrane	other
STEAP1B	STEAP family member 1B	0.041	-4.39	Other	other
DMKN	dermokine	0.001	-5.28	Extracellular Space	other

Table 5. Top ranking differentially up and down-regulated significant genes in CAM vs ATM AGS conditioning data set.
Data was ranked by fold change.

2.3.4.2 Pathway analysis

Pathways analysis was performed using the Ingenuity software platform following application of a 1.6 fold change cut off and a p-value cut off of <0.5 to the batch corrected RMA normalized microarray data set for CAM vs serum free control, ATM vs control and CAM vs ATM. This analysis generated pathway reports containing information on differentially regulated canonical pathways, ranked by assignation of p-value within the data, as well as ratio of molecules within the data set to those in the pathway. Ingenuity uses Fisher's exact test right-tailed to calculate the significance (-log of p-value). The ratio is calculated as follows:

$$\frac{\text{Number of genes in a given pathway that meet your cutoff criteria}}{\text{Total number of genes that make up that pathway and that are in the reference gene set.}}$$

Analysis showed a significant and marked increase in pathways associated with interferon signalling [figure 2.11], with the number of positive hits on this pathway being significantly down regulated. These results also concur with the raw gene expression analysis. Analysis also showed a significant and marked increase in load on pathways associated with immunoregulation within the cells, again correlating with a number of decreased gene signatures associated with these pathways in the raw dataset [table 6]. Pathways associated with antigen presenting, and also macrophages, fibroblasts and endothelial cells were also significant [table 6] implicating the immune response and t-cells as key processes affected by CAM conditioning.

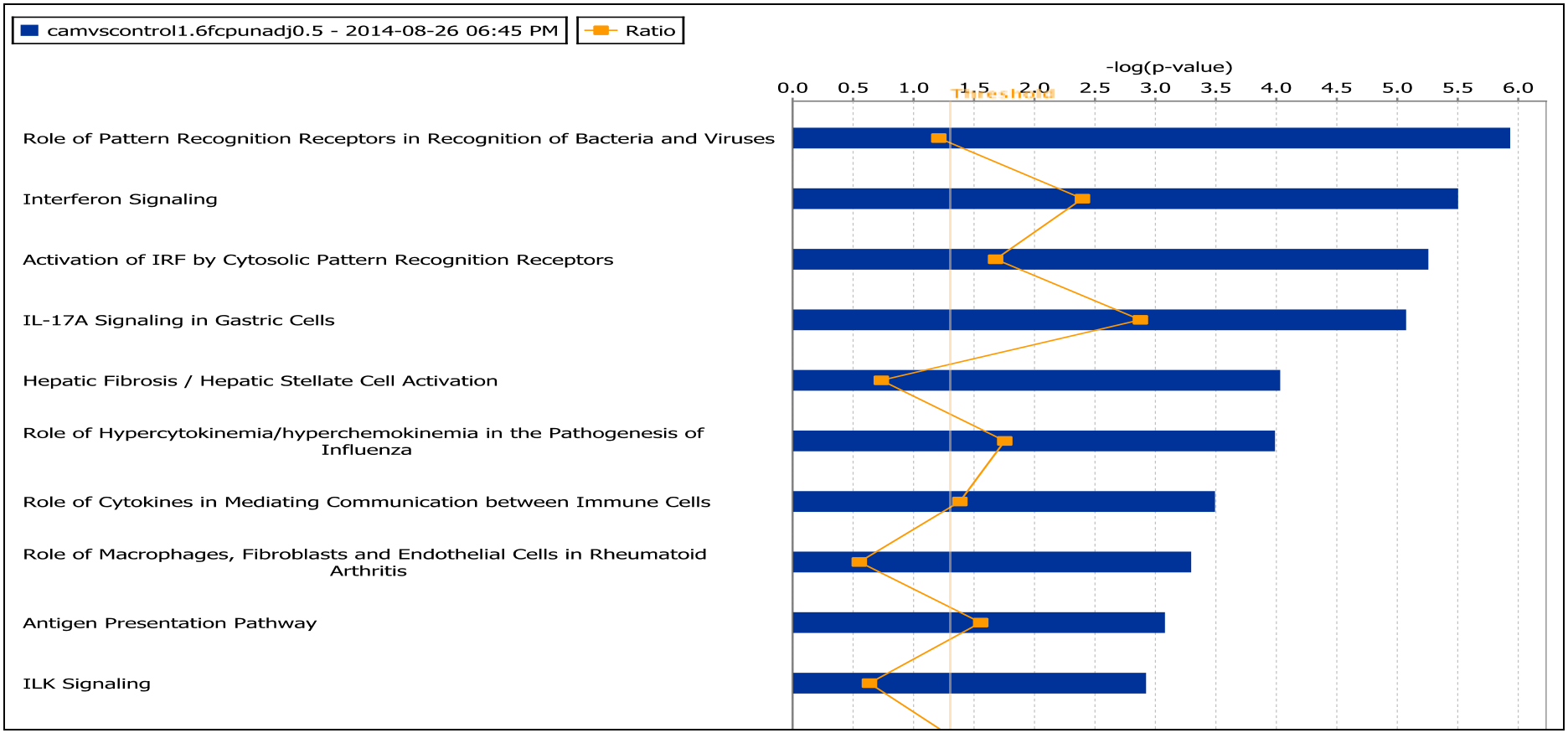

Figure 2. 11. Table showing ranked canonical pathways from Ingenuity pathway analysis on CAM vs Control AGS treated microarray data set (p<0.05, fc >-1.6, >1.6).
Data plotted shows the top ten ranked pathways in order of significance.

Ingenuity Canonical Pathways	-log(p-value)	Ratio	Molecules
Role of Pattern Recognition Receptors in Recognition of Bacteria and Viruses	5.93E00	8.4E-02	IFIH1,CXCL8,OAS1,IRF7,OAS2,PIK3C2A,IL10,DDX58,IFNB1,OAS3
Interferon Signaling	5.5E00	1.67E-01	IFIT3,IFIT1,OAS1,MX1,IFNB1,TAP1
Activation of IRF by Cytosolic Pattern Recognition Receptors	5.26E00	1.17E-01	IFIH1,IRF7,IL10,DDX58,IFNB1,IFIT2,ISG15
IL-17A Signaling in Gastric Cells	5.07E00	2.0E-01	CXCL10,CXCL8,FOS,CXCL11,EGFR
Hepatic Fibrosis / Hepatic Stellate Cell Activation	4.03E00	5.1E-02	CXCL8,COL4A1,IL10,LEPR,COL8A1,MMP13,TNFSF10,IGFBP5,COL28A1,EGFR
Role of Hypercytokinemia/hyperchemokinemia in the Pathogenesis of Influenza	3.99E00	1.22E-01	CXCL10,CXCL8,IL15,IFNB1,IFNL1
Role of Cytokines in Mediating Communication between Immune Cells	3.49E00	9.62E-02	CXCL8,IL10,IL15,IFNB1,IFNL1
Role of Macrophages, Fibroblasts and Endothelial Cells in Rheumatoid Arthritis	3.3E00	3.83E-02	CXCL8,SOCS3,FOS,PIK3C2A,IL10,PRSS2,IL15,MMP13,CREB5,PRSS3,PRSS1
Antigen Presentation Pathway	3.08E00	1.08E-01	PSMB9,NLRC5,TAP1,TAP2
ILK Signaling	2.92E00	4.42E-02	DOCK1,FOS,PIK3C2A,RHOB,MUC1,ITGB8,ITGB6,CREB5

Table 6. Ranked canonical pathways from Ingenuity pathway analysis of CAM vs Control AGS treated microarray data ($p<0.05$, fc >-1.6, >1.6).
Plots shows ranked pathways, significance, ratio and differentially regulated molecules in the data set.

Analysis of ATM vs control conditioning data also showed a significant increase in pathways associated with the cytokine response, including pathways associated with IL-17A as well as a general cytokine signalling pathway being differentially regulated. Results also showed the interferon signalling pathway as being the most statistically significant changed pathway [figure 2.12]. Analysis again also showed a significant and marked increase in load on pathways associated with immunoregulation within the cells, implicating a critical role of the immune response in this system [table 7].

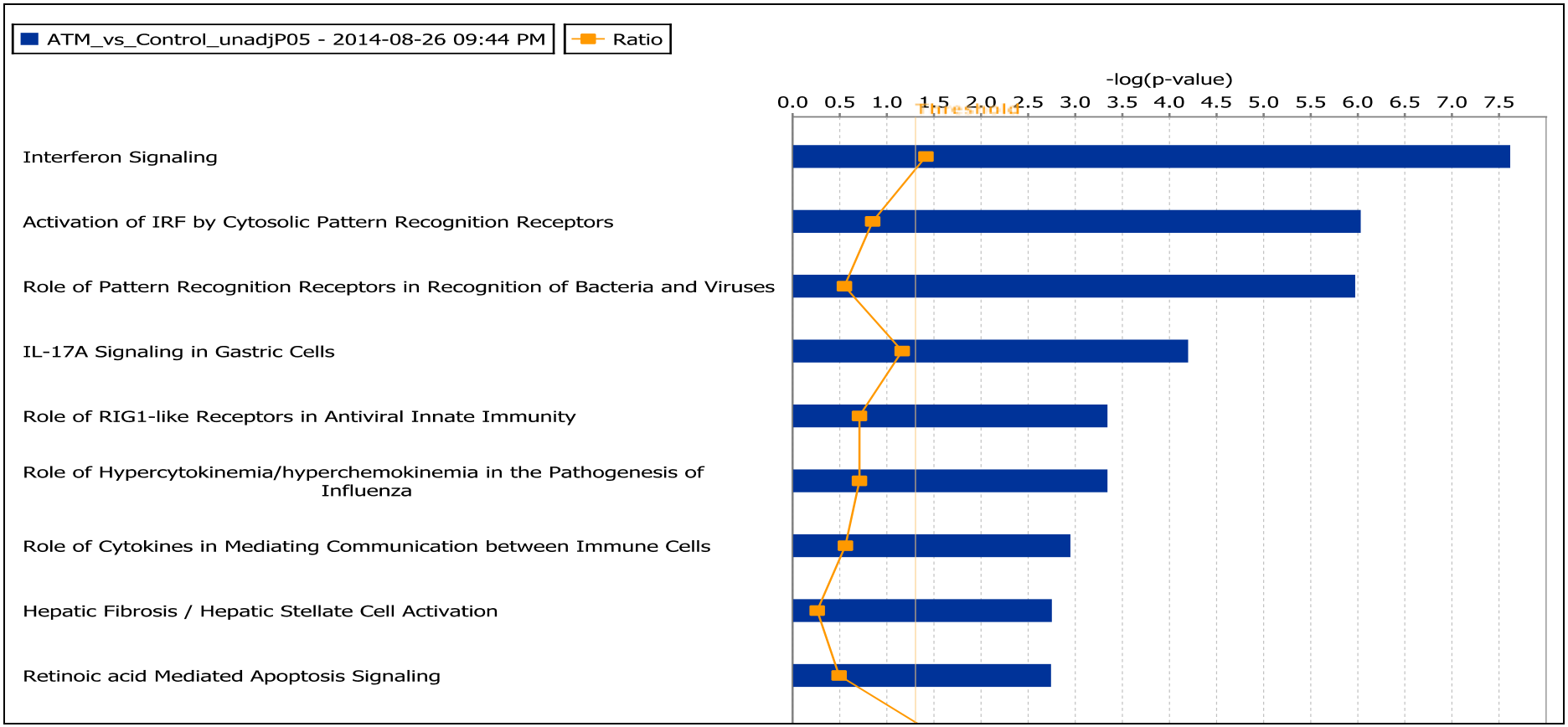

Figure 2. 12. Data to show ranked canonical pathways from Ingenuity network analysis on ATM vs Control AGS treated microarray data set (p<0.05, fc >-1.6, >1.6).
Data plotted shows the top ten ranked pathways in order of significance.

Ingenuity Canonical Pathways	-log(p-value)	Ratio	Molecule
Interferon Signaling	7.62E00	1.94E-01	IFIT3,IFIT1,OAS1,MX1,IFNB1,IFI35,TAP1
Activation of IRF by Cytosolic Pattern Recognition Receptors	6.03E00	1.17E-01	IFIH1,IRF7,IL10,DDX58,IFNB1,IFIT2,ISG15
Role of Pattern Recognition Receptors in Recognition of Bacteria and Viruses	5.97E00	7.56E-02	IFIH1,CXCL8,OAS1,IRF7,OAS2,IL10,DDX58,IFNB1,OAS3
IL-17A Signaling in Gastric Cells	4.2E00	1.6E-01	CXCL10,CXCL8,CXCL11,EGFR
Role of RIG1-like Receptors in Antiviral Innate Immunity	4.2E00	9.76E-02	IFIH1,IRF7,DDX58,IFNB1
Role of Hypercytokinemia/hyperchemokinemia in the Pathogenesis of Influenza	3.34E00	9.76E-02	CXCL10,CXCL8,IFNB1,IFNL1
Role of Cytokines in Mediating Communication between Immune Cells	3.34E00	7.69E-02	CXCL8,IL10,IFNB1,IFNL1
Hepatic Fibrosis / Hepatic Stellate Cell Activation	2.95E00	3.57E-02	CXCL8,COL4A1,IL10,MMP13,TNFSF10,IGFBP5,EGFR
Retinoic acid Mediated Apoptosis Signaling	2.75E00	6.78E-02	IFNB1,TNFSF10,PARP9,PARP14
Pathogenesis of Multiple Sclerosis	2.74E00	2.22E-01	CXCL10,CXCL11

Table 7. Ranked canonical pathways from Ingenuity pathway analysis of ATM vs Control AGS treated microarray data ($p<0.05$, fc >-1.6, >1.6).
Plot shows ranked pathways, significance, ratio and differentially regulated molecules.

Analysis of CAM vs ATM conditioning data showed a distinct difference in gene signatures compared to the other analyses [figure 2.13], with no inflammatory pathways being reported. Differentially regulated pathways identified included MAPK signalling, PPAR- **α** and epithelial adherens junction signalling [table 8].

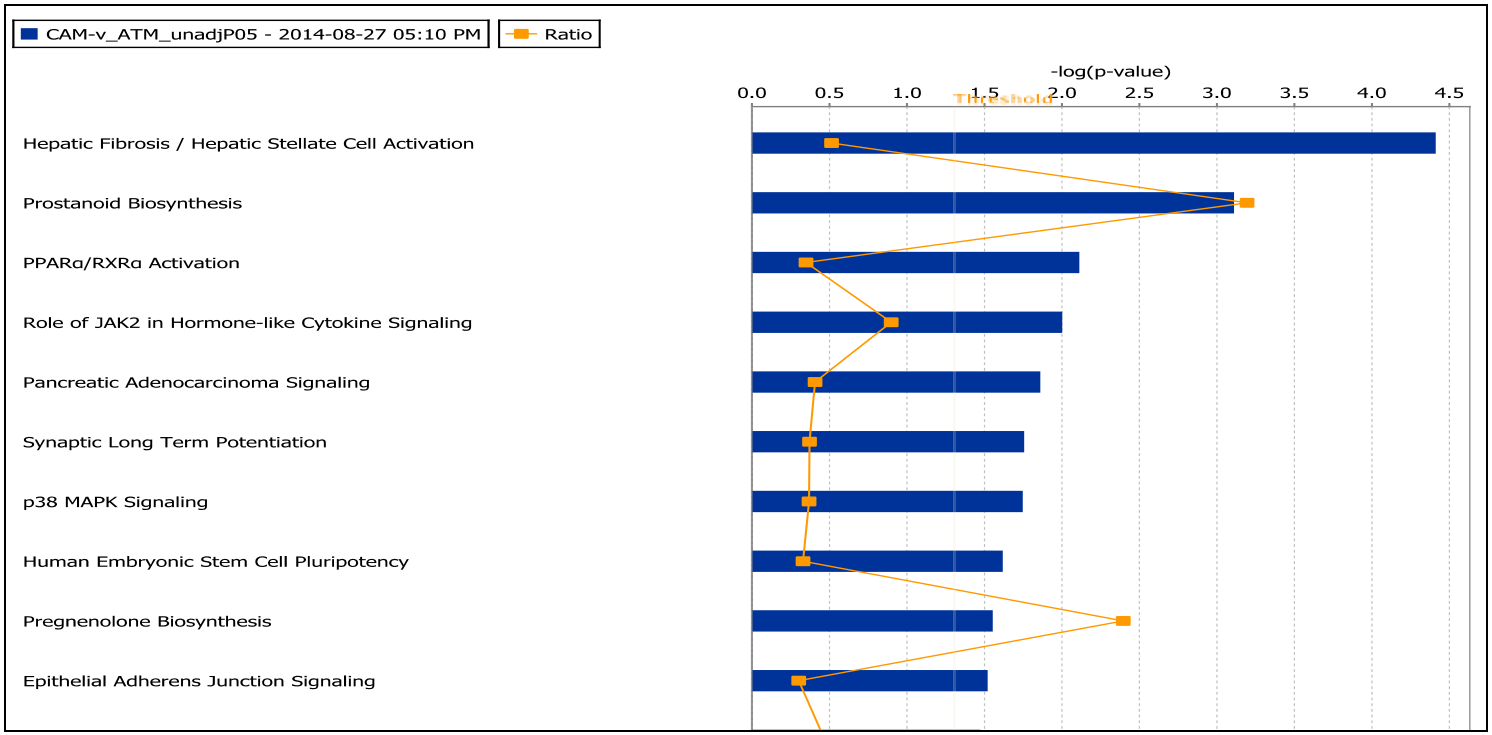

Figure 2. 13. Graph to show ranked canonical pathways from Ingenuity network analysis on CAM vs ATM AGS treated microarray data set (p<0.05, fc >-1.6, >1.6).
Data plotted shows the top ten ranked pathways in order of significance.

Ingenuity Canonical Pathways	-log(p-value)	Ratio	Molecules
Hepatic Fibrosis / Hepatic Stellate Cell Activation	4.41E00	3.57E-02	COL8A2,COL5A2,CYP2E1,HGF,TGFB2,TNFRSF1B,PDGFC
Prostanoid Biosynthesis	3.11E00	2.22E-01	PTGES,PTGDS
PPARα/RXRα Activation	2.11E00	2.42E-02	GHR,TGFB2,BMPR2,ABCA1
Role of JAK2 in Hormone-like Cytokine Signaling	2E00	6.25E-02	GHR,SH2B3
Pancreatic Adenocarcinoma Signaling	1.86E00	2.83E-02	CYP2E1,TGFB2,PDGFC
Synaptic Long Term Potentiation	1.76E00	2.59E-	ITPR3,PPP1R14A,GRIA3
p38 MAPK Signaling	1.75E00	2.56E-02	DUSP1,TGFB2,TNFRSF1B
Human Embryonic Stem Cell Pluripotency	1.62E00	2.29E-02	TGFB2,BMPR2,PDGFC
Pregnenolone Biosynthesis	1.55E00	1.67E-01	CYP2E1
Epithelial Adherens Junction Signaling	1.52E00	2.1E-02	HGF,TGFB2,BMPR2

Table 8. Data to show ranked canonical pathways from Ingenuity network analysis on CAM vs ATM AGS treated microarray data set (p<0.05, fc >-1.6, >1.6).
Data plotted shows the top ten ranked pathways in order of significance.

2.3.4.3 Network Analysis

In order to generate a thorough analysis of the data and generate as many potential interesting targets as possible, network mapping was performed on the data sets. Ingenuity Software suite was used to analyse batch corrected RMA normalized microarray data which passed both p-value and fold change cut-off criteria (<0.5 and 1.6 respectively) for the CAM vs serum free control data set. Ingenuity network reports were generated providing analysis of differentially regulated networks within the dataset that are mapped to specific diseases and functions, ranked according to significance. Networks identified by this analysis may explain gene expression changes, as novel upstream regulators control small hierarchical networks, which do not require all the molecules to have direct connection to the dataset. Scoring criteria provide a means to prioritise the most interesting and relevant trends associated with the phenotype of interest. In this instance, for both CAM and ATM treated AGS gene expression profiles [table 9 and table 10], the inflammatory response was ranked as the most significant network. This result concurs with the raw data analysis, which showed down-regulation of genes corresponding to cytokines and proteins in the interferon pathway. Canonical pathway mapping also using Ingenuity showed significant pathway load of down-regulated genes on inflammation and infectious disease response.

Rank	Top Diseases and Functions
1	Infectious Disease, Antimicrobial Response, Inflammatory Response
2	Antimicrobial Response, Inflammatory Response, Dermatological Diseases and Conditions
3	Infectious Disease, Cell Signalling, Cancer
4	Cell-To-Cell Signalling and Interaction, Cell-mediated Immune Response, Cellular Movement
5	Cell Death and Survival, Cancer, Cellular Development
6	Lipid Metabolism, Small Molecule Biochemistry, Nervous System Development and Function
7	Dermatological Diseases and Conditions, Cancer, Endocrine System Disorders
8	Endocrine System Disorders, Gastrointestinal Disease, Inflammatory Disease
9	Cellular Development, Cellular Growth and Proliferation, Cardiovascular System Development and Function
10	Cell Death and Survival, Cancer, Gastrointestinal Disease
11	Drug Metabolism, Molecular Transport, Lipid Metabolism
12	Infectious Disease, Cell Morphology, Cellular Assembly and Organisation
13	Cell-To-Cell Signalling and Interaction, Cellular Assembly and Organization, Tissue Development

Table 9. Table to show ranked networks from Ingenuity network analysis on CAM vs Control AGS treated microarray data set ($p<0.05$, fc >-1.6, >1.6). Ingenuity network reports of all the differentially regulated networks within the dataset were generated. These were then ranked according to significance with 1 being most significant network and 13 least significant network.

Network analysis in CAM vs control and CAM vs ATM conditioning data set showed multiple networks relating to cancer and cancer progression [table 9 and table 11], which would perhaps be expected. However, it is interesting to note that these networks were not identified in ATM vs control comparisons [table 10]. This suggests that whilst there may be similar signatures in ATM conditioned AGS gene expression profiles, there are significantly more genes relating to carcinogenesis and cancer progression in the CAM conditioned media datasets.

Gastrointestinal disease networks were also pulled out in this analysis, which again may be expected reflecting the origins of these cell lines. Cell to cell signalling and interactions were also identified in the CAM datasets [table 9 and table 11] with the majority of ATM networks being associated with inflammation and the immune response [table 10]. Networks associated with the cell cycle, cell death and survival were also identified. Evasion of cell death and deregulated cell cycle are all hallmarks of cancer and cancer progression, the presence of these networks was identified in all three groups, suggesting that both CAM and ATM conditioning experiments have the ability to induce changes associated with cell-cycle functioning. Networks connected with metabolism, molecular transport and lipid metabolism were also within the top ranking significant functions list for the CAM vs control datasets [table 9]. These networks were not identified in the ATM vs control dataset, suggesting these changes are unique to CAM conditioning.

Rank	Top Diseases and Functions
1	Infectious Disease, Antimicrobial Response, Inflammatory Response
2	Dermatological Diseases and Conditions, Infectious Disease, Cell Cycle
3	Cell Cycle, Cell Death and Survival, Cellular Function and Maintenance
4	Dermatological Diseases and Conditions, Antimicrobial Response, Inflammatory Response
5	Connective Tissue Disorders, Immunological Disease, Inflammatory Disease
6	Infectious Disease, Antimicrobial Response, Inflammatory Response
7	Organismal Injury and Abnormalities, Cellular Development, Cellular Growth and Proliferation
8	Cell Cycle, Connective Tissue Disorders, Developmental Disorder

Table 10. Table to show ranked networks from Ingenuity network analysis on ATM vs Control AGS treated microarray data set ($p<0.05$, fc >-1.6, >1.6). Ingenuity network reports of all the differentially regulated networks within the dataset were generated. These were then ranked according to significance with 1 being most significant network and 8 least significant network.

Rank	Top Diseases and Functions
1	Tissue Morphology, Cellular Growth and Proliferation, Cellular Movement
2	Cancer, Cell Cycle, Cell Death and Survival
3	Protein Synthesis, Cellular Movement, Hematological System Development and Function
4	Cancer, Cell Death and Survival, Cellular Development
5	Cardiovascular Disease, Organismal Injury and Abnormalities, Reproductive System Disease
6	Developmental Disorder, Endocrine System Disorders, Gastrointestinal Disease
7	Cell-To-Cell Signaling and Interaction, Reproductive System Development and Function, Cell Morphology
8	Cellular Assembly and Organization, Cellular Development, Cellular Function and Maintenance
9	Cancer, Cell Death and Survival, Embryonic Development

Table 11. Table to show ranked networks from Ingenuity network analysis on CAM vs ATM AGS treated microarray data set ($p<0.05$, fc >-1.6, >1.6). Ingenuity network reports of all the differentially regulated networks within the dataset were generated. These were then ranked according to significance with 1 being most significant network and 9 least significant network.

2.3.4.4 Transcription Factor Analysis

Comparative microarray gene expression data was further analysed using the Ingenuity™ data analysis software suite, after a fold change cut off of 1.6 and a p-value cut off of <0.5 was applied to batch corrected RMA normalized microarray data for: (1) CAM vs serum free controls, (2) ATM vs serum free controls and (3) CAM vs ATM comparisons. An Ingenuity™ transcription factor reports was generated for each dataset, providing information on differentially regulated transcription factors and 'hub' transcription factors, which controlled multiple differentially regulated genes within each dataset [figure 2.14].

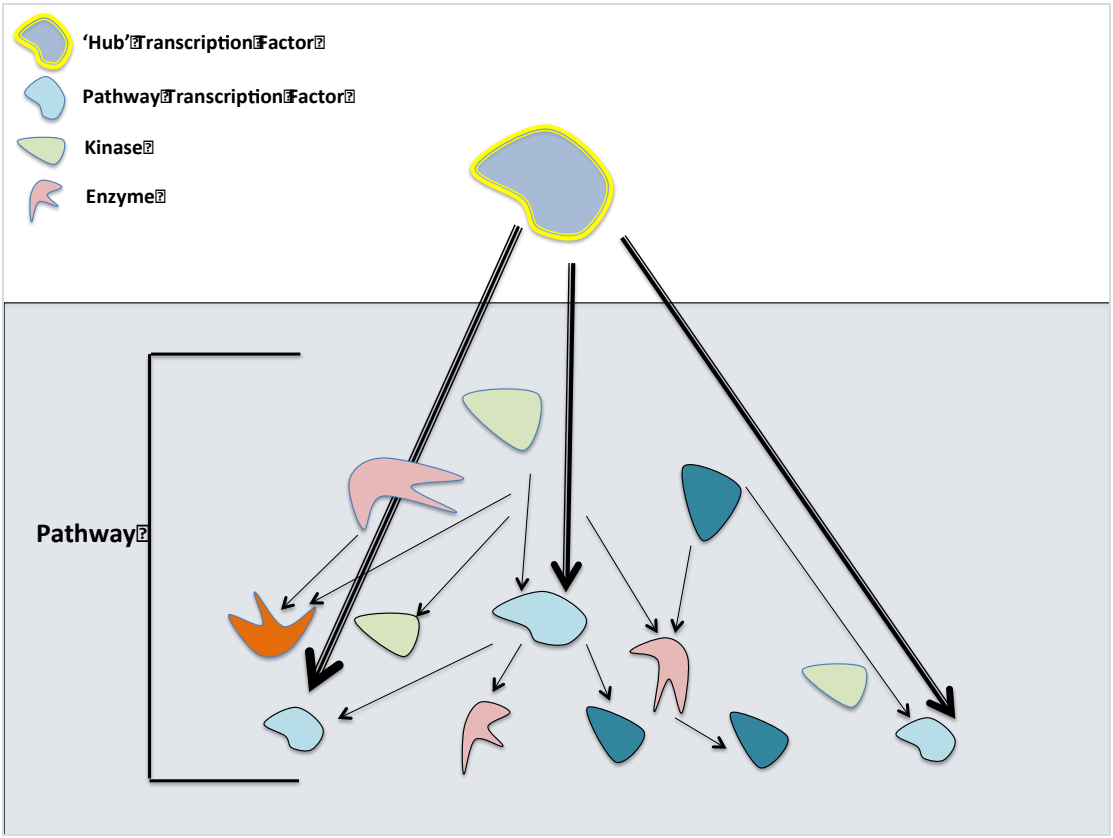

Figure 2. 7. Schematic to show transcriptional regulation in canonical pathways.
'Hub' transcription factors control multiple down-stream effectors, which are differentially regulated in pathways. Pathways also contain modulated transcription factors that are up or down regulated.

CAM vs Control comparison generated data showing transcription factors ATF3, NUPR1 and HDAC8 as being significantly ($p<0.05$) up regulated [figure 2.15]. Activating transcription factor 3 (ATF3) is a member of the ATF/cyclic AMP response element-binding family (Yin *et al.,* 2008) and has been reported to have both pro and anti-tumour effects (Yuan et al 2013 and Yin *et al.,* 2012). Four of the transcription factors identified in the CAM conditioning dataset were also identified in the ATM conditioning dataset [figure 2.16], showing down-regulation of NLRC5 and IRF7 and also up-regulation of HDAC8 and NUPR1. No differentially regulated transcription factors were pulled out from the CAM vs ATM date set analysis due to the stringency of this analysis.

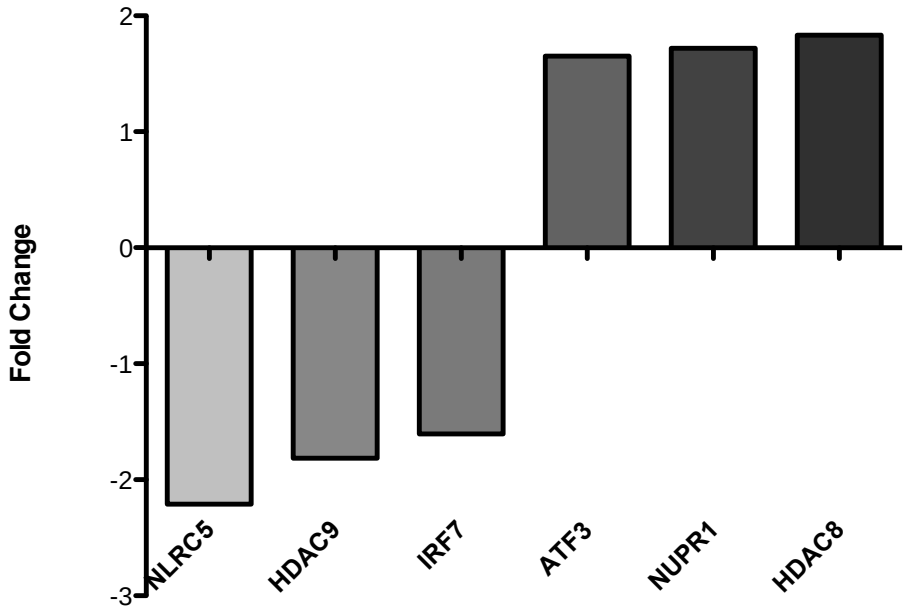

Figure 2.15. CAM induced changes in AGS transcription factor expression profiles.
Six transcription factors involved in cellular processes were found to be differentially regulated from CAM vs Control AGS conditioned gene expression profiles.

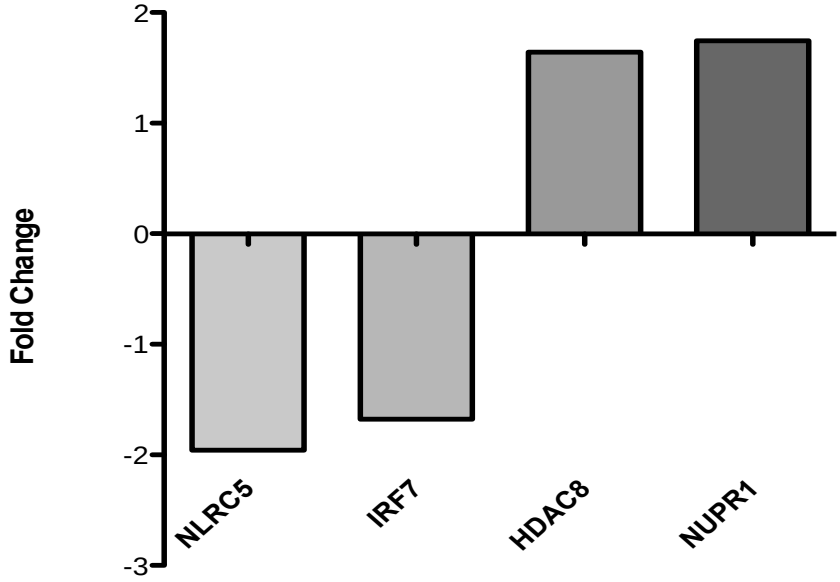

Figure 2.16. ATM induced changes in AGS transcription factor expression profiles.
Six transcription factors identified as differentially regulated from ATM vs Control AGS conditioned gene expression profiles.

Following investigation of differentially regulated transcription factors, upstream analysis was carried out to identify any 'hub' transcription factors which are not themselves changed, but regulate a number of differentially expressed genes [as depicted in figure 2.14]. The outcomes of this analysis produced highly interesting results: firstly, interferon pathway transcription factors were pulled out in both CAM and ATM conditioning studies [table 12 and table 13], a result which concurs with previous pathway and network analysis in this chapter, these include STAT3, STAT2, and IRF3, IRF1 and IRF7. The TP53 (p53) gene was also identified as significant in the CAM conditioning dataset; tumour suppression by p53 occurs by transcription-dependent activities in the nucleus where p53 regulates transcription of cell-cycle related genes, DNA repair, apoptosis, signalling, transcription, and

metabolic genes. (Dai and Gu., 2010). Results suggest down-stream dis-regulation of p53 targets, or even p53 itself, which controls these targets, causing a knock-on effect on cell cycle regulation and evasion of apoptosis. Transcription factor SP1 was also identified as being a controlling transcription factor in the analysis, but only in the CAM vs control dataset, not in the ATM data sets [table 12].

Transcription Factor	p-value
IRF3	1.31E-11
STAT2	2.53E-11
IRF1	7.53E-09
STAT1	3.05E-07
CEBPA	3.59E-05
IRF7	8.32E-05
RELA	8.58E-05
SMARCB1	9.99E-05
SP1	1.21E-04
TP53	1.22E-04

Table 12. Significant 'Hub' transcription factors that control downstream differentially regulated effector genes within CAM vs control AGS conditioned data set.
Transcription factors are ranked according to p-value, generated from total number of downstream effector molecules changed within the dataset.

Transcription Factor	p-value of overlap
CNOT7	4.02E-26
STAT2	5.50E-16
IRF3	9.90E-13
STAT1	9.78E-11
IRF1	2.40E-08
IRF9	2.77E-07
CENPA	4.19E-07
SMARCA4	6.43E-06
IRF7	1.97E-05
FOX03	2.65E-05

Table 13. Significant 'Hub' transcription factors that control downstream differentially regulated effector genes within ATM vs control AGS conditioned data set.
Transcription factors are ranked according to p-value, generated from total number of downstream effector molecules changed within the dataset.

2.3.4.5 Gene Set Enrichment Analysis

The purpose of microarray experiments is to profile and compare the expression of thousands of genes across a number of samples. Ordinarily this involves detailed analysis, restricted to focusing on a smaller number of the most 'interesting' genes. The most common approach to this analysis is usually identifying the genes which are most up or down regulated then choosing a cut off value to shorten of the list to a handful of genes for further investigation, however there are other, more stringent approaches to analysing microarray data. Gene Set Enrichment Analysis (GSEA) is a computational method that determines whether an *a priori* defined set of genes shows statistically significant differences between two phenotypes. In this instance, gene enrichment was carried out on AGS microarray data, which had been generated from AGS cells conditioned with media from CAM, ATM, or control media, it is essentially another, more stringent way of analysing this microarray dataset. GSEA focuses on cumulative changes in the expression of multiple genes as a group, which acts to shift the emphasis from individual genes to groups of genes. By looking at several genes at once, GSEA can identify pathways where several genes each change a small amount, but in a coordinated way, this can help elucidate the complexities of co-regulation.

Gene enrichment analysis was carried out in collaboration with Dr Helen Smith (Manchester University), results generated 27 gene signatures in CAM vs control AGS conditioning data set, 83 signatures in ATM vs control data set and 46 signatures in the CAM vs ATM dataset. Full details of GSEA data reports can be found in the appendix [supplementary file II, figure 2.0.] The

highest-ranking signatures for all data sets are shown below (table 14, table 15 and table 16). Interestingly, the top hits of pathways which were generated using Ingenuity™ were also identified using GSEA, such as immune response, cell cycle control and also metabolic pathways. Indeed, the CAM vs ATM data set included a number of gene signatures relating to metabolic regulation [supplementary file II, 2.0.] suggesting a high amount of gene changes produced by CAM conditioning lead induction in metabolically linked genes and pathways. Identifying similar patterns in differentially regulated signatures using a more stringent analysis technique like GSEA gives more confidence in the results generated by bioinformatics analysis.

NAME	SIZE	ES	NES	NOM p-val	FDR q-val	FWER p-val
REACTOME_REGULATION_OF_ _HIF_BY_OXYGEN	22	0.425	1.650	0	1.000	0.730
REACTOME_LOSS_OF_NLP_FROM_MITOTIC_CENTROSOMES	47	0.455	1.559	0	1.000	0.810
REACTOME_PRE_NOTCH_EXPRESSION_AND_PROCESSING	37	0.344	1.469	0	1.000	0.990
SIG_PIP3_SIGNALING_IN_B_LYMPHOCYTES	34	0.498	1.467	0	1.000	0.990
PID_HIF2PATHWAY	30	0.548	1.445	0	1.000	1.000
PID_BCR_5PATHWAY	64	0.391	1.443	0	1.000	1.000
REACTOME_PPARA_ACTIVATES_GENE_EXPRESSION	84	0.339	1.438	0	1.000	1.000
BIOCARTA_NDKDYNAMIN_PATHWAY	17	0.421	1.421	0	0.969	1.000
PID_HES_HEYPATHWAY	44	0.383	1.405	0	0.941	1.000

Table 14. Table to show ranked networks from Gene Set Enrichment Analysis on CAM vs control AGS treated microarray data set.

NAME	SIZE	ES	NES	NOM p-val	FDR q-val	FWER p-val
BIOCARTA_FAS_PATHWAY	30	0.522	1.741	0	1.000	0.340
TRANSCRIPTION_COUPLED_NER_TC_NER_REPAIR_COMPLEX	28	0.495	1.706	0	0.719	0.490
ST_GRANULE_CELL_SURVIVAL_PATHWAY	26	0.535	1.654	0	1.000	0.670
BIOCARTA_TNFR1_PATHWAY	29	0.390	1.626	0	1.000	0.730
KEGG_GLIOMA	63	0.454	1.616	0	0.961	0.760
BIOCARTA_EGF_PATHWAY	30	0.574	1.579	0	0.820	0.980
PID_P38_MK2PATHWAY	21	0.526	1.572	0	0.636	0.980
REACTOME_SIGNALING_BY_CONSTITUTIVELY_ACTIVE_EGFR	17	0.691	1.564	0	0.640	0.980
BIOCARTA_BCR_PATHWAY	33	0.474	1.539	0	0.749	1.000

Table 15. Table to show ranked networks from Gene Set Enrichment Analysis on ATM vs control AGS treated microarray data set.

NAME	SIZE	ES	NES	NOM p-val	FDR q-val	FWER p-val
BIOCARTA_CTCF_PATHWAY	22	0.530	1.578	0	1	0.78
REACTOME_GLYCOLYSIS	26	0.466	1.565	0	1	0.88
KEGG_VASOPRESSIN_REGULATED_WATER_REABSORPTION	44	0.550	1.562	0	1	0.88
ST_GRANULE_CELL_SURVIVAL_PATHWAY	26	0.421	1.531	0	1	0.92
ST_ERK1_ERK2_MAPK_PATHWAY	31	0.489	1.525	0	1	0.94
PID_PI3KCIPATHWAY	41	0.457	1.520	0	1	0.95
PID_E2F_PATHWAY	65	0.334	1.494	0	1	0.95
KEGG_VALINE_LEUCINE_AND_ISOLEUCINE_DEGRADATION	43	0.628	1.494	0	1	0.95
REACTOME_GLUCONEOGENESIS	30	0.476	1.492	0	1	0.95

Table 16. Table to show ranked networks from Gene Set Enrichment Analysis on CAM vs ATM AGS treated microarray data set.

2.3.4.5 GeneVestigator

GeneVestigator is a software platform that can be used to obtain information and insight into expression profiles of specific genes of interest, including; identifying cancers, diseases or conditions, which overexpress the target gene. The software can also cluster related genes to investigate co-expression

Clustering related genes or multiple genes of interest to look at co-expression and down-stream targets. In this instance a number of analyses were carried out, firstly observing gene expression across the gastric neoplasms database, and secondly analysing metabolic transporter genes of interest to determine expression in gastric cell lines and primary samples [figure 2.17]. A number of genes from the monocarboxylate transporter family (MCTs) were selected to determine expression across AGS gastric cancer cells in various experiments. GeneVestigator analysis showed up – regulation of SLC161 genes (MCT1) and SLC16A3 and A4 as most up-regulated. Further interesting gene signatures in gastric samples established using the GeneVestigator software were also identified [supplementary file II, figures 2.1, 2.2,and 2.3].

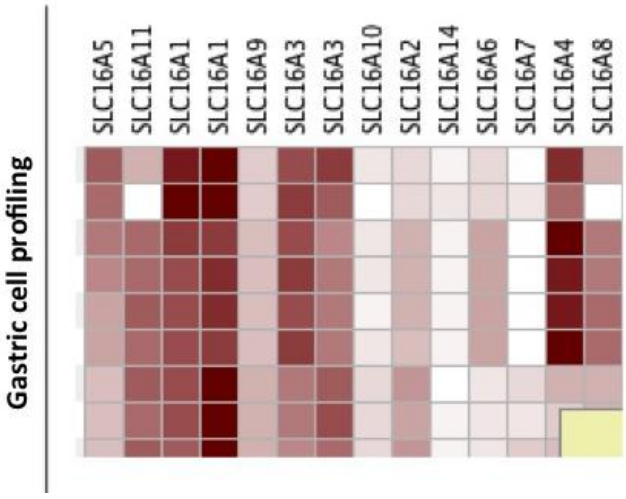

Figure 2. 17. Snapshot of GeneVestigator analysis in Gastric cancer cells. MCT family of small molecule transporters were selected for expression analysis in gastric cell lines.

2.3.5 **Raw Data Analysis Of Single Patient Data**

Whilst grouped analysis is useful for detecting statistical trends within datasets, some signatures or unifying trends can be lost between patients. For example different changes, or different numbers of gene changes within a common pathway may be differentially affected in different patients. Previous analysis of CAM gene expression profiles (Jones *et al.,* unpublished data) revealed distinct patient subgroups, so it was decided that single patient analysis would be performed on the individual CAM datasets to establish any potential differences in patient subgroup on conditioning experiments. Pathway and network analysis were also carried out, as for grouped patient data. In general signatures from these analyses were similar to those obtained from combined group data; with interferon and inflammatory signalling being key pathways down-regulated across patients within the datasets and significant networks relating to cell-cycle, inflammation and gastrointestinal disease being ranked highly [supplementary file II; figure 2.4].

There were some differences in gene expression from AGS conditioned with 294 CAM media (a “good” prognostic CAM) across single patient gene expression data including higher expression of ubiquitin enzymes COQ3 and UQCC3 [table 17].

Patient 305	Fold Change	Patient 308	Fold Change	Patient 192	Fold Change	Patient 294	Fold Change	Patient 190	Fold Change
CEACAM 5	3.764	CEACAM 5	2.578	CEACAM 5	2.57			CEACAM 5	2.75
PRSS1	3.2	PRSS1	2.395	PRSS1	2.44			PRSS1	2.41
PGBD1	2.6	PGBD1	2.458	PGBD1	2.49	PGBD1	3.03	PGBD1	2.66
		METTL10	2.358	METTL10	2.38	METTL10	3.02	METTL10	2.38
MX2	-3.3	MX2	-3.51	MX2	-3.54	MX2	-3.57	MX2	-3.48
PMCH	-2.7	PMCH	-3.398	PMCH	-2.96	PMCH	-3.002	PMCH	-3.01
IFI44L	-3			IFI44L	-2.77			IFI44L	-2.58
RSAD2	-2.7	RSAD2	-2.817					RSAD2	-2.71
				ZNF114	-2.69			ZNF114	-2.58
TFF1	2.9	SPP1	-2.793	IDI	2.2	MIR5188	-3.14		
FOSB	2.7					MMP13	-3.23		
IFIT1	-2.7					HK1	2.75		
						COQ3	2.57		
						UQCC3	2.55		

Table 17. Data to show top hits for up-regulated and down-regulated genes for single patient AGS conditioning data with CAM media. Commonly differentially regulated genes between single patients are in the first part of the table, up-regulated genes are shown in red whilst down- regulated are shown in green. The second half of the table shows patient unique transcription factors

2.3.5.1. Transcription Factor Analysis of Single Patient Data

To establish further trends and potential candidate genes of interest between the datasets, comparative gene expression data was analysed using Ingenuity™ data analysis software, after a fold-change cut-off of 1.6 was applied to batch corrected RMA normalized single-patient CAM vs controls and ATM vs control datasets. Ingenuity™ transcription factor reports were generated for each dataset, providing information relating to 'hub' transcription factors, which controlled multiple differentially regulated genes within each dataset [table 18]. Analysis showed FOS and NLRC5 transcription factors were common across the AGS samples. Data also showed some unique signatures in transcriptional regulation; IRF8 was identified in the 294-conditioning sample, which was from a patient with good survival and prognostic scoring (Varro lab and Jones *et al.,* unpublished data). FOSB was identified in the AGS treated with media from myofibroblast cells from the patients with the worst prognosis and survival scores (305 and 190). Whilst differences in transcriptional profiling may be patient subgroup dependant, microarray profiling of AGS cells conditioned with media from a larger cohort of patient myofibroblasts in order to draw any firm conclusions on patient-specific trends.

Patient 305	Fold Change	Patient 308	Fold Change	Patient 192	Fold Change	Patient 294	Fold Change	Patient 190	Fold Change
FOS	2.332	**FOS**	1.812			**FOS**	1.707	**FOS**	1.94
FOSB	2.776							**FOSB**	1.926
NLRC5	-2.099	**NLRC5**	-2.169	**NLRC5**	-2.329	**NLRC5**	-2.25	**NLRC5**	-2.21
HDAC8	1.757			**HDAC8**	1.657	**HDAC8**	1.875	**HDAC8**	1.715
ATF3	2.007					**IRF8**	-1.77	**IRF7**	-1.606
NUPR1	1.973								

Table 18. Data to show top hits for up-regulated and down-regulated transcription factors for single patient AGS conditioning data with CAM media.
Common transcription factors between single patients are in the first part of the table, up-regulated transcription factors are shown in red whilst down- regulated are shown in green. The second half of the table shows patient unique transcription factors.

2.3.5 Phenotypic Effects of CAM conditioned media on AGS cells

AGS cells were treated with CAM conditioned media from patient myofibroblast cells for 24h before performing EdU proliferation assay. Results showed an increase in AGS cell proliferation upon addition of CAM cell media, compared to the serum free control [figure 2.19 A]. This data was also expressed as an average across the AGS cells treated with conditioned media from a cohort of CAM cell lines [figure 2.19 B]. Results show a statistically significant increase in AGS cell proliferation compared to the serum free control.

A

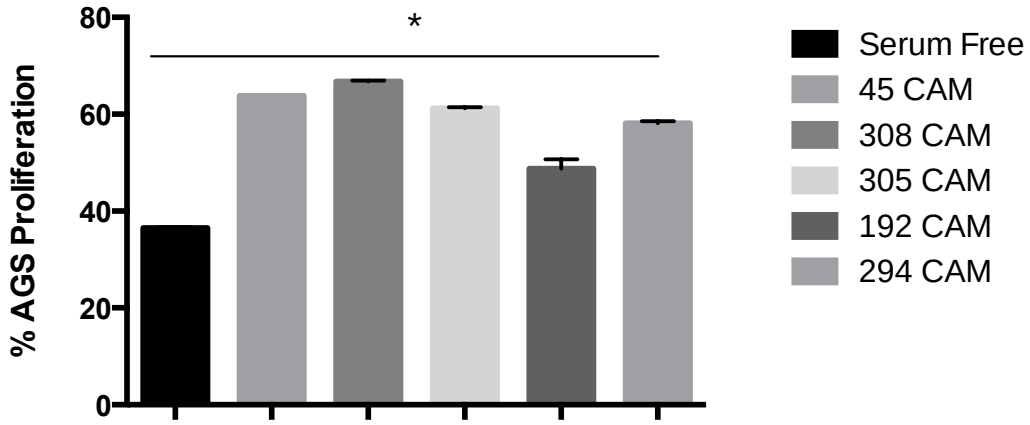

B

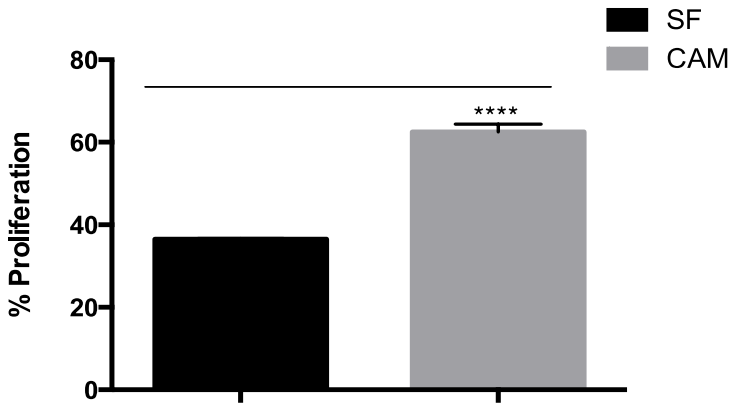

Figure 2. 19. Effects of CAM conditioned media on AGS cell proliferation. AGS cells were conditioned with CAM media for 24h. Results were quantified as percentage of cells stained positive for EDU, out of total cell population, and expressed as either as single patient data [A] or as an average across CAMs [B]. ANOVA analysis of single patient data showed a significant increase (indicated by an asterisk (*) in proliferation of AGS cells upon treatment with CAM media across all cell lines ($p<0.05$). Students T-Test analysis of combined data, also showed statistical significance in AGS cell proliferation of (indicated by an asterisk (*), N=3, error bars represent standard deviation.

To investigate effect on AGS cell migration, AGS cells were seeded in boydon chamber plates together with CAM conditioned media from three representative patient primary myofibroblast cells lines for 24h before performing migration assays. Results showed an increase in AGS cell migration upon addition of CAM cell media, compared to the serum free control [figure 2.20].

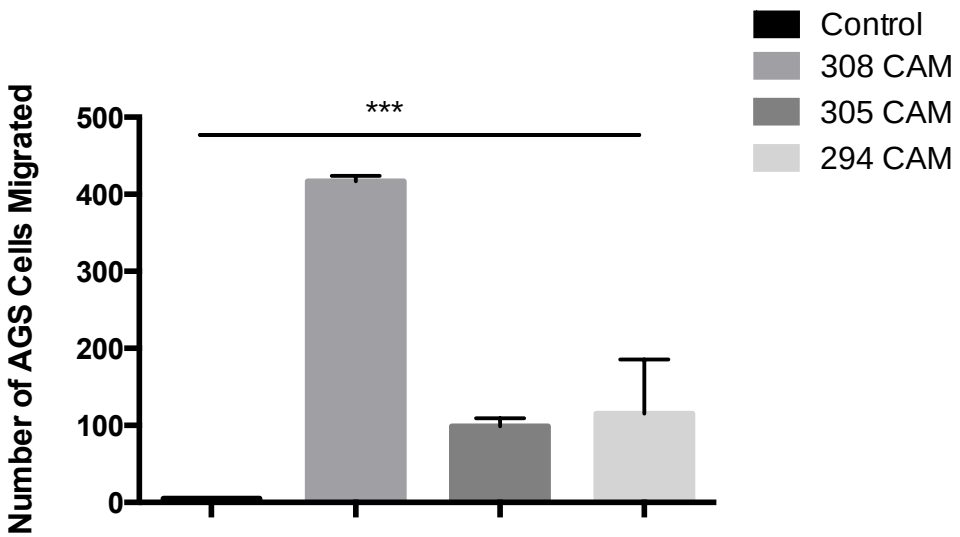

Figure 2. 20. Effects of CAM conditioned media on AGS cell migration.
AGS cells were conditioned with CAM media for 24h. Results are expressed as single patient data. ANOVA analysis of single patient data showed a significant increase (indicated by an asterisk (***) in proliferation of AGS cells upon treatment with CAM media across all cell lines ($p<0.05$), N=3, error bars represent standard deviation.

2.4 Discussion

This purpose of this chapter was to establish any differential effects that CAM-conditioned, ATM-conditioned, or control media have on AGS gene expression profiles. Preliminary analysis confirmed that stocks of primary myofibroblasts used in these studies exhibit previously defined properties, including differential induction of AGS/cancer cell migration and proliferation (Holmberg *et al.,* 2012). In addition, the quality of microarray data was confirmed using standard microarray quality analysis software prior to subsequent data processing and analysis. Trends observed in primary microarray data were also experimentally verified by targeted qPCR studies, thereby confirming the validity of differential gene expression profiles and demonstrating the retention of differential properties in each myofibroblast population. Having established the validity of primary gene expression profiles, bioinformatics tools were then used to further investigate consistent trends in gene expression profiles. This analysis generated interesting trends in metabolic gene signatures and pathways, however trends based on patient subgrouping could not be made due to the small samples size (n=5, with patients from different subgroups). A larger scale microarray study using AGS conditioned with a greater number of myofibroblast patient media would be needed to be carried out to make conclusions about sub-group specific trends.

The purpose of the microarray data analysis was exploratory and hypothesis generating; it was used to establish any trends within the conditioning data set and to look at together with previous microarray analysis (Dr Helen Jones, unpublished data). Initial comparison of gene expression profiles identified interesting trends within grouped patient data. CEACAM5 up regulation has been reported in many cancers and has been shown to be a major target for Smad3-mediated TGF- β signalling (Blumenthal *et al.*, 2007). IGFBP5 has been shown to aid cell survival in low nutrient conditions, which has implications in cancer progression and survival (Akkiprik et al, 2009). The gene CYP1A1 was also identified up regulated in the CAM conditioning dataset. Significantly, this gene is known to be involved in metabolism and causes bioactivation of benzo[a]pyrene, which forms DNA adducts resulting in enhanced levels of mutagenesis (Costa *et al.,* 2010).

In this instance, for both CAM and ATM treated AGS gene expression profiles, the inflammatory and immune response were ranked as the most significant networks. Interferon proteins are part of the cytokine family, involved in numerous functions, including antiviral and antimicrobial response, apoptosis, cell-cycle control and facilitating other cytokines (Slattery *et a*l, 2011). Down-regulation of these proteins may have numerous implications including the cancer cell's ability to evade the immune response and apoptosis. This result concurs with the raw data analysis, which showed down-regulation of genes corresponding to cytokines and proteins in the interferon pathway. Canonical pathway mapping also using Ingenuity,

showed significant pathway load of down-regulated genes on inflammation and infectious disease response.

Results from Ingenuity transcriptional analysis of grouped patient data showed a significant increase of ATF3 in the CAM conditioning dataset, which was not present in ATM vs control conditioning dataset. Transcription factor ATF3 has been reported to have pro-tumour effects, increasing metastatic potential in breast cancer and the inflammatory response (Wolford *et al.,* 2013, Hai *et al* ., 2010). More recently ATF3 has been linked to metabolic regulation and energy metabolism (Lee *et al.,* 2013). Interestingly, other transcription factors associated with metabolic activity in the cell were also identified as up- regulated, SP1 and p53, both 'hub' transcription factors. SP1 is known to regulate a number of genes, but particularly those associated with metabolism, specifically pyruvate kinase and fatty acid synthase (Archer *et al.,* 2011). Dis-regulation of P53 is associated with enabling cells to resist the shift to glycolysis (Cheung *et al.,* 2010). The identification of p53 as a hub transcription factor is interesting, as this acts to regulate transcription of cell-cycle related genes, DNA repair, apoptosis, signalling, transcription, and metabolic genes. In addition, p53 can also induce apoptosis and autophagy in the cytoplasm through transcription independent activities (Dai and Gu., 2010). The presence of p53 in this analysis is interesting taken in context of the cell-cycle networks identified in the previous analysis. Results suggest down-stream dis-regulation of p53 targets, or even p53 itself, which controls these targets, causing a knock-on effect on cell cycle regulation and evasion of apoptosis.

The most interesting and striking data generated from the microarray gene analysis performed in this chapter were the variations seen across a number of metabolic genes and transcription factors associated with metabolic regulation. The metabolic signatures generated from both grouped and single patient CAM data are particularly relevant when considered in the context of previous work (Jones *et al.,* unpublished data) carried out on the myofibroblast cell lines, which were used to provide the conditioned media in this study.

Briefly, differential gene expression profiles of CAMs, ATMs or NTMs were analysed to generate microarray data, which was investigated by several methods including multivariate and correspondence analysis (Jones *et al.,* 2012, unpublished data). These studies allowed differentially affected genes and pathways to be considered at the same time with both corresponding changes being plotted on the 3D graph to generate functionally related clusters. These clusters were then analysed systematically using odds ratios to define not only pathways containing the greatest number of differential gene expression but more importantly, differentially expressed genes that form an intersection between multiple canonical pathways. As such, these genes potentially represent a key subset of differentially expressed genes that have the potential to impose maximal impact on the system, or to confer specific functional or prognostic phenotypes (Jones *et al.,* unpublished data). Overall, these results show that the CAM vs. NTM comparison produced the greatest number of differentially regulated genes relating to fatty acid-β-

oxidation and metabolic pathways. The expression of genes within these pathways were generally found to be significantly up–regulated in CAMs compared to NTMs [table 19].

Gene name	Over-represented pathway	Fold change
SLC2A11	Facilitative Na+-independent glucose transporters	1.75
SLC2A10	Facilitative Na+-independent glucose transporters	1.41
SLC16A3	Bile salt and organic anion SLC transporters	5.43
SLC16A7	Bile salt and organic anion SLC transporters	-1.49
SLC27A1	Transport of fatty acids	1.42

Table 19. Pathways identified in CAM vs NTM myofibroblast analysis.
Over-represented transporter pathways (odds ratios >2) identified within the Reactome database and associated with differentially regulated transporters ($p \leq 0.05$), for the CAM vs. NTM data set. (Jones *et al.,* unpublished data).

Combined analysis of CAM gene-expression profiles and myofibroblast conditioning studies, provides the basis for a proposed model of energy metabolism in gastric cancer [figure 2.26]. Signatures from these collective studies were further investigated to establish if these trends could be functionally validated in available primary myofibroblast cell lines.

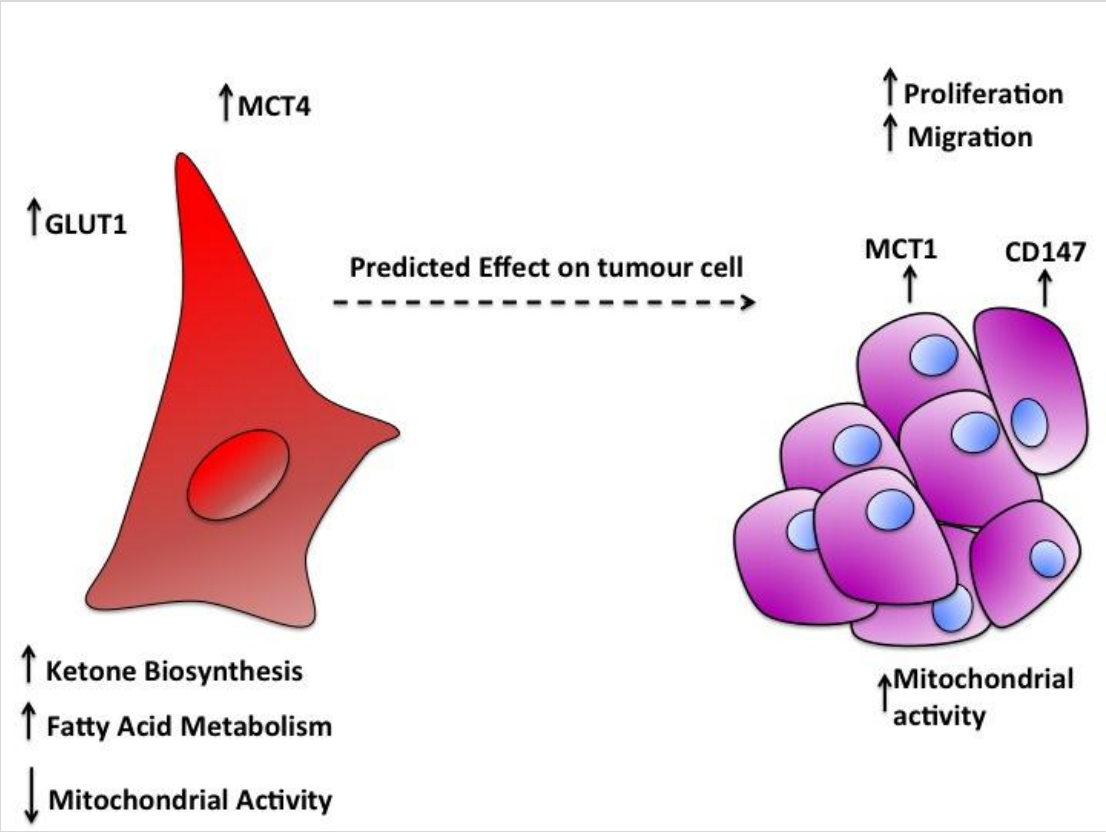

Figure 2. 8. Schematic representing predictive model of paracrine communication between myofibroblast cells and AGS epithelial gastric cancer.
This was based on microarray data analysis of primary gastric myofibroblast cell lines and AGS cancer cells conditioned with CAM media to investigate paracrine signalling.

Chapter Three

Metabolic Reprogramming in the Gastric Cancer Microenvironment

3.0 Introduction

Paracrine communication between cancer cells and the tumour microenvironment has become an area of increasing interest in recent years, with the focus of academia and industry alike looking to target the cells supporting tumour growth, as well as tumour cells alone. The immune response of the tumour microenvironment (Zhou *et al.,* 2014): the role of cytokines (Wilson *et al.,* 2002): and activation of transcription factors (Yu *et al.,* 2007), are all well established areas of therapeutic interest within the tumour-microenvironment's paracrine system, however, little is understood regarding reciprocal communication in the field of cell metabolism and cancer development. Despite this fact, the concept of paracrine communication in relation to cellular metabolism is not entirely a new one; as early as the 1950s, the work of McIlwain showed lactate as an energy substrate for cells in brain tissue. Subsequently, reciprocal communication has been shown between astrocytes and neurone cells, with astrocytes supplying substrates to neurons from their glycogen stores and from glycolysis (Genc *et al.,* 2011, Allaman *et al.,* 2011). The parallels of this relationship can be seen in the 'Reverse Warburg Effect', first postulated by the Lisanti research group (Pavlides *et al.,* 2009). This model shows a metabolic switch of stromal myofibroblasts to a glycolytic phenotype, which acts to support and enhance tumour growth via transport of high-energy metabolic products (Pavlides *et al.,* 2009, Bonuccelli *et al.,* 2010 and Sotgia *et al.,* 2012).

The complexities of energy metabolism in the tumour and its stroma have not yet been presented in a gastric cancer model. The goal of this chapter was to determine the metabolic status of gastric cancer cell lines and primary gastric myofibroblasts, based on the previous microarray data analysis of both myofibroblast and AGS co-cultured experiments, to provide a thorough representation of energy metabolism in the microenvironment of gastric cancer.

3.1 Aims and Hypotheses

This chapter addresses induced metabolic changes that occur in primary human gastric myofibroblasts and AGS gastric cancer cells under co-culture conditions. We aimed to test the hypothesis that CAM and AGS cells have distinct metabolic profiles and to see if co-culture and conditioned media experiments would induce reciprocal metabolic changes in each cell type.

Briefly, the primary aims of the chapter were:

1. To analyse and compare the basal levels of mitochondrial activity in primary gastric myofibroblasts and AGS cells.

2. To determine if CAM and NTM cell-lines retain innate metabolic properties, which are maintained in low passage cultures.

3. To use co-culture and conditioned media experiments to investigate imposed reciprocal changes in each cell type.

3.2 Chapter Specific Materials and Methods.

Full and extensive details of materials and methods used in this chapter can be found in Chapter VI.

3.2.1 XF-Extracellular Flux Analyser

3.2.1.1 Myofibroblast Cells

To investigate the glycolytic capacity and oxygen consumption rate of Myofibroblasts, low passage (P5-P10) primary CAM cell lines (308, 305, 294, 42 and 45) and primary NTM cell lines (334, 196 and 241), were each seeded into 24-well XF seahorse Flux analyser cell dishes, which were pre-treated with Cell-Tak. Cellular glycolytic function and oxygen consumption rate testing was carried out in n=5 replica. Control wells were not treated with any drugs or compounds.

3.2.1.2 AGS Cancer Cells

To determine the range of metabolic changes imposed in AGS gastric cancer cells following exposure to CAM conditioned media; AGS cells were seeded at a density of 80,000 cells/well, in n=5 replica format in Cell-Tak treated 24 well XF Seahorse Flux analyser cell dishes. Adherent cells were cultured for 24 hours in full media before being washed three times in DPBS. Cells were then cultured overnight in CAM 308, or CAM 294 conditioned media or in serum free control media. In each case, the cellular glycolytic capacity and oxygen consumption rate were recorded.

3.2.2 Mitotracker® Staining

Low passage (P5-P10) CAM and NTM cell lines and AGS cells were cultured to ≈ 80% confluence prior to performing assays and Mitotracker® staining was carried out. For each assay twenty images were taken using a 63X oil objective on a Ziess multiphoton 2 confocal microscope. Whole cell image intensity levels were quantified using ImageJ software. Results were analysed as both single patient/cell-line specific data and as combined CAMs vs NTMs comparisons.

3.2.3 Immunofluorescence for GLUT1 Transporter Channel

Low passage (P5-P10) CAM and NTM cell lines between were grown on glass coverslips in DMEM full-media for 24 hours to achieve ≈ 80% cell confluence. Cells were processed for immunofluorescence as previously described and stained with GLUT1 antibody.

3.2.4 Real Time PCR for CAM Conditioning Experiments

AGS cells grown to 60-70 % confluence in 10cm dishes were washed three times in PBS before adding 10ml of conditioned media from CAMs (190, 192, 305, 308 or 294) or NTM 334. After a 24h incubation cells were prepared for RNA extraction.

3.2.5 Western Blotting for CAM, NTM and AGS Conditioning Experiments

CAM cell lines 308 and 294, and NTM cell line 334 (P5-P10) were grown to 80% confluence. In each case cells were harvested and processed for western blotting as previously described. Membranes were probed for MCT4 and tubulin for loading. AGS cell lines were split and grown until 80% confluent before being treated for 24 hours with CAM or NTM conditioned media. Cells were harvested and processed for western blotting. Membranes were incubated with MCT1, CD147 and tubulin antibodies.

3.3 Results

3.3.1 Comparison of mitochondrial activity in CAMs, NTMs and AGS gastric cancer cells

It is well established that cancer cells modify their metabolic pathways in order to provide sufficient energy to drive enhanced cell proliferation, invasion into surrounding tissue and migration (Yi *et al.,* 2012, Bonuccelli *et al.,* 2010 and Schulz *et al.,* 2006). Warburg first proposed the hypothesis that cancer cells undergo a change in mitochondrial function, such that they become more dependent on glycolysis, than mitochondrial respiration to generate ATP (Warburg, 1956). Since the proposal of this hypothesis there have been many publications supporting the concept that tumour cells have altered mechanisms of ATP production (Christofk *et al.,* 2008, Harjes *et al.,* 2012 and Heiden, 2012). However, more recently the role of the tumour microenvironment has been re-evaluated in relation to paracrine communication between tumour cells and cells within the adjacent stroma, or tissue. This concept of reciprocal paracrine communication within the tumour microenvironment is a complex issue, which remains poorly characterised for many forms of tumour. Several issues currently limit a full understanding of the molecular processes that drive, or facilitate, metabolic balance within the microenvironment of gastric tumours. Different metabolic states may operate at different stages of tumour development and at different sites within a tumour; depending on local levels of acidity, hypoxia, inflammation and nutrient availability. Therefore, to provide improved insight into this process, it is important to first define the inherent metabolic properties of both gastric cancer cells and gastric stromal myofibroblasts. Armed with this information it is then possible to define changes imposed on

each cell type as a result of paracrine communication under different conditions. To address these questions, experiments were designed to define basal and imposed metabolic activity in gastric cancer cells and primary gastric myofibroblast cell lines.

The Seahorse XF Flux analyser provides a gold standard method for measuring cellular respiratory metabolism, In brief; mitochondrial function (oxygen consumption rate or: 'OCR' levels) is determined by measuring the level of dissolved oxygen in the seahorse cell media (minimal media without serum or glucose). The Seahorse also measures extracellular acidification rates ('ECAR'), produced by levels of secreted protons, which are indicative of levels of cellular glycolytic capacity. While these measurements are being taken, three substrates are sequentially injected into the cell media: (1) glucose to act as a substrate for glycolysis, (2) oligomycin to inhibit ATP synthase and (3) 2-deoxyglucose (2DG), to inhibit glycolysis. Due to the inherent complexity of these assays a representative selection of available CAMs and NTMs were selected for detailed analysis, in order to assess the validity of preliminary semi-qualitative live-cell Mitotracker analysis performed in conjunction with these experiments. Seahorse data was derived from AGS cells or primary CAM cell lines that are representative of sub-groups of CAMs isolated from patients with either early or late-stage tumours; each of which was compared to a representative gastric NTM cell line. The oxygen consumption rate of AGS cells, CAMs and NTMs was measured and recorded [Figure 3.1]. Results showed an overall increase in the rate of oxygen consumption in AGS cells compared to all selected CAM or

NTM cell-lines. Inhibition of ATP synthesis by oligomycin A, significantly reduces electron flow through the electron transport chain, therefore cells dependent on mitochondrial respiration, rather than glycolysis, will be more dramatically affected by addition of this drug. This can been seen in figure 3.1, where upon injection of oligomycin there is a significant drop in OCR reading in AGS cells, compared to that observed in either CAM or NTM cells.

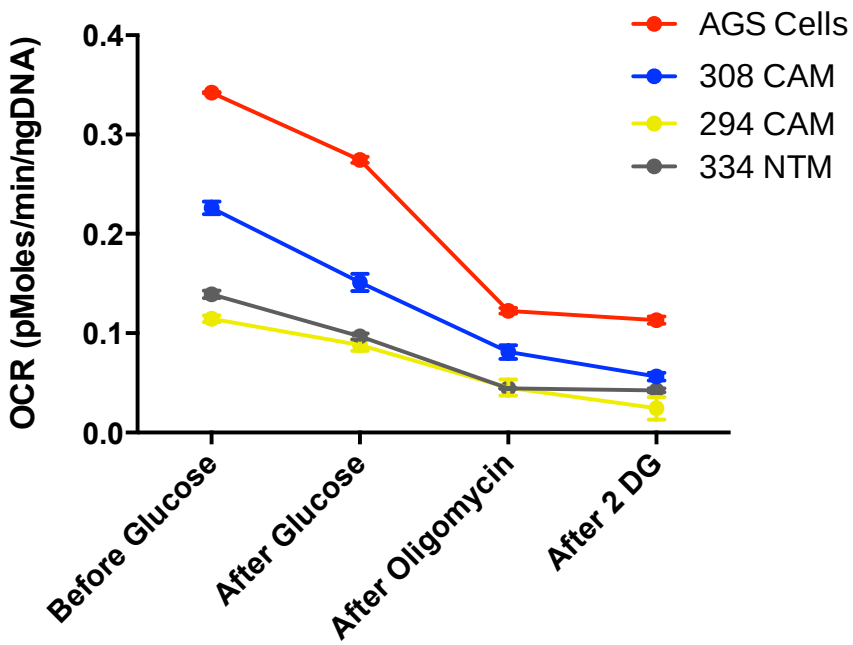

Figure 3. 1. Oxygen Consumption Rate of AGS, CAM and NTM cells.
The extracellular acidification rate and oxygen consumption rate of AGS (red) CAMs 308 (blue) CAM 294 (yellow) and NTM 334 (grey) cells was recorded using the seahorse XF flux analyser. n=5, error bars represent standard deviation. Data was normalised to DNA concentration.

Mitotracker® mitochondrial dye was used to further confirm the results from the Seahorse, utilising the same myofibroblast cell lines as in the Seahorse, and keeping the cell passage numbers consistent in both experiments. Results showed a statistically significant (students t-test, $p<0.0001$) increase in Mitotracker® staining in AGS cells compared to CAMs 308 and CAM 294 and NTM 334 [figure 3.2].

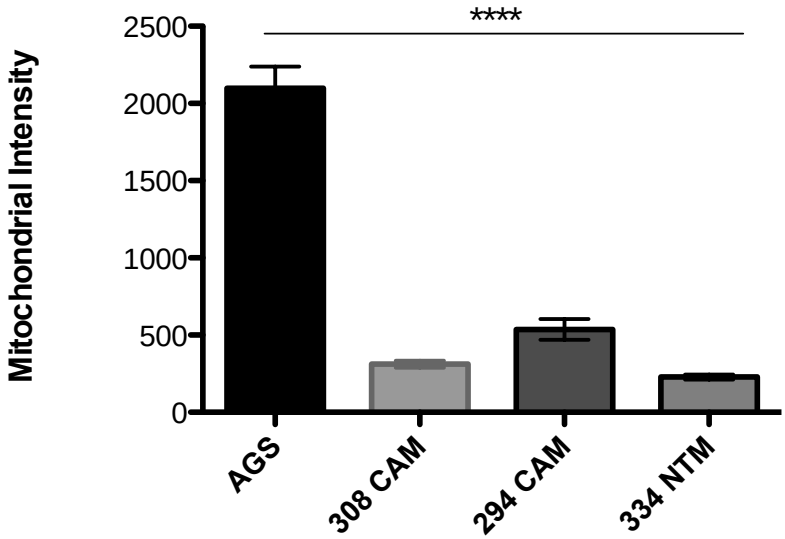

Figure 3. 2. Mitochondrial intensity of AGS, CAM and NTM cells.
Mitotracker Red CM Ros stain was incubated with cells, prior to live-cell imaging. The relative intensity of mitochondrial staining was measured (n=20) as a semi qualitative measure of mitochondrial activity using ImageJ intensity quantification of pixels function. ANOVA analysis of data showed AGS cells had a significant ($p<0.001$) increase (indicated by asterisks (****) in mitochondrial stain compared to CAM or NTM cell-lines (n=3).

Mitochondrial activity was also measured using Mitotracker® stain across an additional panel of three CAM and three NTM cell lines to further investigate trends seen in cell lines chosen for use in seahorse studies. Image analysis of mitochondrial staining [figure 3.3A] showed a consistent reduction in mitochondrial activity across eight CAM and NTM cell lines compared to levels observed in AGS cells [figure 3.3B]. Due to the intense fluorescent signal detected from the AGS cells it was difficult to discern comparatively subtle differences in mitochondrial staining between myofibroblast subsets. Therefore, a further set of independent experiments were performed to examine the innate properties of these myofibroblasts using more sensitive settings on the multiphoton 2 microscope, which will be described later in this chapter.

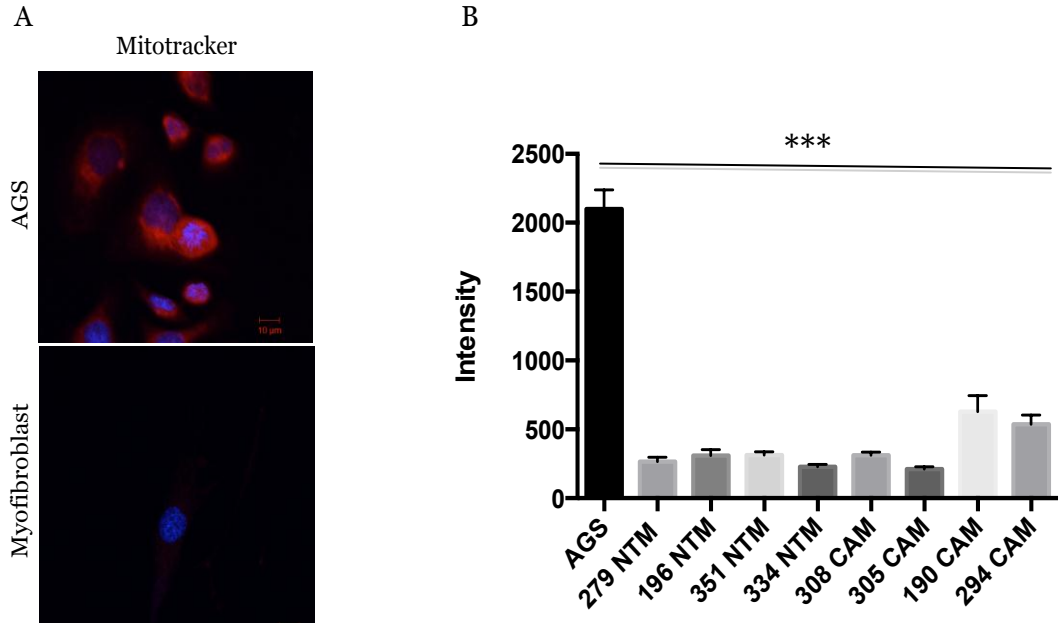

Figure 3. 3. Mitochondrial intensity of AGS cells and a panel of primary NTM and CAM cell-lines.
Mitotracker Red CM Ros stain was added to AGS, CAM and NTM cells before live-cell imaging. Mitochondrial intensity was measured (n=20) using ImageJ, intensity quantification of pixels function. A one-way ANOVA was performed to determine significance between cell lines. AGS cells showed a statically significant increase in mitochondrial stain compared to all CAM or NTM cells tested ($p<0.001$, indicated by an asterisk (***)).

3.3.2 Regulation of Transporter Channels in CAM and NTM Primary Cell Lines

A series of reciprocal conditioning experiments was performed to investigate the effects of paracrine communication between AGS cells and myofibroblasts, as described previously [results chapter one], microarray studies were carried out to establish the effects that CAM conditioned media have on global gene expression profiles in gastric AGS cancer cells. Following normalisation and batch correction, lists of genes showing significant imposed changes in expression were used to perform gene and pathway enrichment studies to provide new insight into the spectrum of functional changes resulting from paracrine communication between gastric cancer cells and associated stromal CAMs. Selected targets were chosen from this analysis for validation and further analysis.

As discussed previously, microarray analysis of primary CAM cell-lines showed an up regulation of various transporter channels involved in cellular metabolic pathways compared to control primary NTM cell-lines (Jones *et al.,* unpublished data). It has also been reported in the literature that glucose transporter one (GLUT1) is up regulated in cells and cell-lines that predominantly rely on glycolysis, rather than mitochondrial respiration (Young *et al*; 2011, Liu *et al*; 2012). The primary CAM, ATM and NTM raw data was re-analysed as single patient data. This was done using mas5 normalisation, then R computer programming to calculate average probe expression for each gene, to establish patient based trends. GLUT1 was selected for further investigation, as it was identified as being a target of

interest by previous work carried out in the lab (Jones *et al.,* unpublished data). Interestingly, this was one of the differentially regulated genes identified in the analysis of single patient gene expression profiles performed in this study [Figure 3.4].

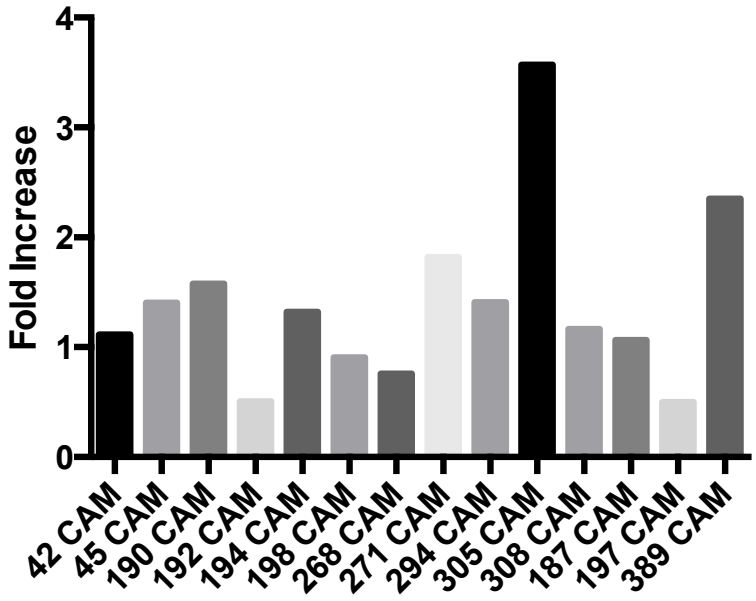

Figure 3. 4. Relative GLUT1 gene expression levels in 14 gastric CAM cell-lines.
Microarray gene expression profiling was carried out across a panel of 14 primary gastric CAM cell-lines. In each case expression levels were normalised to average levels of GLUT1 expression detected across a panel of primary gastric NTM cell-lines.

A panel of CAMs and NTMs was selected to assess relative levels of GLUT1 expression in tumour or normal tissue derived myofibroblasts. CAM cell-lines 305, 308 and 294 and NTM cell lines 334, 241 and 196 were fixed and stained for GLUT1. Relative staining intensity was then quantified using ImageJ software (n=20 for each cell line). Variance analysis of this data showed a statistically significant difference between levels of GLUT1 expression observed in CAM and NTM cell-lines [figure 3.5A]. A Tukey's multiple comparisons test was also carried out [figure 3.5B] to examine the differences between means of intensity for a selection of patient myofibroblasts. However, results from this analysis showed no significant difference (with the exception of CAM 308) between the means observed for each CAM cell-line. Equally, no difference was observed between the mean values of the three NTM cell lines (NTM 196, NTM 334 and NTM 241). There was however, statistical significance ($p<0.05$) between the means of all CAM and NTM cell-lines studied [figure 3.5B]. Immunofluorescence images show distinct differences in GLUT1 staining between CAM and NTM cell-lines [Figure 3.5C]. Finally, when the average single-patient intensity values for both CAMs and NTMs was combined (n=3) and a t-test carried out between the two groups, a statistically significant difference ($p<0.05$) in GLUT1 stain was observed between the two groups, [Figure 3.5D].

A

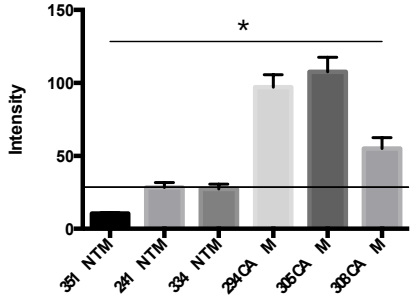

B

Tukey's multiple comparisons test	Mean Diff.	95% CI of diff.	Significant?	Summary
351 NTM vs. 241 NTM	-17.83	-44.15 to 8.485	No	ns
351 NTM vs. 334 NTM	-16.79	-43.11 to 9.523	No	ns
351 NTM vs. 294 CAM	-86.58	-112.9 to -60.27	Yes	****
351 NTM vs. 305 CAM	-97.02	-123.3 to -70.71	Yes	****
351 NTM vs. 308 CAM	-44.57	-70.89 to -18.26	Yes	****
241 NTM vs. 334 NTM	1.039	-25.28 to 27.35	No	ns
241 NTM vs. 294 CAM	-68.75	-95.07 to -42.44	Yes	****
241 NTM vs. 305 CAM	-79.19	-105.5 to -52.87	Yes	****
241 NTM vs. 308 CAM	-26.74	-53.06 to -0.4237	Yes	*
334 NTM vs. 294 CAM	-69.79	-96.11 to -43.47	Yes	****
334 NTM vs. 305 CAM	-80.23	-106.5 to -53.91	Yes	****
334 NTM vs. 308 CAM	-27.78	-54.09 to -1.462	Yes	*
294 CAM vs. 305 CAM	-10.44	-36.75 to 15.88	No	ns
294 CAM vs. 308 CAM	42.01	15.70 to 68.33	Yes	***
305 CAM vs. 308 CAM	52.45	26.13 to 78.77	Yes	****

C

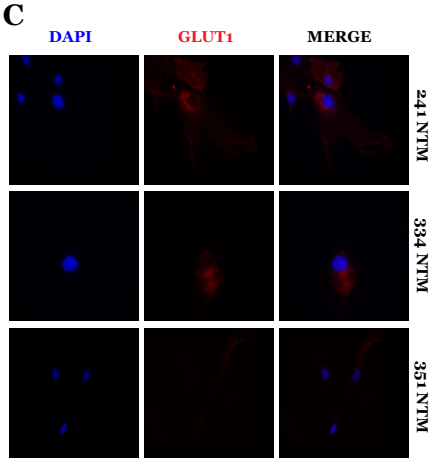

D

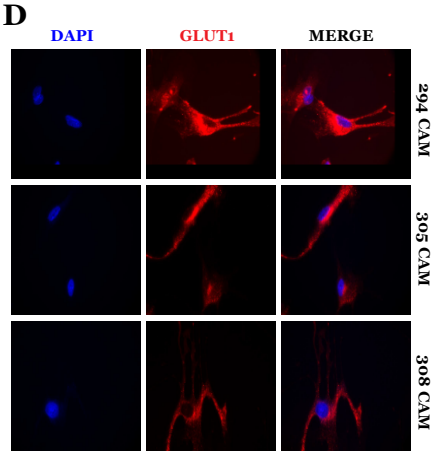

E

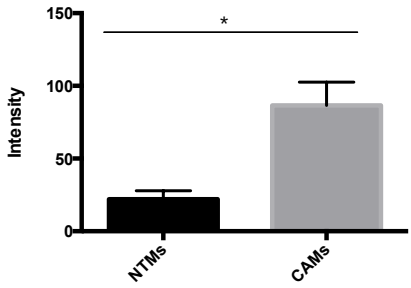

Figure 3. 5. GLUT1 expression in CAMs and NTMs.
Cells were fixed and stained with Rb anti-GLUT1. Relative levels of GLUT1 expression were assessed by measuring fluorescence intensity across a representative selection of myofibroblasts (n=20) using ImageJ intensity quantification of pixels function. Results are shown for individual patients. A one-way ANOVA ($p<0.05$, indicated by an asterisk (*)) (A) and a Tukey's Multiple Comparison Test (B) were performed to establish statistical significance of observed differences in GLUT1 expression. Representative images of GLUT1 expression in NTMs and CAMs are shown in panels (C) and (D) respectively. The students t-test was also performed on average expression values across NTMs and CAMs, showing a statistically significant difference in GLUT1 stain between the two groups ($p<0.05$, indicated by an asterisk (*)).

Monocarboxylate transporter 4 (MCT4) was also identified to be up-regulated across CAMs, following analysis of single-patient gene-expression data [Figure 3.6]. This trend was also identified in a previous correspondence analysis of CAM specific gene expression profiles (Jones *et al.,* unpublished data). Studies in breast and prostate cancer have also identified MCT4 as an important indicator of metabolic status (Bonuccelli *et al.,* 2010, Sotgia *et al.,* 2012). Therefore, MCT4 was selected as a potential marker of altered metabolic status.

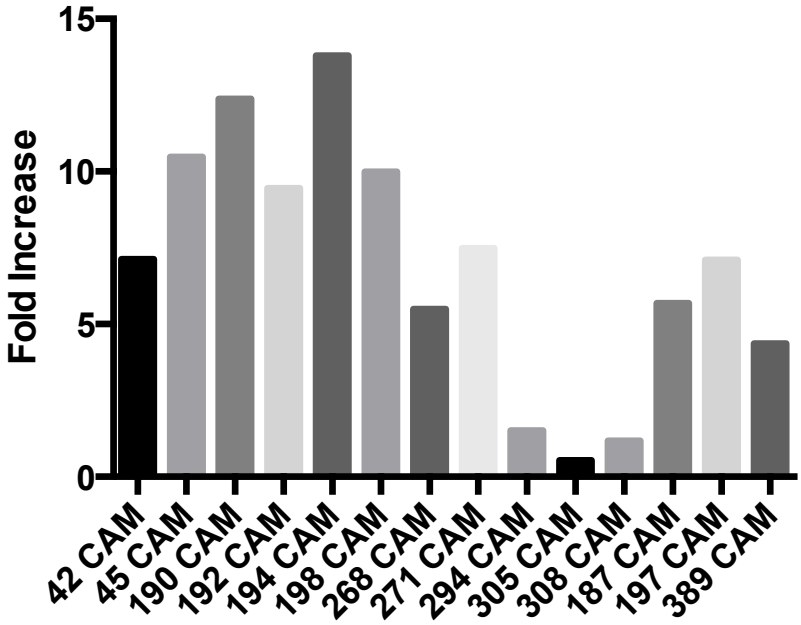

Figure 3. 6. Relative MCT4 gene expression levels in 14 gastric CAM cell-lines.
Microarray gene expression profiling was carried out across a panel of 14 primary gastric CAM cell-lines. In each case expression levels were normalised to average levels of MCT4 expression detected in a panel of 8 primary gastric NTM cell-lines.

Relative levels of MCT4 protein expression were analysed in a selection of primary CAM and NTM cell lines by semi-quantitative western blotting [Figure 3.7A]. These cell-lines were selected for this study as they represent primary CAMs derived from the site of both early and late stage tumours. In addition, they were also the cell-lines used in previous AGS conditioning microarray studies that have been discussed in results chapter one.

Results from western blot analysis show a clear increase in expression of MCT4 in CAM 308 and CAM 294 cells compared to control NTM 334 cells. In this analysis protein levels were quantified using ImageJ and normalised to the tubulin loading control [figure 3.7B].

A

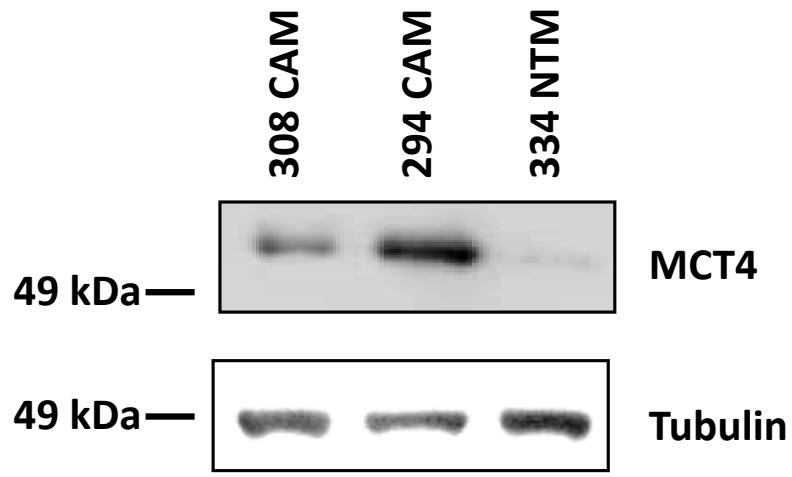

B

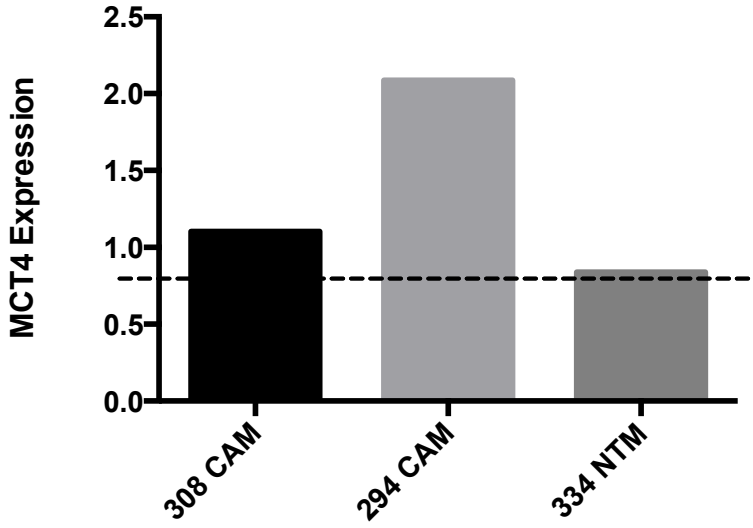

Figure 3. 7. Relative levels of MCT4 expression in CAM and NTM cells.
Western blots were performed on equivalent samples of whole cell lysates prepared from CAM or NTM cell-lines. Blots were probed with mouse monoclonal anti-MCT4 to assess levels of MCT4 protein in each cell line (A). Intensity values were quantified using Image J intensity quantification of pixels function and normalised to corresponding levels of tubulin detected in each sample (B).

3.3.3 Analysis of changes in transporter channel expression in AGS cells following exposure to CAM conditioned media

Monocarboxylate transporter channel one (MCT1) was selected as a candidate for further investigation. Analysis from the CAM microarray data set (Jones *et al.,* unpublished data) identified this as a potential gene of interest, predicted by reciprocal patterns in gene changes such as MCT4 and ketone biosynthesis. MCT1 has also been identified in numerous published studies (Le Floch et al 2011, Zhao et al 2014) whereby it has been established as a marker indicative of altered metabolic status. This has also been reported in other solid-tumours, including breast (Whitaker-Menezes et al 2011), and prostate cancer (Sanità et al 2014) therefore determining the MCT1 status of AGS gastric cancer cell lines was important for the purposes of this study. CD147 is a glycoprotein which exists on the plasma membrane; it contains a single transmembrane domain and also two immunoglobulin-like domains (Kirk *et al.,* 2000). It known to form a complex with MCT1 and is reported to be responsible to the localisation and regulation of MCT1 with the cell, therefore CD147 was also selected for analysis by western blotting in these experiments.
Firstly qPCR analysis was carried out after 24h conditioning of AGS cells with CAM conditioned media, results were normalised to beta-actin and expressed relative to control media. Results showed statistically significant increase (students t-test, $p<0.001$) of MCT1 transporter channel in AGS cells following incubation with CAM media, compared to control media [figure 3.8].

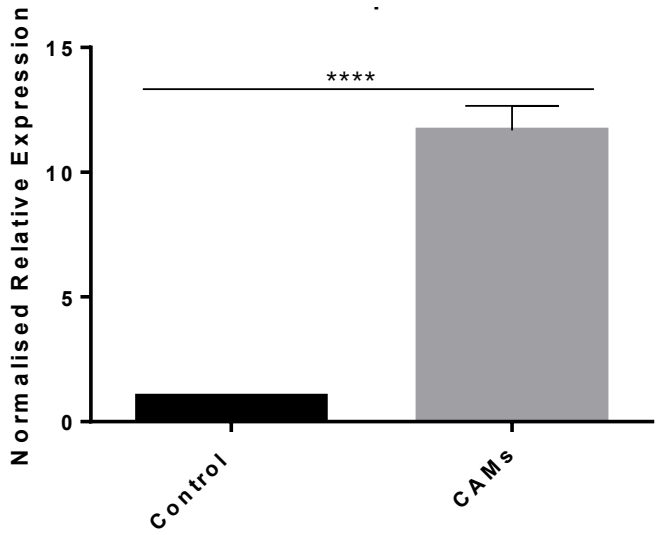

Figure 3. 8. Relative changes in levels of MCT1 gene expression following exposure to of AGS cells to CAM conditioned media.
Relative levels of MCT1 expression were quantified by qPCR following exposure of AGS cells to either serum free or CAM conditioned media for 24 hours. In each case expression levels were normalised to both beta actin and serum free expression levels. Students t-test showed significance ($p<0.001$, indicated by asterisk (****)) between control and CAM MCT1 gene expression.

After preliminary qPCR was performed to investigate regulation at mRNA level, further analysis was carried out using western blotting to determine the protein levels of MCT1 and CD147 following conditioning with CAM media. 24h conditioning of AGS cells with media from CAM 308 and 294 showed an increase in CD147 and also MCT1 expression [figure 3.9]. MCT1 expression was already detected at a protein level in AGS cells which would be expected, as this suggests the AGS cells already have high levels of mitochondrial function; however CD147 was clearly up regulated in CAM conditioned media.

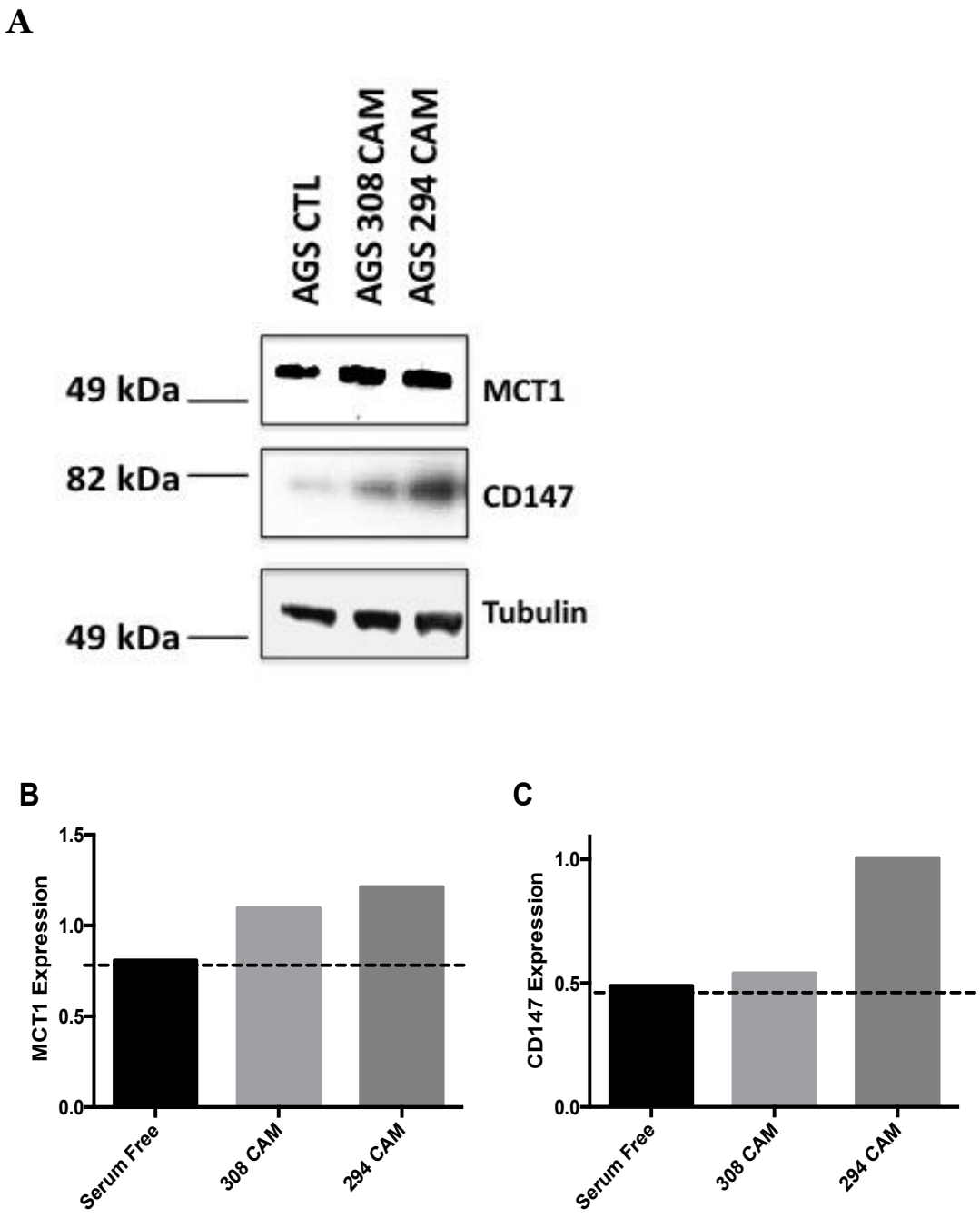

Figure 3. 9. Relative induction of MCT1 protein expression levels in AGS cells following exposure to CAM conditioned media.
AGS cells were incubated for 24 hours with conditioned media from either CAM-308 and CAM-294 or serum free media (CTL). Western blots of whole cell lysates were probed with mouse monoclonal anti-MCT1 and rabbit polyclonal anti-CD147 antibodies and mouse monoclonal ant-tubulin as a loading control (A). Relative levels of protein expression were measured by ImageJ using the intensity quantification of pixels function, and values for MCT1 expression were normalised to respective levels of tubulin expression, panels (B) and (C) respectively.

3.3.4 Analysis of glycolytic capacity and oxygen consumption in AGS cells following exposure to CAM conditioned media

Results presented in this chapter show for the first time that isolated gastric primary CAM cell lines, retain inherently modified metabolic signatures, however the effect that CAM conditioned media may have on the metabolic status of gastric AGS cancer cells has not yet been established. To investigate this question, two primary gastric CAM cell-lines were selected to generate CAM-conditioned media. Again CAMs used in these studies were selected to correspond with available microarray data, and secondly to investigate any potential variability that may exist between CAMs derived from earlier or later stage tumours. In this analysis, AGS cells were treated with conditioned media for 24h before the Seahorse XF analyser was used to generate a metabolic profile of treated AGS cells. Control conditions for these experiments were designed to directly match control conditioned used in the preparation of samples for microarray gene expression profiling (Varro lab). Interestingly, data showed that following 24 hours incubation with media from CAM 308, AGS cells show an overall increase in ATP production. Most importantly, CAM 308 conditioned media imposed a significant increase in oxygen consumption rate, indicating a clear potential for CAM induced changes in AGS cell metabolism, potentially effecting levels of both glycolysis [supplementary file 3; figure 3.1] and mitochondrial respiration [figure 3.10].

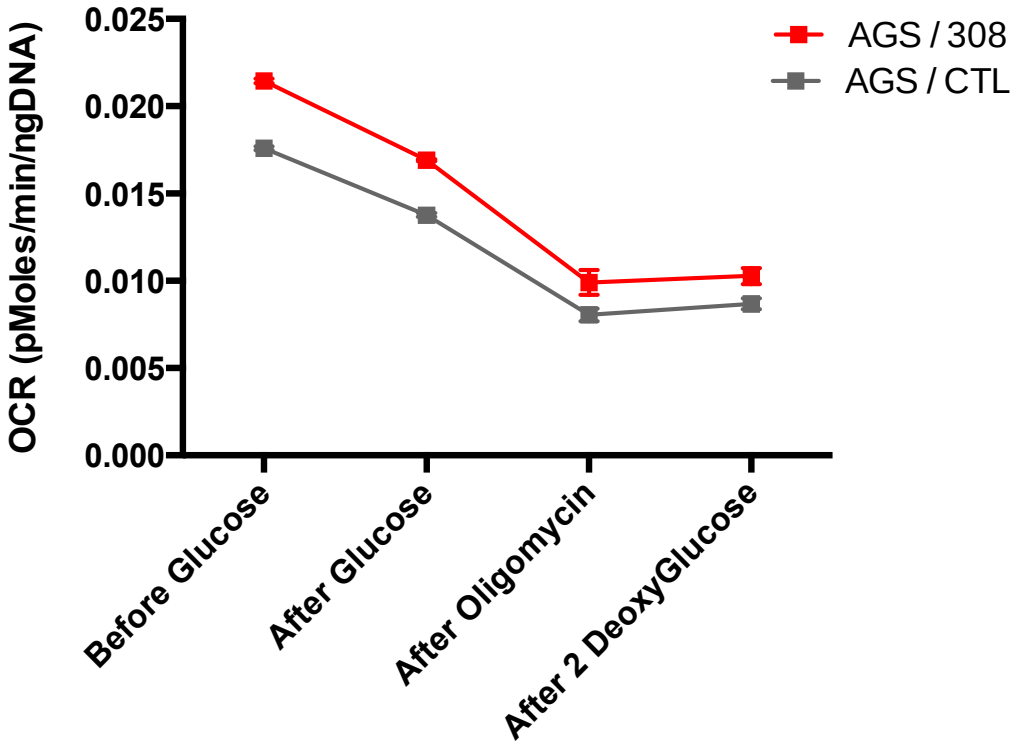

Figure 3. 10. Oxygen consumption rate of AGS cells treated with control or CAM conditioned media.
The oxygen consumption rate of AGS cells treated with CAM conditioned media from patient 308 (red) or serum free media (dark red) was measured using the Seahorse XF Flux analyser. n=5, error bars represent standard deviation. Data was normalised to DNA concentration.

In contrast, conditioned media from CAM 294, a primary cell-line isolated from a less advanced tumour compared to CAM 308, showed no difference in glycolytic function [supplementary file 3; figure 3.2], and a slight decrease in oxygen consumption rate of AGS cells [figure 3.11]. This result suggests that the ability of CAMs to influence cancer-cell metabolism may be linked to the stage of tumour development. Given that myofibroblasts may themselves be programmed by exposure to signals from cancer cells it is logical that longer exposure may confer a greater ability to drive paracrine reprogramming of cancer cells, thereby satisfying the growing need for energy production in late-stage tumour development. However, to establish the broader significance of this observation similar, or complementary studies would need to be performed on AGS cells treated with a broader selection of CAM conditioned media. Despite the different induced metabolic changes observed by Seahorse analysis after 24 hours, both CAM 308 and CAM 294 cell-lines were found to induce up-regulation of MCT1 and CD147 in AGS cancer cells as demonstrated previously in this chapter. Therefore, expression of protein markers such as MCT1 may be an indication of metabolic potential rather than an accurate indication of functional balance between glycolytic activity and oxidative respiration. To look more closely at metabolic regulation in these cells Mitotracker® cell stain was used to look at this phenotype across a panel of CAMs.

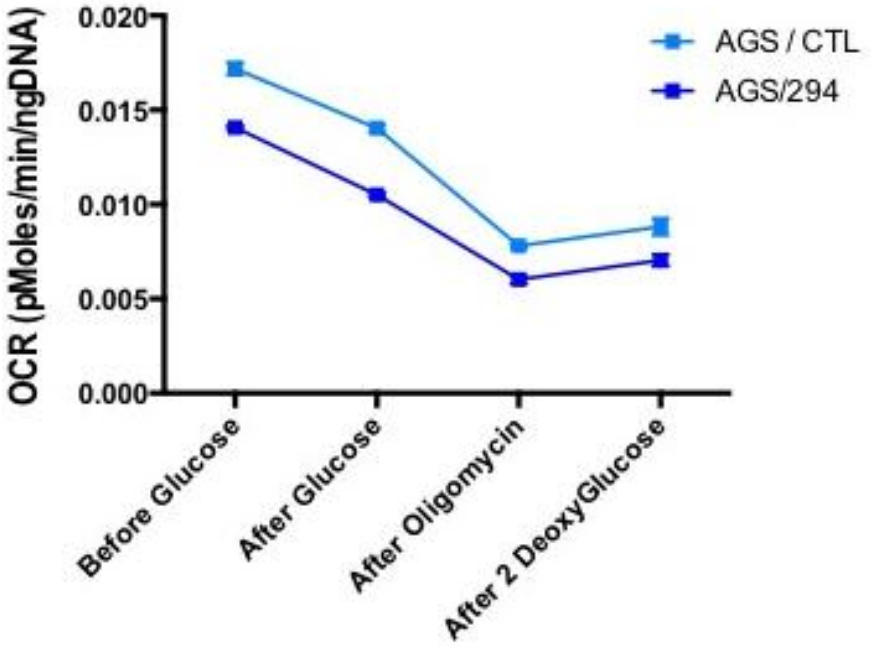

Figure 3. 11. Oxygen consumption rate of AGS cells.
The oxygen consumption rate of AGS cells treated with CAM-294 conditioned media (dark blue) or serum-free media (light blue) was measured using the Seahorse XF Flux analyser. n=5, error bars represent standard deviation. Data was normalised to DNA concentration.

3.3.5 Comparison of mitochondria activity of primary gastric CAM and NTM cells

As stated earlier in this chapter, in order to look more closely at the mitochondrial activity in myofibroblast cells, a sensitive experiment was set up which was specifically designed to examine and compare any potential differences in mitochondrial function by live-cell imaging. A panel of CAM cell-lines isolated from patients from the worst patient prognosis sub-group (CAM 308, CAM 305 and CAM 45) and NTMs (NTM 334, NTM 241 and NTM 196) were incubated with Mitotracker mitochondrial stain and representative images of live-cells (n=20) were recorded and fluorescence intensity was quantified using ImageJ software. Results from this analysis show interesting patient subgroup-related trends (Figure 3.12A) and an average percentage decrease in mitochondrial activity in CAMs compared to NTMs ($p<0.01$) (Figure 3.12B). Representative images are shown (Figure 3.12C). This data shows that CAM cell-lines consistently exhibit lower mitochondrial staining, implying reduced levels of mitochondrial activity and oxidative respiration, than observed for comparative NTM cell-lines.

A

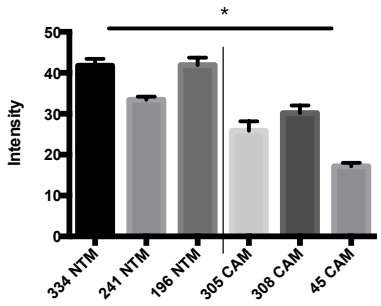

B

Tukey's multiple comparisons test	Mean Diff.	95% CI of diff.	Significant?	Summary
334 NTM vs. 241 NTM	6.432	-5.969 to 18.83	No	ns
334 NTM vs. 196 NTM	-2.019	-14.42 to 10.38	No	ns
334 NTM vs. 305 CAM	14.07	1.673 to 26.47	Yes	*
334 NTM vs. 308 CAM	14.19	1.789 to 26.59	Yes	*
334 NTM vs. 45 CAM	22.91	10.50 to 35.31	Yes	***
241 NTM vs. 196 NTM	-8.451	-20.85 to 3.950	No	ns
241 NTM vs. 305 CAM	7.642	-4.759 to 20.04	No	ns
241 NTM vs. 308 CAM	7.758	-4.642 to 20.16	No	ns
241 NTM vs. 45 CAM	16.47	4.073 to 28.87	Yes	**
196 NTM vs. 305 CAM	16.09	3.692 to 28.49	Yes	**
196 NTM vs. 308 CAM	16.21	3.809 to 28.61	Yes	**
196 NTM vs. 45 CAM	24.92	12.52 to 37.33	Yes	***
305 CAM vs. 308 CAM	0.1165	-12.28 to 12.52	No	ns
305 CAM vs. 45 CAM	8.831	-3.569 to 21.23	No	ns
308 CAM vs. 45 CAM	8.715	-3.686 to 21.12	No	ns

C

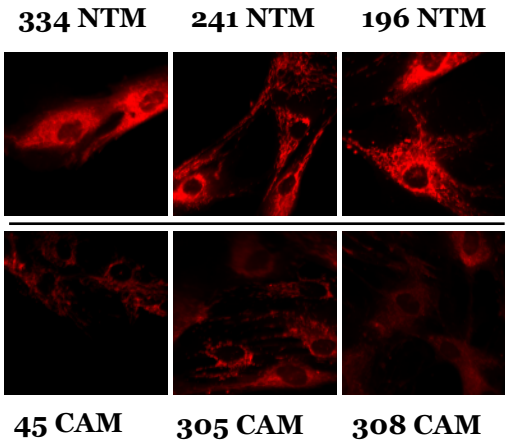

D

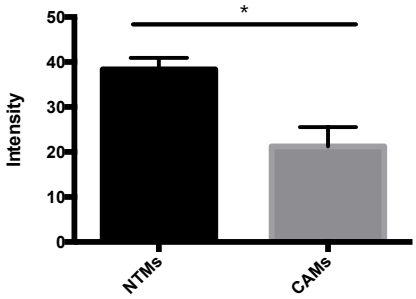

Figure 3. 12. Analysis of relative levels of mitochondrial activity in primary gastric NTM or CAM cells.
Live NTM (334, 241 and 196) and CAM (305, 308 and 45) cells were stained with Mitotracker Red CM Ros using ImageJ intensity quantification of pixels function. Trends observed across individual cell-lines are shown in panel (A). A one-way ANOVA ($p<0.05$, indicated by asterisk (*)) and a Tukey's Multiple Comparison Test (B) were performed to establish statistical significance of variability between observed activity in CAM and NTM cells. Representative images of levels of staining are shown in panel (C). Average differences in levels of mitochondrial staining between NTMs and CAMs (n=3) are shown in panel (D) (t-test showed significance of $p<0.05$, indicated by asterisk (*)).

3.3.4 Comparing inherent glycolytic capacity and oxygen consumption rate of gastric CAMs and NTMs

To look more closely at the metabolic trends indicated by Mitotracker staining analysis, the seahorse XF flux analyser was also used to perform a more detailed metabolic profiling of these cell-types. Again, due to the inherent complexity of these experiments, representative CAM and NTM cell-lines were selected for comparison. Results presented in figure 3.13 show comparative data for CAM 308 and NTM 334, which have been used consistently throughout this results chapter. However, replicate experiments show these trends are also representative of values detected in other CAM and NTM cell-lines [supplementary file 3; figure 3.3]. Seahorse experiments were performed as described previously, and myofibroblast cell-lines were treated in the Mitotracker experiments, in order to minimise variability and keep comparisons as similar as possible. Results showed that the representative CAM cell line had an increased level of extracellular acidification compared to the control 'NTM' cell line. There is a statistically significant difference between the two cell lines, with a decrease in acidification much more pronounced in the CAM than the NTM cell line after addition of 2-deoxyglucose [figure 3.13].

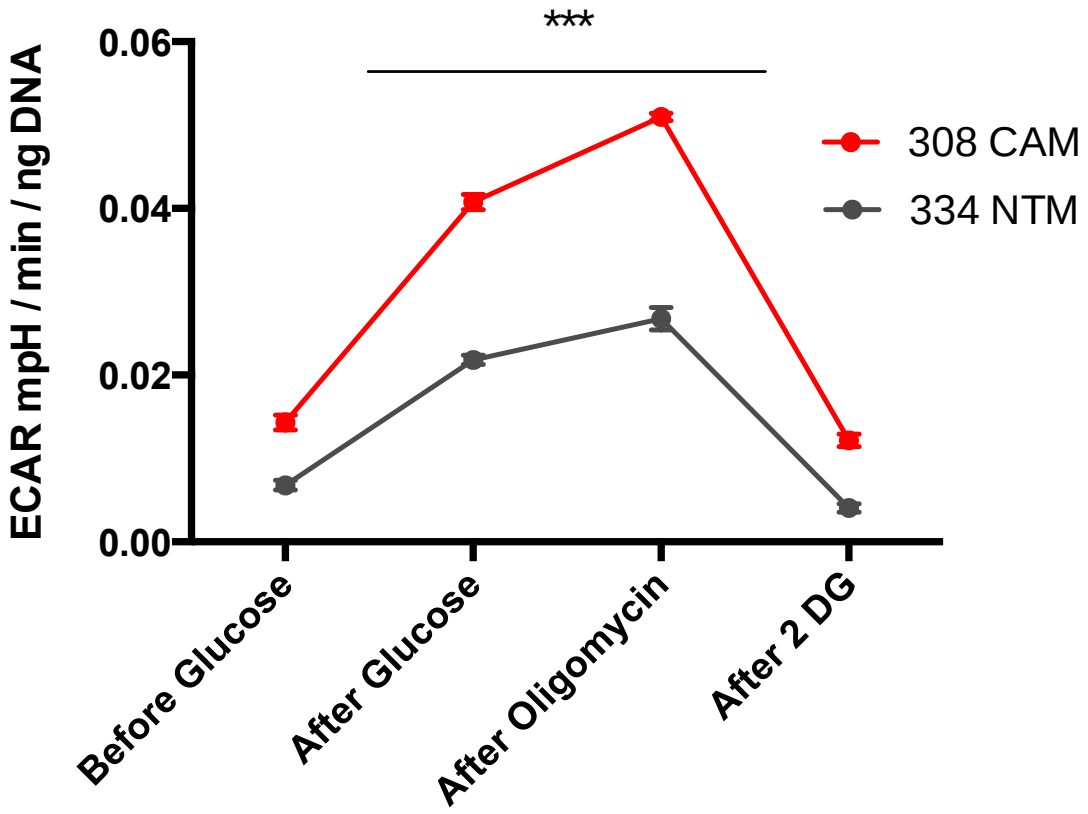

Figure 3. 13. Glycolytic capacity of CAMs and NTM cells.
ECAR rates were measured for bad prognostic patient CAM-308 (red) and NTM-334 (grey) using the Seahorse XF analyser. Results were normalized to DNA concentration. ANOVA analysis was carried out between conditions and showed there was a significant difference ($p<0.01$) between glycolytic capacity of 308 CAM and 334 NTM cells indicated by asterisk (***). Error bars represent standard deviation, n=5)

3.4 Discussion

Energy metabolism is a key factor in tumour development, as cancer cells require a constant supply of energy and biosynthetic nutrients to support proliferation (Rossignol, *et al.,* 2004 and Moreno-Sánchez *et al.,*2011). Data presented in this chapter provide new insight into the inherent and induced metabolic status of primary gastric myofibroblasts and AGS cells. To date, there is little information relating to the metabolic properties of gastric cancer cells or their effect on the metabolism of cells within the surrounding stroma. While data from other cancer models, have described characteristic changes in metabolic transporters, results remain incomplete with different models of classical and reverse Warburg effects being reported in different studies and tumour types (Cai *et al.,* 2010, and Martinez-Outschoorn *et al.,* 2011). There is also still very little known about the mechanisms of induction or regulation of these metabolic changes in cancer models.

This chapter aimed to test the hypothesis that CAM and AGS cells have distinct metabolic profiles. Data presented in this chapter show that AGS gastric cancer cells have a much greater rate of oxygen consumption than that observed in stromal myofibroblasts. Addition of Oligomycin A to inhibit ATP synthesis (Symersky et al,. 2012) in Seahorse metabolic profiling experiments, showed that AGS cells predominantly utilise mitochondrial respiration, rather than glycolysis as a primary mechanism of energy production. This signature of high-level mitochondrial activity is supported by Mitotracker data showing higher levels of mitochondrial activity in AGS cells compared to stromal

myofibroblasts. Collectively, this data is indicative of a reverse Warburg effect, in which cancer cells utilise oxidative phosphorylation as a primary source of energy. Interestingly, this is in contrast to the classical Warburg effect, which continues to be described in many publications (Schulze *et al.,* 2011, Salminen *et al.,* 2010 and Cai *et al.,* 2010); stating that cancer cells rely on glycolysis, not mitochondria for respiration as a primary source of energy.

We also aimed to test the hypothesis that co-culture of AGS and myofibroblast cells, and conditioned media experiments would cause paracrine induced metabolic changes in each cell type. Our data clearly demonstrates that AGS cells treated with CAM conditioned media leads to induction of MCT1 and CD147 expression, which is associated with a corresponding increase in the rate of oxygen consumption. In agreement with our findings, the Lisanti group have shown that treatment of MCF-7 breast cancer cells with high-energy metabolites showed an increase in both mitochondrial activity and mitochondrial biogenesis (Martinez-Outschoorn *et al.,* 2011). In our model we predict that CAMs become programmed by cancer cells to produce a range of nutrients and high-energy metabolites, which are then supplied to the cancer cells to support proliferation and tumour development.

Although characteristic markers such as α–smooth muscle actin (SMA) and vimentin have been identified for myofibroblasts (Sharon *et al.,* 2013), CD44 for mesenchymel stem cells (Spaeth *et al.*, 2013) and E-cadherin as a marker for epithelial cells (Kuphal and Bosserhoff, 2006), there are still very few markers recognised for metabolic status among cells of the stroma. In this study, a panel of CAMs and NTMs were selected to look more closely at

GLUT1 activity within different populations (CAM, ATM or NTM) of myofibroblasts. Results from immunofluorescence experiments performed in this study reveal consistent differences in GLUT1 staining between CAM and NTM cell lines; with the average intensity for CAMs and NTMs combined showed an overall statistically significant difference ($p<0.05$) in GLUT1 stain between the two groups. Therefore, we would propose that the presence of GLUT1 in stromal cells could be used as a potential marker for more aggressive/late-stage tumours that have succeeded in transforming the surrounding stromal myofibroblast cells to support and enhance growth. This information may aid more appropriate therapeutic stratification of patients, or inform development of improved forms of 'Precision Medicine'. Results from our studies strongly support the concept of a 'reverse Warburg' effect, in which stromal cells, instead of cancer cells, up regulate transporter channels associated with export of the products of glycolysis. Interestingly, although most reports in the literature associate GLUT1 over-expression with tumour development, most studies report increased GLUT1 in cancer cells, not stromal cells (Amann., et al 2009, Chandler *et al.,* 2006 and Young *et al.,* 2011). This pattern of expression is typical of the classical Warburg effect, whereby cancer cells up regulate GLUT1 as the tumour cells switch to glycolysis rather than oxidative phosphorylation. This suggests that different metabolic states or mechanisms may operate in different tumours, at different stages or development or even in different regions of a solid tumour. Our data strongly suggests that gastric cancer cells may favour mitochondrial respiration over aerobic glycolysis. Seahorse oxidative stress tests showed that the observed drop in oxygen consumption in NTM and CAM cells after the addition of oligomycin A was much more reduced than that observed with

AGS cells (0.055 pMoles/min/ngDNA compared to 0.15 pMoles/min/ngDNA in AGS cells), indicating that myofibroblasts in general are actually programmed to rely less on mitochondria for energy metabolism. Significantly we also observed that the extracellular acidification rate was also higher in CAMs compared to NTMs, which is consistent with an increase in the production and secretion of ketone bodies or lactate in myofibroblasts from cancer stroma, rather than normal tissue, and indicate high glycolytic activity. This result was again reflected in correlated Mitotracker studies, which show a consistent increase in Mitotracker staining in NTMs compared to CAMs, thereby indicating that they have more active mitochondria. This data again suggests fundamental differences in metabolic activity between these two forms of activated myofibroblasts., which are retained even after isolation and restricted passage in culture. Relative levels of MCT4 expression were also investigated in primary myofibroblasts (308 CAM, 294 CAM and 334 NTM). As previously stated, these cells lines were chosen as they represent CAMs from both 'good' and 'bad' patient prognostic groups. In addition, these CAMs were also used in AGS conditioning studies previously described (results chapter II). Western blotting results showed an increase in expression of MCT4 in CAM cells 308 and 294 compared to the control NTM 334 cells. Indicating that CAMs maintain a metabolic phenotype that is distinct from NTMs. Interestingly, these results concur with microarray data, which shows increased levels of MCT4 compared to NTM controls. MCT4 over-expression is synonymous with an increase in ketone and lactate transport, particularly in relation to cancer. Studies by Lisanti *et al.,* also show an increase in MCT4 expression in histological analysis of breast cancer stroma (Witkiewicz *et al.,* 2010). Moreover, in these studies the presence of MCT4 staining was

associated with a poor prognosis and a decrease in patient survival, which suggests the potential prognostic value of MCT4 detection in gastric cancer models. A recent study in head and neck squamous carcinoma (HNSCC) also found MCT4 positive staining in stromal fibroblasts, and the presence of this was also found to be associated with a late stage tumours (Curry *et al.,* 2013). Results therefore identify a potential prognostic value for GLUT1 and MCT4 as prognostic markers in gastric cancer stroma.

Findings presented in this work show CAM conditioning of AGS cells for 24 hours led to an increased rate of AGS cell proliferation and migration. Short term CAM conditioning of AGS cells also induced increased expression of MCT1, when analysed by qPCR, in addition, western blot results showed increased levels of both MCT1 transporter channels and CD147, which co-localises with MCT1 and is required for its functional regulation and location. The observed elevation of MCT1 and CD147 expression is indicative of increased up regulation of the transport of ketone bodies and other high-energy metabolites into the cancer cells. Whilst there are publications supporting the concept of paracrine communication, and the 'feeding' of cancer cells with high energy building blocks for ATP generation (Pavlides *et al* 2009, and Sotgia *et al.,* 2012), there are also conflicting reports in the literature. Data published by Fine et al (2009) showed that ketone bodies actually act to inhibit cell growth, via over expression of uncoupling protein 2 (UCP2). This data is discussed in the context of a modified version of the 'Randle Cycle', which was first proposed in 1963 as ground breaking work in the field of metabolism in diabetes (Randle *et al.,* 1963). The Randle cycle shows that ketone bodies and fatty acids act to inhibit glycolysis to ensure the

stable production of ATP, however in an adapted cancer cell model, production of ATP is not stable, due to dis-regulation of UCP2. Data produced by Fine *et al.,* suggests that ketone bodies metabolised in cancers that over express uncoupling proteins, may inhibit glycolysis. Without the ability to produce ATP via oxidative phosphorylation, cell growth would be impaired. It has been proposed that exposure to reactive oxygen species (ROS) and induction of HIF-1∝ may regulate UCPs, potentially leading to their over expression (Fine *et al.,* 2009 and Nishio *et al.,* 2005), thereby linking hypoxia and oxidative stress to the inhibition of cancer cell proliferation, due to dis-regulation of mitochondrial electron transport proteins.

Data presented in this chapter show high levels of mitochondrial respiration in AGS cancer cells after conditioning with media from associated CAMs. Analysis of microarray data from conditioning experiments show statistically significant ($p<0.05$) down regulation of UCP1 and UCP3 with no statistical change in UCP2 [supplementary file III; figure 3.4]. Taken together with phenotypic assays of CAM conditioning experiments, whereby we noted a corresponding change in AGS cell proliferation, suggesting that without UCP over-expression, CAM media rich in ketones and other high energy metabolites serves to drive AGS cancer growth. This lack of over-expression of UPCs together with up regulation of ketone bodies in the CAM media is consistent with a model of pseudo-hypoxia, rather than hypoxia itself. In this model cancer cells maintain their mitochondrial function yet enforce or 'trick' stromal cells to switch to a more glycolytic phenotype via secretion of factors that induce oxidative stress. To further understand the paracrine communication between tumour cells and stroma myofibroblasts, more experiments are needed to investigate the differential effects of hypoxia.

Performing proliferation assays on co-cultured cells exposed to conditions mimicking hypoxia such as treatment with hydrogen peroxide, or incubation in a hypoxic chamber, would establish whether there is an inhibition of growth in these conditions, as well as determining levels of UCPs by qPCR.

Up regulation of MCT1 observed in these co-culture experiments also concurs with data in the previous chapter, whereby pathway analysis of conditioning data showed activation of the PPAR- α pathway in CAM cells compared to ATM conditioning. Whilst there is still much to learn about the complex regulation of MCT1, it is known that activation of transcription factor peroxisome proliferator-activated receptor (PPAR)-α causes up-regulation of genes involved in ketone body synthesis (Kersten *et al.,* 2001). Further work in this area *in vivo* provided data showing that activation of PPAR- α was directly linked to increased mRNA levels of MCT1 (Konig *et al.,* 2008). This is interesting in context of data from co-culture microarrays and supportive co-culture lab work carried out in this study. These results provide indications of the potential pathways by which MCT1 is activated and regulated, however currently this knowledge is very limited, and there is much more to elucidate concerning the conditional regulation of transporter channels within different cell types.

Elevated MCT1 expression has also been linked to increased invasion in lung cancer, colorectal cancer and also in malignant pleural mesothelioma, whereby siRNA silencing of MCT1 expression led to decreased invasion (Mogi *et al.,* 2012, Pinheiro *et al.,* 2008 and Izumi *et al.,* 2011). Little is known about the mechanisms of this phenotype, however our data supports this concept. As previously discussed, CD147 is responsible for regulation of MCT1 expression

and subcellular localisation (Walters *et al.,* 2013). Our data shows that CD147 expression is highly up regulated in AGS cells after CAM conditioning. As CD147 is known to form a complex with MCT1, (Kirk *et al.,* 2000) it is not surprising that its expression pattern closely mimics that of MCT1 in these cells. Interestingly, CD147 is also known to regulate and induce MMP expression in neighbouring myofibroblast cells (Gabison *et al.,* 2005 and Jouneau *et al.,* 2011). It is possible that the invasive properties linked to MCT1, could actually be facilitated by the MCT1-CD147 complex, and the induction of MMPs by CD147, which would contribute to degradation of the extracellular matrix, thereby enhancing tumour cell invasion.

Chapter Four

Metabolic Reprogramming of Normal Tissue Myofibroblasts

4.0 Introduction

Myofibroblasts play an important role in the normal wound–healing process, however they are not usually found in healthy uninjured tissues (Eyden, 2005). Current dogma suggests that prolonged exposure to inflammatory signals, or tissue injury may drive a two-phase process in which fibroblasts are first converted into protomyofibroblasts, expressing both β and γ actin, before progressing to 'activated myofibroblasts', which express α-smooth muscle actin (∝-SMA) (Micallef *et al.,* 2012). Two factors, which contribute to this process, are transforming growth factor (TGF)-β and endothelin-1 (ET-1) (Phan *et al.,* 2003).

The microenvironment of gastric tissue is unique as even under healthy 'normal' conditions both epithelia and underlying tissues may be exposed to environmental stress, inflammation, and signals that drive constant tissue regeneration [figure 4.1]. As cells within the gastric environment are in constant contact with these inflammatory signals, activated myofibroblast cells make up part of the natural cell population of gastric tissue. These cells, however, are functionally different to cancer-associated myofibroblasts taken from the site of a tumour or from tissue adjacent to developing tumours. These distinctions in gene expression profiles have been previously reported (Jones *et al,*. unpublished data) and have also been discussed in chapters II and III in this thesis.

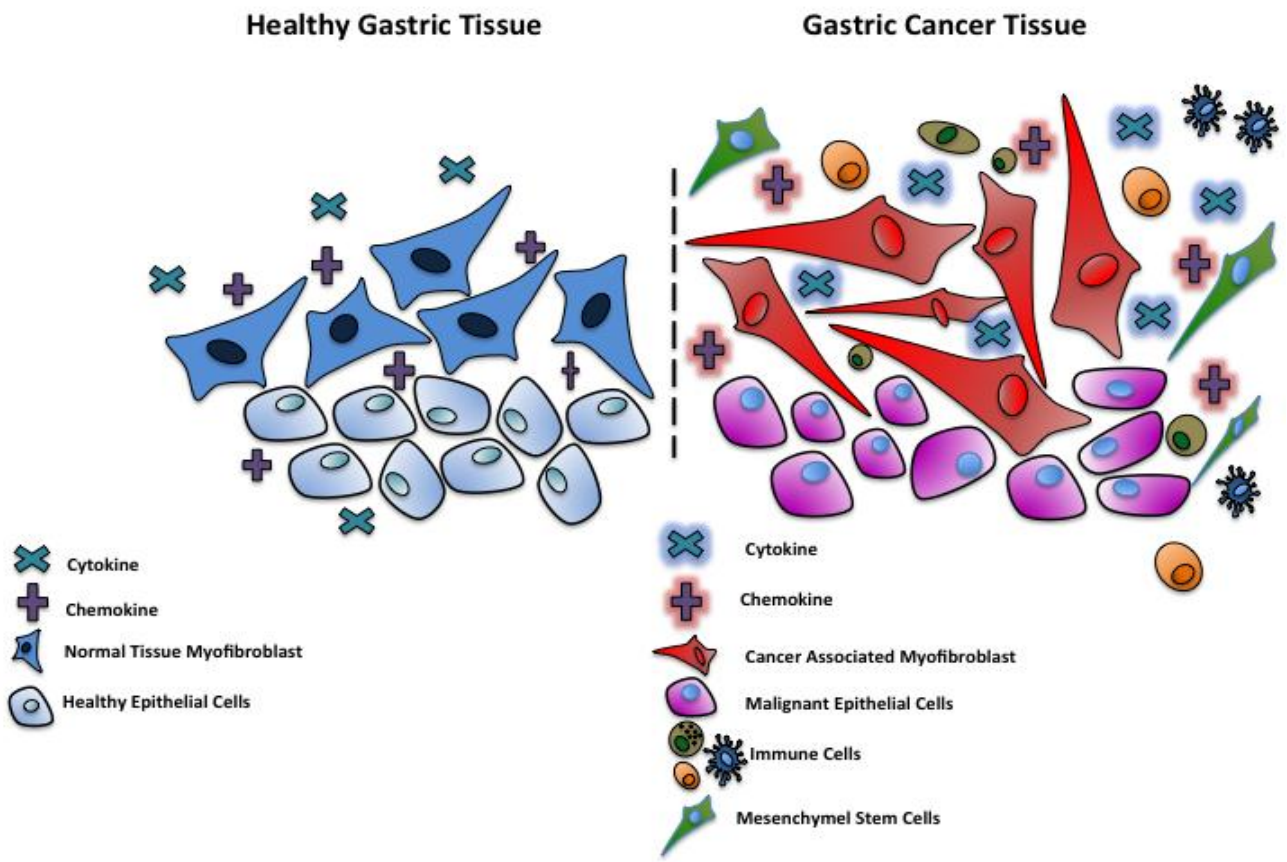

Figure 4. 1. Schematic representing differences between communication in normal 'healthy' gastric tissue and gastric cancer tissue.

In normal gastric tissue, balanced paracrine communication exists between myofibroblasts and epithelial cells. In cancer, cross–talk between CAMs and cancer cells leads to changes and activation of cancer promoting cytokines, chemokines and recruitment of adapted immune cells such as cancer associates macrophages and mesenchymel stem cells to the tumour site, creating an environment supportive of tumour growth.

The metabolic properties of healthy "normal" primary stromal cells has not yet been reported in the literature, nor have primary gastric myofibroblast cells taken from healthy tissue been used to resolve questions regarding metabolic re-programming within a cancer model. As myofibroblast cells are vital for the wound healing process (Li and Wang, 2011) and cancer is often described as 'the wound, which does not heal' (Dvorak., 1986), using healthy myofibroblast cells to investigate the model of gastric cancer and cell reprogramming is potentially more clinically relevant than using an immortalised or primary fibroblast cell lines. Data presented in this chapter is novel work in the field, and aims to provide a more comprehensive and clinically relevant model of tumour – stroma interactions.

4.1 Aims and Hypothesis

This chapter aimed to test the hypothesis that conditioned media from AGS cancer cells is able to induce CAM related functional and metabolic reprogramming of NTMs. The primary aim of work described in this chapter is to further examine inherent properties of gastric NTMs, and assess the potential for cancer cell mediated metabolic reprogramming into CAM like 'feeder cells'.

1. To assess the inherent metabolic status of NTMs including analysing relative expression of CAM related markers of metabolic status

2. To perform co-culture and cancer-cell conditioned-media studies to assess induced changes in NTM metabolic status.

3. To establish if NTM cells can be functionally reprogrammed to adopt CAM-like metabolic properties.

4.2 Chapter Specific Materials and Methods

Detailed materials and methods can be found in chapter six, however, below is a brief outline:

4.2.1 Proliferation and Migration Assays

EdU proliferation assays and boydon chamber migration assays were carried out as described previously. Low passage (P4-P9) NTM cells lines 334, 351 and 241 were used in both proliferation and migration assays. In each case, serum-free media was used as a control, to ensure consistency with growth and cell maintenance conditions used in preparation of samples for associated microarray studies.

4.2.2 Transwell Co-Cultures

Long-term transwell co-cultures were set up in 10cm dishes using 2% serum media with AGS and NTM 334 cells seeded on the bottom and top compartments of the transwell culture units respectively at a density of 300,000 cells/ml. Cells were fed every 72 hours, before being processed for RNA extraction or western blotting on day seven. AGS cells cultured at the same density for equivalent time in un-conditioned 2% serum media were used to define control levels of RNA and protein expression.

4.3 Results

4.3.1 Phenotypic Effects of NTM conditioned media on AGS cells

As previously discussed, there are distinct and definite differences in gene expression profiles between normal 'healthy' myofibroblasts and myofibroblasts taken from the cancer microenvironment. Microarray analysis of CAM, NTM and NTM data, showed distinct and highly dissimilar gene expression patterns between NTMs, and CAM and ATM cell lines (Jones *et al.,* unpublished data). Principle component analysis of microarray data showed segregation of cell types, and NTMs were shown to have unique global gene expression patterns compared to CAMs and ATMs [figure 4.2].

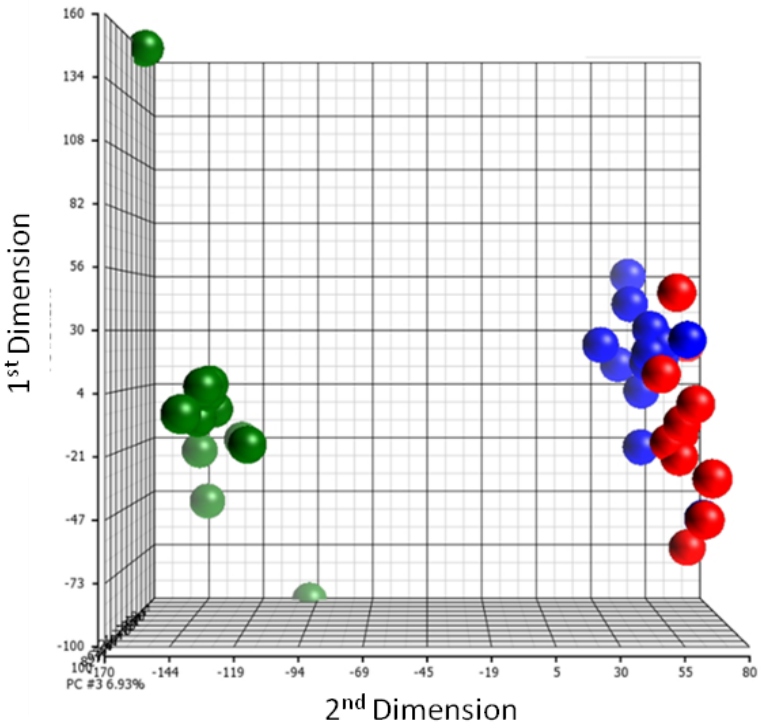

Figure 4. 2. Principal component analysis of all CAM (RED), ATM (BLUE) and NTM (GREEN) patient samples.
PCA shows distinct segregation of myofibroblast cell types. Figure taken from Jones *et al.,* unpublished data.

To examine more closely the inherent properties of gastric NTMs and to establish the potential for cancer cell mediated metabolic reprogramming into CAM like 'feeder cells,' a series of experiments were carried out. Firstly, to establish the phenotypic effects of exposing AGS cells to NTM conditioned media, short term conditioned media proliferation and migration assays were performed as previously described (Holmberg et al, 2012). Results from these experiments show a significant and consistent increase in AGS cell proliferation and migration after treatment with conditioned media from NTM cell lines [figure 4.3]. Thereby demonstrating that non-cancer associated NTMs secrete factors that promote or encourage proliferation and migration of AGS cells. Observed NTM mediated increase in AGS cell proliferation was not, however, as high as that induced by equivalent CAM conditioned media [chapter III].

The total number of migrated and proliferating AGS cells was variable between NTM patients, for example media from patient 334 induced less migration than patient 351; however the increase in migrated and dividing cells was still significant across all patients compared to the control media. Data from migration and proliferation assays were expressed across the three individual NTM cell lines [figures 4.3A and B], and as an average across all three cell lines [figures 4.3C and D] to illustrate both relative trends in each individual primary cell line as well as the overall NTM patient trend.

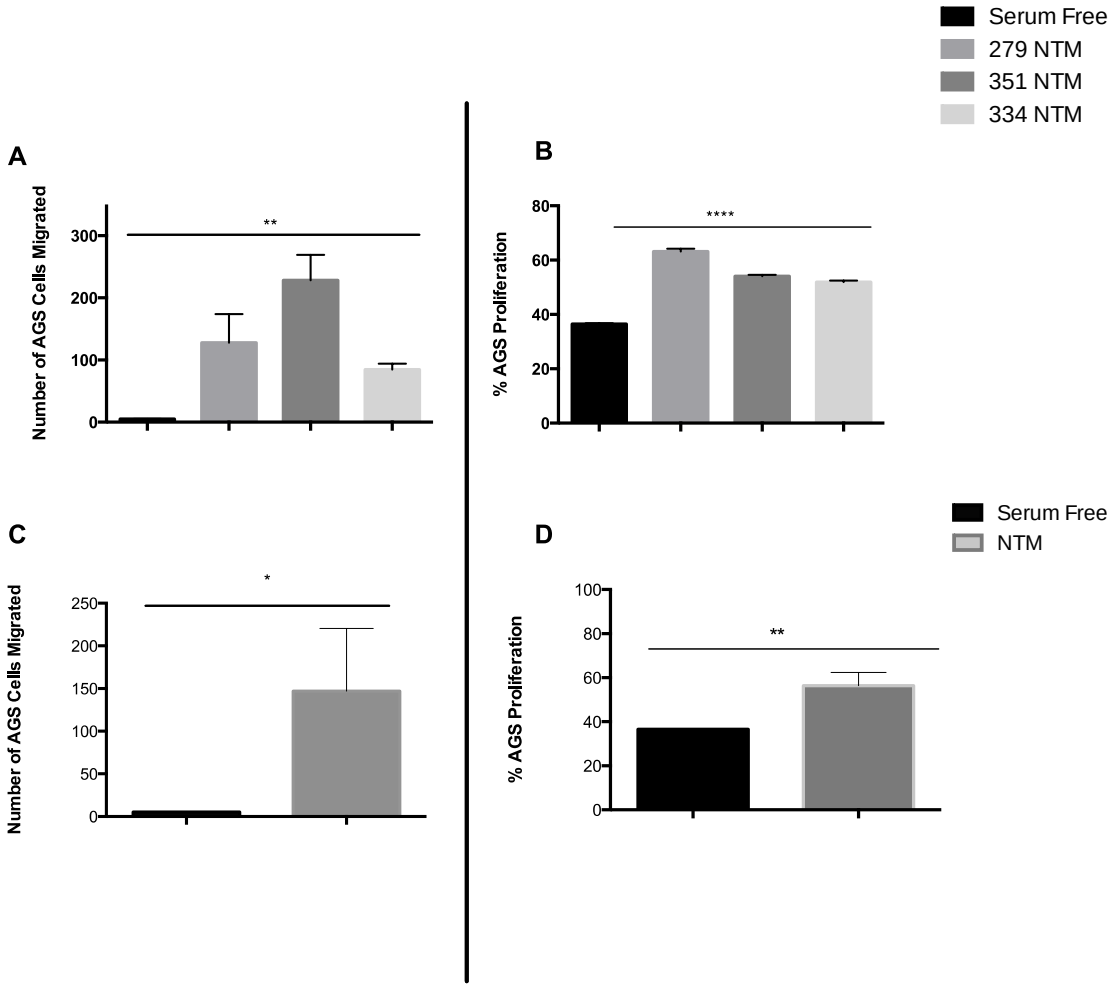

Figure 4. 3. EdU proliferation and boydon chamber migration assays representing NTM-conditioning effects on AGS cells.
Boydon chamber assays showed increase in AGS cell migration, results were expressed as both single patient NTM data [A] and [C] combined average numbers of migrating cells. ANOVA analysis of single patient data showed a significant increase (indicated by an asterisk (**)) in migration of AGS cells upon treatment with NTM media across cell lines ($p<0.01$). Students T-Test analysis of combined data, also showed statistical significance in AGS cell migration after treatment with conditioned media (indicated by an asterisk (*), N=3, error bars represent standard deviation. For proliferation assays, EdU dye was incorporated into AGS cells treated with NTM conditioned media, before FACS analysis was performed to determine % of proliferating cells. Results show [B] single patient NTM and [D] combined average numbers of proliferating cells following conditioning with either serum free or conditioned media (n=3) error bars represent standard deviation. ANOVA analysis of single patient data showed a significant increase (indicated by an asterisk (****) in proliferation of AGS cells upon treatment with NTM media across all cell lines ($p<0.001$). Students T-Test analysis of combined data, also showed statistical significance in AGS cell proliferation after treatment with conditioned media (indicated by an asterisk (**), N=3, error bars represent standard deviation.

4.3.2 Validation of Microarray Targets in AGS cells co-cultured with NTM cell lines by qPCR

24h conditioning was carried out as previously described to investigate NTM mediated changes in AGS gene expression. A series of qPCR experiments were designed to compare the top differentially regulated genes observed in the CAM conditioning experiments set with the NTM conditioning set.

Data shows that the highest ranking up regulated genes in CAM conditioning data sets; HK1, CEACAM5 and GLUT1 were down regulated in NTM conditioning data sets [figure 4.4]. OAS1, one of the most greatly down regulated genes in the CAM conditioning data set, was only down regulated marginally, not significantly, in the NTM data sets. This confirms the microarray analysis and principle component analysis showing differences in gene expression between CAM and NTM cell lines [figure 4.5]. Whilst NTM conditioning has been shown to induce AGS proliferation and migration, it is apparent that there are many differences between the genes induced by conditioning, suggesting fundamental genetic differences between a CAM and NTM conditioning phenotype.

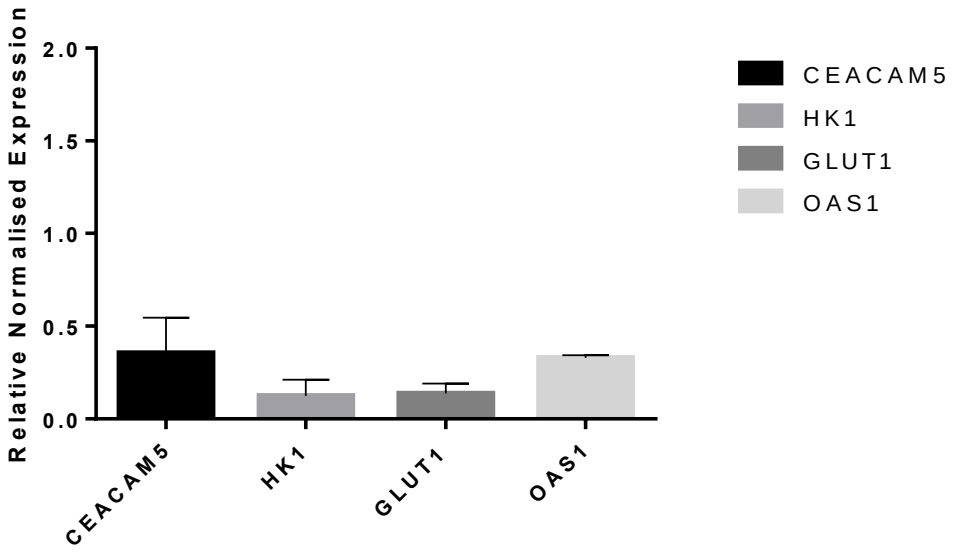

Figure 4. 4. qPCR to determine NTM-conditioning effects on AGS cells.
Data presented shows gene expression in AGS cells following 24 hour conditioning with NTM 334 cell media, n=3, error bars represent standard deviation. In each case expression levels were normalised to both beta actin and serum free expression levels.

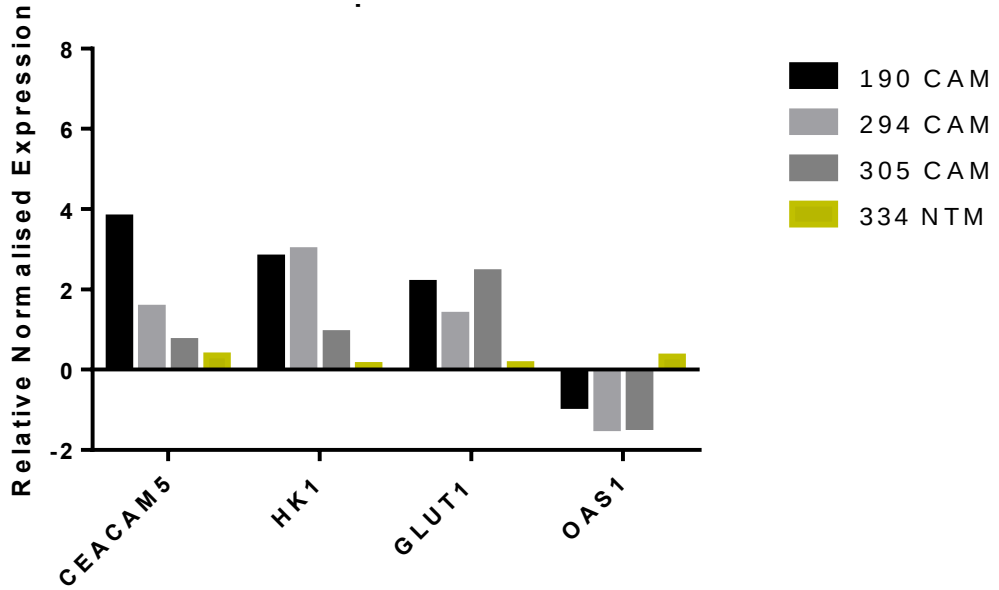

Figure 4. 5. qPCR shows NTM-conditioning effects on AGS cells.
Data presented shows gene expression in AGS cells following 24 hour conditioning with CAMs 190, 294 and 305 and NTM 334 cell media, n=3. In each case expression levels were normalised to both beta actin and serum free expression levels.

4.3.3 Short Term NTM conditioning of AGS cells induced changes in AGS related gene expression profiles and protein expression

AGS cells were conditioned with NTM media for 24 hours then qPCR was carried out to determine the levels of MCT1. Results showed there was a significant increase in MCT1 in AGS treated with NTM cell media, compared to AGS cells treated with control cell media [figure 4.6]. AGS cells treated with CAM conditioned media for 24 hours was also included for comparison. Following qPCR data analysis, western blot experiments were also carried out to determine the protein levels of MCT1 and CD147 in AGS cells following conditioning with NTM media. Western blotting analysis showed NTM cells induced expression of MCT1 and CD147 in AGS cells after 24 hour conditioning [figure 4.7], this was comparable to the induction of these transporter channels by CAM media.

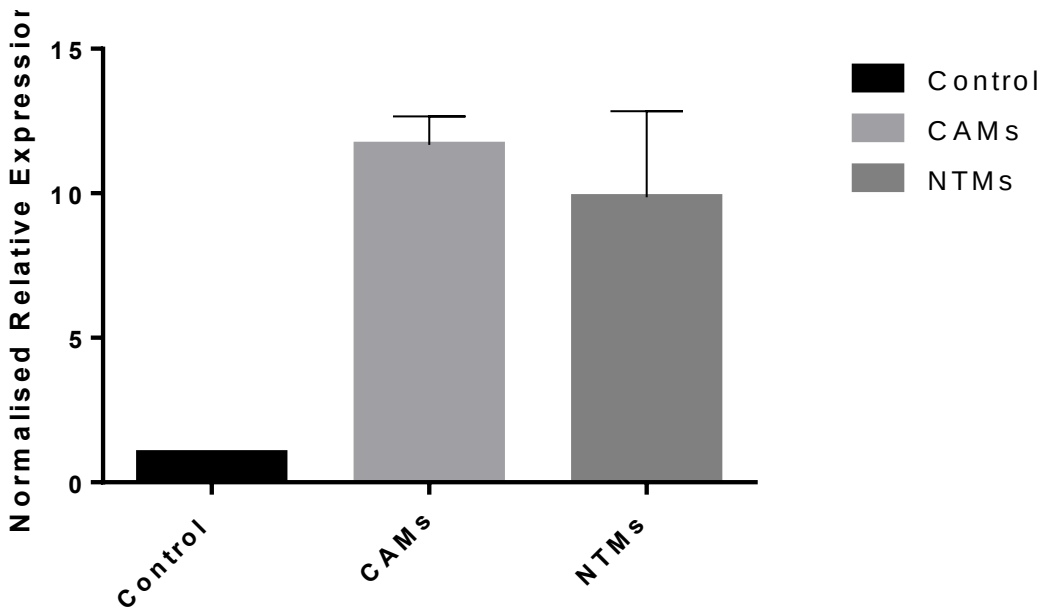

Figure 4. 6. Relative changes in levels of MCT1 gene expression following exposure to of AGS cells to NTM conditioned media.
Relative levels of MCT1 expression were quantified by qPCR following exposure of AGS cells to either serum free or NTM conditioned media for 24 hours, n=3, error bar represent standard deviation. In each case expression levels were normalised to both beta actin and serum free expression levels.

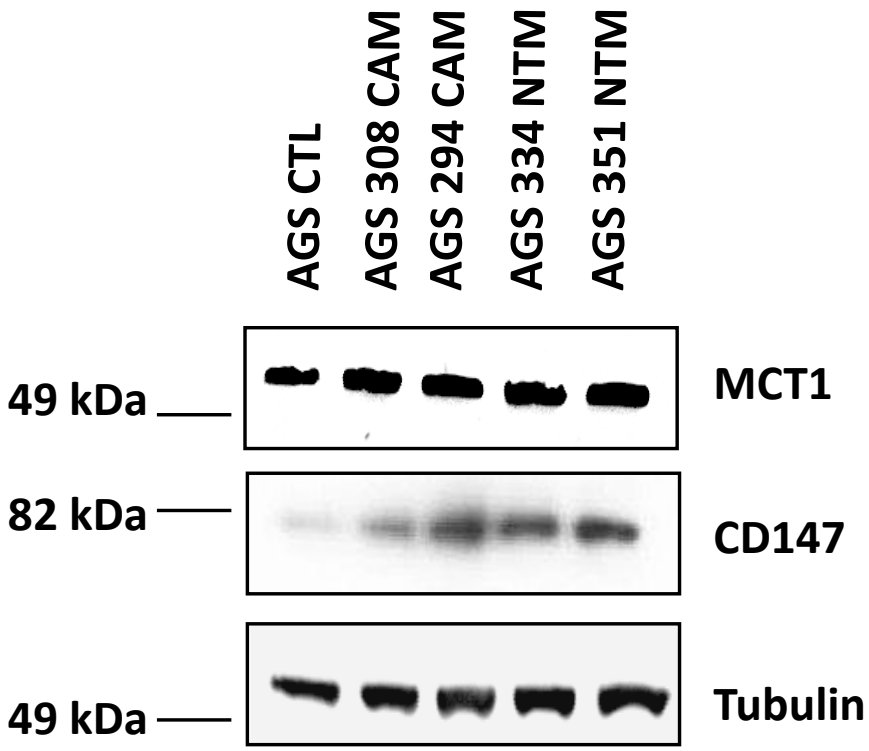

Figure 4. 7. Western blot to show MCT1 and CD147 protein levels following exposure of AGS cells to NTM conditioned media.
Western blots were carried out following exposure of AGS cells to either serum free, CAM or NTM conditioned media for 24 hours. Tubulin was used as a loading control to check for equal loading.

4.3.4 Long Term AGS cells conditioning induced changes in NTM related gene expression profiles

Following 24hr AGS conditioning with NTM media, a series of experiments were designed to test the hypothesis that AGS cells grown in co-culture with NTM cells could induce 'CAM like' changes in gene expression in NTM cells. Previous data from CAM, ATM and NTM microarrays showed primary gastric NTM cells have uniquely different gene expression profiles compared to gastric CAMs (Jones *et al,*. unpublished data). Specifically, NTM cell lines appear to have little to no expression of metabolic related transporter channels, such as GLUT1 and MCT4. In addition, results from seahorse metabolic profiling experiments and Mitotracker cell staining performed in this study, also show a marked difference in metabolic status between NTM and CAM cell lines [chapter III]. This data infers that in normal 'healthy' myofibroblast cells, mitochondria mediated oxidative respiration is predominantly used to generate ATP. Given the inherent differences observed between NTM and CAM metabolism, a series of experiments were designed to investigate whether it was possible to re-programme NTMs with cancer cell media, to determine if they acquire CAM-like metabolic feeder properties. This information would be advantageous in generating a more realistic model for tumour–stroma interactions in the early stages of tumours, particularly in relation to metabolic changes within the tumour microenvironment.

To investigate changes in NTM gene expression profiles following exposure to AGS cells or AGS-conditioned media, long-term co-cultures were carried out in 10cm transwell plates. Transwell plates allow for the movement of small

molecules such as cytokines through the 0.4uM membrane, but do not allow for the movement of cells, thus ensuring two separate monolayers in each compartment, but the free exchange of media and components between cells. This allows for the understanding of effects of paracrine communication between these two cell subsets.

Firstly, as GLUT1 was previously identified as being up regulated in CAMs but not in NTM cell lines [chapter III] it was selected as a target for further investigating in long- term NTM conditioning experiments. qPCR experiments were carried out on transwell lysates to investigate the changes in induction of GLUT1 in NTM cells. Previous data presented in this work showed that expression of GLUT1 is inherently low in these cell types.

After 7 day co-culture with AGS cancer cells, GLUT1 was up regulated 15 fold compared to cells cultured alone [figure 4.8]. For both cancer treated and control transwell plates, the seeding densities and the cell culture media used was consistent, and cells were fed every 72 hours. This data illustrates how rapidly and robustly paracrine communication between cell types can act, and how within just seven days, NTM cell line 334 is showing changes at the mRNA level in GLUT1, which has been previously demonstrated in CAM cell lines.

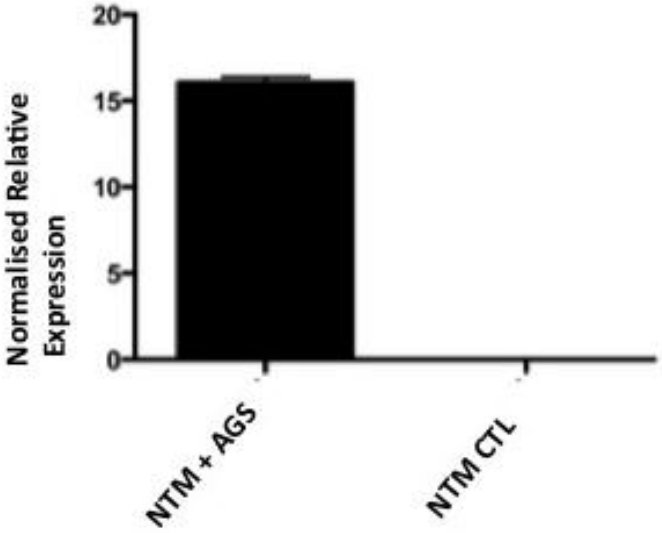

Figure 4. 8. Relative changes in levels of GLUT1 gene expression following co-culture of AGS cells with NTM cells.
qPCR was carried out on NTM cells line 334 after 7 days of co-culture with AGS cell to investigate levels of GLUT1. Co-cultured cells were compared to the non-treated control cells. Results represent n=3, data was normalised to beta actin as a stable housekeeping gene, error bars represent standard deviation.

4.3.5 Long Term AGS cells conditioning induced changes in NTM related protein expression profiles

Due to the nature of these studies, for determining protein expression, comparative profiling was performed on one representative cell line from the 'normal' myofibroblast cell bank, NTM 334, plus cancer associated myofibroblast cell lines from both 'good' and 'bad' prognostic patients, CAM 308 and CAM 294. Results showed that after 7-day co-culture with AGS cells, NTM 334 up-regulated MCT4 transporter channel to a comparable level to that observed in CAM cells [figure 4.9A]. No up-regulation of MCT4 was observed in control myofibroblast cells, which had not been co-cultured with AGS cells [figure 4.9B]. This data indicates paracrine communication exists between AGS cancer cells and primary NTM cells, which is sufficient to induce MCT4 expression in theses "normal" myofibroblast cells after just 7 days of co-culture.

A

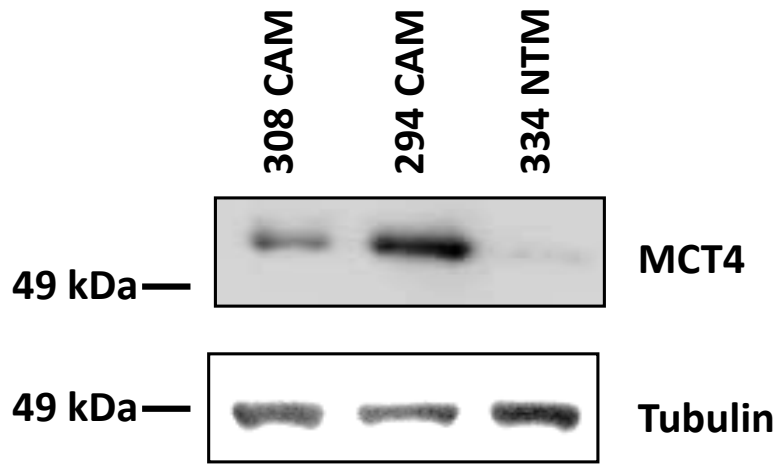

B

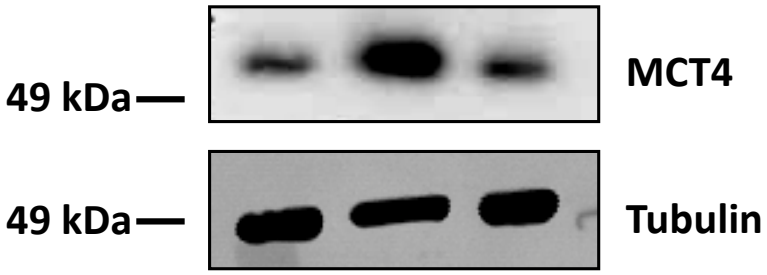

Figure 4. 9. Western blot to show comparison of CAM and NTM cells after co-culture.
Myofibroblast cell lines were cultured for 7 days alone in media containing 2% FBS [A], or together with AGS cells in media containing 2% FBS [B]. Following cell lysis, BCA was carried out for protein normalisation and then samples were processed for western blotting. Membranes were probed for MCT4 and tubulin was used as a loading control.

4.3.6 NTM induced changes in AGS Cell Protein Expression

To investigate the reciprocal responses induced in AGS cells co-cultured with NTM cell lines, lysates were collected from corresponding AGS cells grown in transwell units for analysis of corresponding markers MCT1 transporter and CD147 expression by western blotting. MCT1 was selected as this was observed previously in the CAM induced phenotype [chapter III], as well as being reported in the literature (Pavlides et al 2009, Bonuccelli *et al.,* 2010 and Sotgia *et al.,* 2012), it is known to be up-regulated in response to transport of small high energy metabolites such as ketone bodies (Cuff *et al.,* 2002).

Results showed levels of MCT1 transporter expression in AGS cells increased in response to both CAM and NTM conditioned media following 7 days co-culture [figure 4.10], MCT1 was also present in the control treated cells (AGS cells grown for 7 days in 2% FBS media), this would be expected as this transporter channel is reported to be differentially regulated in some cancers (Curry *et al.,* 2012, Zhao *et al.,* 2014 and Pinheiro *et al.,* 2011) and analysis using Genevestigator software also showed this gene has been pulled out of microarray analysis from the gastric cancer database [chapter II]. MCT1 up-regulation is usually observed when oxidative cancer cells increase importation of lactate or ketone bodies to fuel their mitochondrial respiration, results showing increased MCT1 in AGS cells co-cultured with NTM cell line therefore suggests increased rate of mitochondrial respiration. CD147, otherwise known as Emmpirin is a member of the immunoglobulin superfamily and is expressed on many cells (Iacono *et al.,* 2007).

It is reported to be essential for maintaining protein expression levels of monocarboxylate transporter channels (Kirk *et al.,* 2000), as well as its primary function of regulating other processes such as MMPs (Chen *et al.,* 2011 and Sun *et al.,* 2001), hence the name, Emmpirin (extracellular matrix metalloproteinase inducer).

Results by western blot showed an increase in CD147 expression, which was detected in its mature, fully glycosylated form in the AGS cells co-cultured with CAM or NTM conditioned media. In contrast, when AGS cells were cultured in control unconditioned 2% FBS media, very little high molecular weight, un-glycosylated CD147 was detected, with the majority of expressed CD147 being detected as the lower molecular weight immature/core glycosylated form [figure 4.10] The observed difference in ratios of mature and immature forms of CD147 is consistent with MCT1 being required for CD147 maturation (from core to a complex form of glycosylation). This data suggests that after co-culture for 7 days, both CAM and NTM cell lines are capable of inducing maturation of CD147, which is consistent with detected increased levels of MCT1.

MCT1 was still observed in the control cells as can be seen by the band in figure 4.10, however it was clear that CD147 levels were different in the CAM and NTM co-culture data, showing a distinct band at 64kDa and a fainter band at 82kDa. This data clearly suggests that overall the CAM and NTM cells have increased turnover and up regulation of MCT1/CD147 levels.

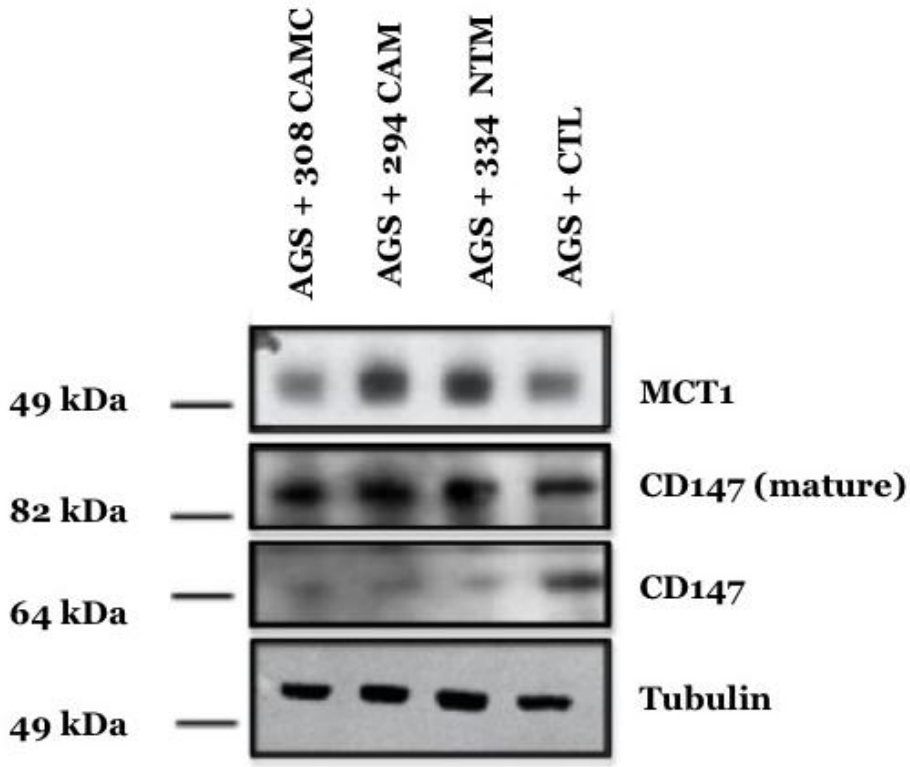

Figure 4. 10. Comparative levels of MCT1 and CD147 expression in AGS cells cultured in the presence or absence of CAM or NTM cells.
AGS cells were cultured for 7 days with myofibroblast cell lines 308, 294 or 334 in media containing 2% FBS, control cells were grown alone in media containing 2% FBS. Following cell lysis of AGS cells, BCA was carried out for protein normalisation and then samples were processed for western blotting. Membranes were probed for MCT1, CD147 and tubulin was used as a loading control.

4.4 Discussion

It is well established that tumour development is driven by reciprocal paracrine communication between cancer cells and cells in the neighbouring tissue or stroma. During this process, cancer cells produce oncogenic and signals, which enhance the growth and invasion into the surrounding stromal cells. Whilst there is supporting evidence for the role of cancer associated fibroblasts (CAFs) in tumour progression, there are also many reports demonstrating that fibroblasts can restrict and contain cancer cells (Alkasalias *et al.,* 2014 and Bisell *et al.,* 2011), in part by preventing EMT and metastasis.

Conversion of fibroblasts to myofibroblasts is hypothesied to be driven by exposure to inflammatory signals, which also attract differentiated myofibroblasts to the site of damage (Cai *et al.,* 2010). Active myofibroblasts secrete ECM degrading proteases, thereby promoting changes in ECM composition and turnover (DeClerck *et al.,* 2004). In addition, myofibroblasts can also modulate immune responses at the site of injury and secrete various growth factors (Kim *et al.,* 2010). Using primary myofibroblast populations, to investigate cancer induced reprogramming is therefore more clinically relevant than using immortalised fibroblast cell lines when investigating molecular processes that drive the development and progression of gastric tumours.

Previous data has shown that NTMs have similar inflammatory properties to CAMs, such as secretion of cytokines and interferon responses (Jones *et al.,*

unpublished data). Also, NTMs are able to stimulate migration and proliferation of AGS cells *in vitro*. Comparison of metabolic profiles in the previous results chapter however, illustrated fundamental differences in primary NTM and CAM cells. In our studies NTMs exhibited much higher mitochondrial activity and significantly less GLUT1 expression, compared to CAMs. Glycolytic stress tests performed using the Seahorse show that CAM cells have increased extra-cellular acidification rates compared to NTM cells. In light of this observation we decided to examine the effects of co-culturing NTM cells with AGS cancer cells, in order to establish if CAM like metabolic profiles could be induced in NTMs, Thereby mimicking processes that may take place during cancer progression.

Data presented in this chapter provides evidence that NTMs can be reprogrammed to adopt CAM like metabolic properties, which would support tumour growth. These changes include the up-regulation of MCT4, GLUT1 with a converse induction of MCT1 and CD147 in AGS cells. Collectively, these results show that prolonged reciprocal paracrine communication between gastric cancer cells and stromal myofibroblasts results in metabolic reprogramming to a pro-tumorigenic phenotype [figure 4.11].

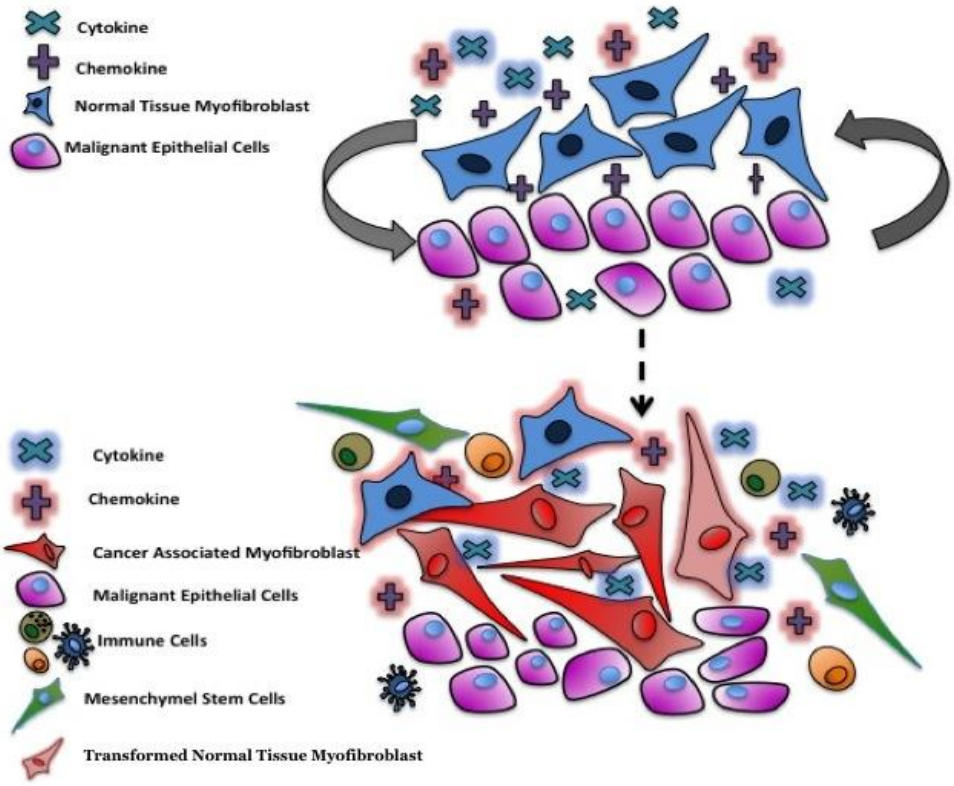

Figure 4. 11. Schematic to show the predicted model of NTM cells transition to a more 'CAM' like phenotype.
Cross–talk between NTMs and cancer cells leads to changes and activation of cancer promoting cytokines, chemokines to the tumour site, driving mutual changes in both cell subsets. NTMs develop CAM- like properties, undergoing changes in metabolism, creating an environment supportive of tumour cell growth.

Currently, there is limited work in the field of cancer related myofibroblast re-programming, especially in the field of gastric cancer. Data from studies on prostate cancer (Ishii *et al.,* 2011) supported the findings presented in this work. Results demonstrated that co-culture of "normal" human prostate stromal cells with prostate cancer cell lines led to the induction of biochemical

properties of "cancer associated" stromal cells, such as up regulation of TGF-β. Conditioning of immortalised fibroblast cell lines with media from cancer cell lines has also been previously shown to induce an increased rate of aerobic glycolysis and energy transfer in the fibroblast cells (Guido *et al.,* 2012 and Martinez-Outschoorn *et al.,* 2012).

Similar work has also been performed in breast cancer models, whereby co-culture of breast cancer cells with 'normal breast fibroblasts' cells promoted cancer cell invasion through up regulation of ADAM metallopeptidases (Tyan *et al.,*2012). Results showed cancer cells are capable of inducing normal stromal fibroblasts to secrete ADAMTS1 after co-culture (Tyan *et al.,*2012). Significantly, this study also highlights the induced change from a 'normal' to 'cancer promoting' myofibroblast phenotype was not a transient process, but were retained after multiple passages, suggesting these changes were in some way epigenetically programmed. In the field of gastric cancer, further work is required to establish whether the induced metabolic phenotype in 'normal myofibroblast' cells is retained after co-culture with AGS cancer cells is stopped. This would provide a more thorough picture to establish if these changes are epigenetic and offer further insight into this model. Additionally, further work establishing the phenotypic effects of these metabolic changes, such as invasion, migration and responses to therapeutic drugs would provide new insight into the molecular mechanisms of tumour progression and novel therapeutic options.

Chapter V

Discussion

5.0 Discussion

5.1 Summary and Conclusions

This study provides novel insight into mechanisms of paracrine communication and stromal cell programming in gastric cancer. Initial analysis of differential gene expression profiles resulting from exposure of AGS cells to conditioned media derived from different populations of primary myofibroblasts demonstrated that cancer derived myofibroblasts have unique properties that are retained in purified low-passage primary cultures. Comparative analysis of differential changes in gene expression profiles also provided new insight into molecular mechanisms, pathways and transcriptional networks, which operate in different classes of stromal myofibroblasts. In particular, we identified a clear pattern of imposed metabolic changes, which may well play a key role in the progression and prognosis of gastric cancer.

5.2 Bioinformatic Analysis of Co-Culture Data

In terms of CAM-to-AGS communication, pathways associated with inflammation and immune evasion were found to be most differentially regulated following exposure of AGS cells to CAM and ATM myofibroblast conditioned media. As chronic inflammation, gastritis and infection, are known to be causative factors in many cases of gastric cancer, this observation is in agreement with currently accepted models of gastric tumour development (Fox *et al.,*2007 and Bornschein *et al.,* 2010).

Previous collaborative work in our laboratories (Varro and Sanderson) identified retained metabolic signatures in primary CAMs (Jones *et al.*, unpublished data). In this study, we wanted to determine whether these changes confirmed reciprocal CAM-specific changes in the metabolic status of AGS cells. Subsequent pathway enrichment analysis showed that CAM conditioned media induced changes in the PPAR–α pathway, which is associated with the regulation of the transporter channel MCT1. Activation of specific metabolically linked transcription factors, such as SP1 (Archer *et al* 2011) were identified in CAM conditioned AGS cells. Interestingly, similar reciprocal changes in metabolic regulation have also been observed in other cancer models, and these changes are often associated with a more aggressive phenotype (Martinez-Outschoorn *et al.,* 2011) and poor patient prognosis. This study suggests that markers of this form of reprogramming may also have utility in diagnosis and prognostic prediction in gastric cancer.

5.3 Metabolic Signatures in CAM cells

Following analysis of data from CAM conditioning of AGS cells, a series of experiments were planned to investigate the metabolic signatures identified from previous microarray analysis (Jones *et al.*, unpublished data). Results from these studies show that CAMs and NTMs retained functional and phenotypic differences both at protein and mRNA levels. In particular, CAM cells showed up-regulation of GLUT1 and MCT4 channels, both metabolic markers that are synonymous with active glycolysis. These cell-types also exhibited low levels of staining with Mitotracker™, indicating predominantly of less ‘active’ aerobic respiration takes place. Whilst these changes were

consistently observed across a selection of primary CAM cell lines, further investigations would need to be carried out to establish if there are more subtle differences between CAMs derived from early or late stage patient subgroups (Varro lab, Jones *et al.,* unpublished data). It may be expected that greater changes in metabolic signatures observed in CAM cell lines might correlate with a worse patient survival and prognosis score, as these metabolic changes feed the cancer cells, supplying more ATP for tumour growth and metastasis. Further analysis of CAM cell lines using other biochemical assays such as ketone and lactate kits would provide further information to quantify the production of Ketone bodies or pyruvate in different myofibroblast populations

5.4 Re-programming of Normal Tissue Myofibroblasts

Gastric tissue is relatively unique as activated myofiboroblasts are also found in normal healthy gastric tissues. These cells, however, are functionally different to CAMs taken from the site of a tumour, or from tissue adjacent to developing tumours, showing differences in microarray gene expression profiles, transcription factor expression and metabolic gene expression. However, data presented in this thesis show that NTMs can be re-programmed *in vitro* by co-culture with AGS gastric cancer cells.

5.5 Future work and the potential for therapeutic intervention

Data presented in this thesis reveal the therapeutic potential of MCTs in the treatment of gastric cancer. The use of MCT inhibitors in the treatment of solid tumors is relatively new; currently an MCT1 inhibitor is undergoing phase 1 clinical trials for the treatment of solid tumours, whilst MCT4 inhibitors are currently undergoing development, but as yet there is no available data on the success of these drugs in the clinic. In general, MCTs offer an attractive option for intervention in the development of aggressive forms of gastric cancer, which are not responding to conventional treatment. Potentially MCT inhibitors could be used after primary patient treatment, to disrupt the paracrine communication between the tumour and it's stroma, and to prevent micro-metastasis and secondary cancer growth.

Intervention using MCT1 inhibitors may however, pose a number of problems; firstly there is an assumption that tumours either rely on mitochondrial respiration or switch to glycolysis. However, this may be a very simplistic view as many late stage tumours may have areas of hypoxia, where cells would preferentially rely on glycolysis. As such, they will have areas of pseudo-hypoxia and they may also have areas of high oxidative phosphorylation. Therefore, inhibition of MCT1 may not be successful in cases where there exists a mixture of tumour niches. Also, where it is effective, blocking intake of high-energy metabolites (by inhibition of MCT1) may cause further evolution of the cell to rely on alternative means of ATP production, such as fatty acid pathways or activation of GCN2, which can act to induce ATF4 which can act to drive cell proliferation, evasion of apoptosis and adapt a metabolic response (Ye *et al.,* 2010).

MCT1 is proposed to be the major regulator of bidirectional monocarboxylic acid transport between the brain and the blood (Smith *et al.,* 2006). As discussed previously, the tumour stroma relationship mirrors the paracrine communication that exists between astrocytes and neurones within the brain. As lactate does not cross the blood-brain barrier easily, neurons obtain lactate from neighboring astrocytes via monocarboxylate transporter channels (Pellerin *et al.,* 1998). Interfering with this natural lactate shuttle in the brain could have serious deleterious effects on neuronal survival and brain function.

The mechanisms by which MCT1 is regulated are still poorly characterised. Whilst its expression varies in response to external environmental stimuli, the controlling pathways and molecular regulation up-stream of this is not well elucidated. In this study we show that the PPAR-α pathway is differentially regulated in response to CAM conditioning of AGS cells. Also, PPAR-α is known to regulate MCT1 expression in cells (König *et al.,* 2008).

Further knowledge and understanding of other pathways controlling the regulation of MCTs would be beneficial and could provide additional therapeutic options; for example, selecting a molecular target up-stream of MCT1, which induces over-expression via a cancer specific pathway could be one way of specifically targeting MCT1 in cancer cells, whilst avoiding detrimental effects in healthy cells. Data presented in this thesis show that CD147 expression is induced in AGS cells treated with CAM media, in the

same pattern as MCT1 expression. CD147 is known to form a complex with MCT1 and MCT4, and could offer further options for therapeutic intervention.

5.6 Concluding Remarks

Since the initial postulation of the 'Warburg Effect', there have been numerous studies that have concluded that cancer cells switch to aerobic glycolysis over mitochondrial respiration (Schulze *et al.,* 2011, Salminen *et al.,* 2010 and Cai *et al.,* 2010). However, many of these studies do not take into account the complex nature of the cancer microenvironment. Results presented in this thesis support a reverse Warburg type effect in gastric cancer, whereby cancer cells program surrounding cells to provide nutrients, thus enabling cancer cells to maintain an increased rate of mitochondrial respiration. Interestingly, we also found that AGS cells also exhibited some markers of glycolysis, such as, up regulation of GLUT1 and HK1. This suggests that cancer cells may either be utilising both forms of respiration, switching from one form to the other, or that different cells within the total population exhibit different profiles. Further studies utilising quantitative *in vitro* and *in vivo* models are required to differentiate between these possibilities.

The dynamic tumour microenvironment, involves a combination of immune cells, stem cells, fibroblasts and proliferative tumour cells ultimately the complex patterns of combinatorial crosstalk between all of these cell types will determine the efficiency of tumour growth. In this context it will be important to develop improved multi cell co-culture systems in which the relative contribution and proportions of each cell type can be studies and quantified in

order to develop mathematical models, which allow the consequences of sequential and combined perturbations to be modelled in order to guide development of optimal therapeutic strategies.

Therefore in conclusion it is important to take into consideration the various factors in the processes of tumour growth and development, and to recognise that tumour cells do not rely on glycolysis or mitochondrial respiration as mutually exclusive events. Work from this thesis has demonstrated that in a gastric cancer model, there can be a switch of stromal cells to become 'feeder' cells, which support the growth of neighbouring cancer cells, and these changes could be exploited to develop novel therapeutic agents to work in conjunction with chemotherapy.

Our data supports the hypothesis that the microenvironment does have an important role to play in energy metabolism and thus the growth of tumour cells. Our results support the concept of tumour compartmentalisation in energy metabolism and the metabolic shunting of high energy metabolites, depending on the needs of the cancer cells. It is evident clear that the tumour microenvironment is a dynamic and evolving system, in which both tumour and stromal cells continually adapt to provide an environment that is supportive of sustained but regulated tumour growth, and continued work in this area will provide more understanding of the complexities of this relationship.

Chapter VI

Materials and Methods

6.1 Materials

6.1.1 Reagents and Materials

AGS gastric cancer cell line was obtained from the American Type Culture Collection (VA, USA)

Antibiotic-antimycotic solution (Sigma, Poole, Dorset, UK)

BCA Protein Assay (Thermo Scientific, UK)

BD Control Cell Culture Inserts and BD BioCoat Matrigel Invasion Chambers (BD Biosciences, Massachusetts, USA)

Blocking Reagent (Biorad UK)

Bovine serum albumin (BSA; Jackson Immuno Research Laboratories, Suffolk, UK)

Cell-Tak Cell Solution (BD Biosciences, UK)

Clarity™ Western ECL Blotting Substrate (Biorad, UK)

Click-iT® EDU proliferation Assay (Life Technologies, UK)

Dulbecco's Modified Eagle's Medium (Sigma, Poole, Dorset, UK)

Fetal bovine serum (FBS; Perbio, Cheshire, UK)

GeneChip©Human Genome U133 Plus 2.0 arrays (Affymetrix, Santa Clara, CA, USA)

Kodak X-Omat XAR-5 film (Sigma, Poole, Dorset, UK)

Mini-PROTEAN pre-cast gels (Biorad, UK)

Mitotracker CMXRos dye (Life Technologies, UK)

Nitrocellulose Membrane (Life Technologies, UK)

Non-essential amino acid solution (Sigma, Poole, Dorset, UK)

PageRulerTM Plus Prestained Protein Ladder (Fermentas, York, UK)

Penicillin-streptomycin solution (Sigma, Poole, Dorset, UK)

Phosphatase Inhibitor Cocktail set II, EDTA-Free (Calbiochem, USA)

Protease Inhibitor Cocktail Set III, EDTA-Free (Calbiochem, USA)

Quant-iT PicoGreen ds DNA kit (Life Technologies, UK)

Quick Diff Kit for cell stain (IBG Immucor Limited)

RNeasy kit (Qiagen, West Sussex, UK)

Sequencing-grade modified trypsin (Promega, WI, USA)

TWEEN20 (Sigma, Poole, Dorset, UK)

Water (H20) used in all experiments was Millipore double filtered water.

Whatman 3mm paper, Z763187 (Sigma, Poole, Dorset, UK)

6.1.2 Solutions and Equipment

The antibodies used for the work carried out in this thesis are listed below [table 20], together with the species of antibody (M= Mouse and Rb=Rabbit) and dilution used. Antibodies were used for both western blotting (WB) and Immunofluorescence (IF) techniques. Antibodies for western blotting were diluted in 5% blocking buffer [table 22], antibodies for immunofluorescence were diluted using 3% BSA [table 20].

Antibody	**Antigen**	**Dilution Factor**	**Buffer**	**Company and lot number**
Rb α MCT1	Human MCT1	1:500		Santa Cruz (sc-14916)
Rb α MCT4	Human MCT4	1:500		Santa Cruz (sc-50329
Rb α GLUT1	Human GLUT1	1:1000	5 % milk in PBST/	Abcam(ab40084)
M α Tubulin	Human Tubulin	1:1000		Abcam(ab6046)
Rb α CD147	Human CD147	1:500		Abcam(ab64616)
Donkey α Rb HRP	IgG	1:10,000	3% BSA	Jackson(715-001-003)
Donkey α M HRP	IgG	1:10,000		Jackson(711-001-003)

Table 20. Antibodies and dilutions used in the work presented in this thesis.

Equipment	Manufacturer and Model
Seahorse metabolic analyser	Seahorse XF^{e} 24 Flux Analyser, Seahorse Biosciences
Benchtop centrifuge	Eppendorf centrifuge
qPCR machine	Biorad CFX Connect
Semi dry blotter	Biorad Trans- Blot
Wet transfer blotter	Biorad Protean
Live cell microscope	Multiphoton two
Fixed cell microscope	Olympus 1x81
Nanodrop 2000	Thermo Scientific

Table 21. Equipment used to carry out the work presented in this thesis.

The compositions of all buffers used within this thesis are described in the table below [table 22]. Water was the standard solvent used unless otherwise stated.

Buffer	Composition
3 x sample buffer	For 100 ml: 2.3 g Tris base, 9.0 g SDS, 30 ml glycerol, adjust volume to 90 ml with dH_2O, 50 mg bromophenol blue, add 10% β-mercaptoethanol
Mammalian cell lysis buffer	100µl RIPA buffer containing 1% protease and 1% phosphatase inhibitors
Ponceau	0.2% Ponceau red in 1% acetic acid
SDS-PAGE stacking buffer	Acrylamide/Bis, ddH2O, 1.5M Tris-HCl pH 8.8, 10% SDS, 10% APS, TEMED
SDS-PAGE separating buffer	Acrylamide/Bis, ddH2O, 1.5 M Tris-HCl pH 8.8, 10% SDS, 10% APS, TEMED
SDS-PAGE running buffer	0.2 g/l Tris base, 188 g/l glycine, 10 g/l SDS
Transfer buffer	14.4 g Glycine, 3.03 g Tris, 800 ml Water and 200 ml methanol
MOPS Buffer	Dilute 20x MOPS buffer in ddH2O
Blocking buffer	5% blocking reagent in 50ml 1XPBS plus 1% tween
Wash Buffer	1XPBS plus 1% tween

Table 22. Buffers used to carry out the work presented in this thesis

6.2 Methods

6.2.1 Primary Myofibroblast Cell Extraction (Varro Laboratory)

Biopsies were taken from 14 patients with gastric cancer in Szeged hospital, Hungary. Myofibroblast cells taken from tissue in the tumour stroma are referred to as cancer associated myofibroblasts (CAMs) in 12 of the patients, biopsies were also taken from the tissue adjacent to the tumour site, these myofibroblast cells are referred to as adjacent tissue myofibroblasts (ATMs). As a control, myofibroblasts from normal tissues were extracted from 12 post mortem organ donors who had no known underlying medical conditions, these cells are referred to as normal tissue myofibroblasts (NTMs). These patient samples are shown in table 23. All work was approved by the Ethics Committees of the University of Szeged, Hungary.

Label	Sample	Sample type
1-CAM	Sz42/1 P5	Cancer
1-ATM	Sz42/2 P5	Adjacent
2-CAM	Sz45/1 P5	Cancer
2-ATMA	Sz45/2 P5	Adjacent 1
2-ATMB	Sz45/22 P7	Adjacent 2
3-CAM	Sz190/1 P4	Cancer
3-ATM	Sz190/2 P4	Adjacent
4-CAM	Sz192/1 P5	Cancer
4-ATM	Sz192/2 P5	Adjacent
5-CAM	Sz194/1 P5	Cancer
5-ATM	Sz194/2 P5	Adjacent
7-CAM	Sz198/1 P5	Cancer
7-ATM	Sz198/2 P5	Adjacent
8-CAM	Sz268/1 P5	Cancer
8-ATMA	Sz268/2 P5	Adjacent 1
8-ATMB	Sz268/22 P5	Adjacent 2
9-CAM	Sz271/1 P5	Cancer
9-ATM	Sz271/2 P5	Adjacent
10-CAM	Sz294/1 P4	Cancer
10-ATMA	Sz294/2 P5	Adjacent 1
10-ATMB	Sz294/22 P4	Adjacent 2
11-CAM	Sz305/1 P5	Cancer
11-ATMB	Sz305/22 P5	Adjacent 1
12-CAM	Sz308/1 P5	Cancer
12-ATM	Sz308/22 P6	Adjacent
13-CAM	Sz187/1 P8	Cancer
14-CAM	Sz197/1 P5	Cancer
15-CAM	Sz389/1 P7	Cancer
15-ATM	Sz389/2 P7	Adjacent
21-ANMA	Sz196/2 P5	Normal Tissue Myofibroblast
22-ANMA	Sz241/2 P6	Normal Tissue Myofibroblast
22-ANMB	Sz241/22 P6	Normal Tissue Myofibroblast
23-ANMA	Sz246/2 P6	Normal Tissue Myofibroblast
23-ANMB	Sz246/22 P6	Normal Tissue Myofibroblast
24-ANMA	Sz261/2 P6	Normal Tissue Myofibroblast
24-ANMB	Sz261/22 P6	Normal Tissue Myofibroblast
25-ANMA	Sz279/22 P4	Normal Tissue Myofibroblast
26-ANMA	Sz334/2 P5	Normal Tissue Myofibroblast
26-ANMB	Sz334/22 P5	Normal Tissue Myofibroblast
27-ANMA	Sz351/2 P5	Normal Tissue Myofibroblast
27-ANMB	Sz351/22 P5	Normal Tissue Myofibroblast
28-ANMB	845P7	Normal Tissue Myofibroblast

Table 23. Table detailing full list and labelling of primary patient myofibroblasts with passage number and sample type

Sz187	Sz197	Sz389	Sz192	Sz45	Sz195	Sz294	Sz268	Sz271	Sz194	Sz308	Sz305	Sz190	Sz198	Sz42	Patient code	
CagA +ve	CagA +v	None	CagA +ve	None	CagA +ve	None	CagA +ve	None	*H.pylori*	*H.pylori*	CagA +ve	None	*H.pylori*	None	*H.pylori* status. H.pylori = infected CagA +ve =cagA strain detected None = No H.pylori infection	
F	M	M	F	M	F	F	M	M	M	M	M	F	M	M	Gender	
39	54	67	49	82	85	84	76	72	76	51	59	65	77	72	Age	
TOTAL	TOTAL	DISTAL	TOTAL	DISTAL	DISTAL	TOTAL	TOTAL	TOTAL	DISTAL	TOTAL	TOTAL	TOTAL	DISTAL	TOTAL	Type of resection	
0	0	1	0	1	1	1	0	0	1	0	0	0	1	0	Anaemia HGB<100G/L or Blood Transfusion	
0	0	0	1	0	0	0	1	1	0	0	1	1	1	0	BMI <19 or Bodyweight loss >10KG	
4	2	3	3	3	1	3	4	4	1	1	3	4	2	1	pTNM	T
2	0	1	2	2	1	0	2	1	0	2	2	0	0	0		N
0	0	0	0	0	0	0	0	0	0	0	0	2	0	0		M
3	3	2	3	3	3	3	3	3	1	3	3	3	2	3	Grade	
0	1	0	1	0	1	0	0	1	0	1	1	1	0	0	Histological type: Intestinal or diffuse	
0	0	0	1	1	0	0	0	0	0	1	0	0	0	0	Lymphatic vessel invasion	
1	0	0	0	0	0	0	1	1	0	0	0	0	0	0	Vascular invasion	
1	0	0	0	1	0	0	0	0	0	1	1	0	0	0	Positive margins of resection	
0	0	0	0	0	0	0	0	0	1	1	1	0	0	0	Serological tumour marker-elevation	
0	0	0	0	0	0	0	0	0	0	1	1	1	0	0	Tumour recurrence	
0	0	0	0	0	0	0	0	0	0	1	0	0	0	0	Synchron or metachron tumour	With surgical intervention
0	0	0	0	0	1	0	0	1	0	0	0	0	1	1		Without surgical intervention
15.5.07	16.8.07	2.7.06	21.5.07	26.6.06	7.8.07	5.12.07	6.11.07	13.11.07	6.8.07	8.1.08	3.1.08	18.5.07	27.8.07	16.6.06	Date of operative	
42	62	50	22	2	13	51	15	24	60	9	17	5	60	75	Survival (months)	
			29.3.09	8.06	14.9.07	12.3.12	2.09		1.9.12	19.10.08	1.8.09	14.10.07	10.9.12		Exit	
11	6	7	11	11	9	7	11	12	4	12	12	13	7	5	Total	
6	6	6	4	6	6	6	6	5	6	3	6	6	4	6	Myoscore	

Table 24. Patient information relating to the scoring details . Row displaying the total represents the prognosis score and is calculated based on the sum of all the variables. If the value is left blank the patient is not deceased.

6.2.2 Myofibroblast Cell Line Generation and Culture

Primary myofibroblast cells were isolated from tissue samples and cultured by Peter Hegyi, (Department of Medicine, University of Szeged, Hungary), as previously described (McCaig *et al.,* 2006). Primary myofibroblasts were cultured in Dulbecco's Modified Eagles Medium supplemented with 10% Fetal Bovine Serum, 2% Antibiotic-Antimycotic solution, 1% Penicillin-Streptomycin Solution, and 1% Non- essential amino acid solution. Cells were maintained at 37 ℃ and 5% CO^2 and media was changed approximately every 60 hours. When the cells reached 70 – 80 % confluence the cells were split by washing in Dulbecco's Phosphate Buffered Saline before adding 0.25% trypsin for 4 to 5 minutes and cell passage number was noted. In all experiments cells were not passaged beyond passage 14 as it has been documented previously that primary cells may become senescent and stop proliferating after this point.

6.2.3 AGS Cell Culture

AGS cells were grown in Dulbecco's Modified Eagles Medium supplemented with 10% Fetal Bovine Serum 1% Antibiotic-Antimycotic and 1% Penicillin-Streptomycin Solution. Cells were maintained at 37 ℃ and 5% CO^2 and cells were passaged or media was changed approximately every 46-72 hours.

6.2.4 Generation of Conditioned Media

CAM cells were seeded at a density of 1,000 cells/ml, and left to grown for 24 hours. After being washed three times in Dulbecco's Phosphate Buffered Saline, Dulbecco's Modified Eagles Medium without fetal bovine serum was added to the cells, and they were left to grown for 24 hours. The following day media was collected and centrifuged for 7 minutes at 800g, the supernatant was removed and this was used for the conditioning experiments.

6.2.5 AGS Cell Conditioning for Microarray Analysis (Varro Laboratory)

AGS cells were cultured onto 10 cm dishes and left to grow for 24 hours at a density of 1 million cells per ml. After being washed three times in Dulbecco's Phosphate Buffered Saline, the conditioned media from cancer associated myofibroblasts and adjacent tissue myofibroblasts was added to a confluent monolayer of AGS cells. Dulbecco's Modified Eagles Medium without fetal bovine serum added to AGS cells was used as the control. After 24 hours the cells were ready to be used for RNA extraction and subsequent microarray analysis.

6.2.6 RNA Extractions, Gene Microarray and Normalisation (Varro Laboratory in Collaboration with Dr Jithesh Puthen, Liverpool University Statistician)

AGS Cells were cultured in conditioned media (as previously described) and RNA was extracted using an RNeasy Kit from Qiagen according to manufacturer's protocol. This work was carried out by Dr I. Steele (Varro Lab). RNA quantity and quality was determined before microarrays were carried out. Gene microarrays were conducted on AGS cells cultured with

media from five patient CAM cell lines, plus their paired ATMs, with serum free media is used as the control [table 25]. The samples were processed using the GeneChip® Human Genome U133 Plus 2.0 Array at the Liverpool Genome Research Facility by Dr Lucille Rainbow.

The Human Genome U133 plus 2.0 Array allows analyses of 38,700 genes. Affymetrix Genechips are designed so that each gene is matched to 11 pairs of probes, which are used to measure the level of expression. These probes are evenly distributed throughout the chip to detect any noise within the genechip and to allow for effective normalisation of the datasets. The probes consist of perfect and mis-match probes; mis-match probes are subtracted from perfect match probes to give the true signal value. Each chip also contains probes which measure non-specific binding of cRNA which is another way to eliminate non-specific signals and to normalise the data effectively. To ensure quality control between different arrays, there is also a selection of normalisation probes, which have constant levels of expression. These are therefore used to normalise signals across multiple arrays.

The GeneChip® Scanner 3000 was used for imaging the arrays, and quality control was performed using Affymetrix micro-array 5 QC metrics by Dr Helen Smith (The University of Manchester). The statistical analysis of gene expression profiles was performed in GeneSpring GX.10 and experiments were normalized by RMA analysis using PARTEK© software (Jithesh Puthen, University of Liverpool). The gene lists were then analysed for differential regulation.

Label	Sample	Sample type
3-CAM	Sz190/1 P4	Cancer
3-ATM	Sz190/2 P4	Adjacent
4-CAM	Sz192/1 P5	Cancer
4-ATM	Sz192/2 P5	Adjacent
10-CAM	Sz294/1 P4	Cancer
10-ATMA	Sz294/2 P5	Adjacent 1
11-CAM	Sz305/1 P5	Cancer
11-ATMB	Sz305/22 P5	Adjacent 1
12-CAM	Sz308/1 P5	Cancer
12-ATM	Sz308/22 P6	Adjacent
CONTROL		
CONTROL		
CONTROL		

Table 25. Table detailing full list and labelling of ASG microarray data generated from conditioning with primary patient myofibroblasts media. Table highlights cells passage number and sample type**.**

6.2.7 Differentially regulated oligonucleotide lists

Microarray data was analysed using Partek© and the data was normalized by RMA and then batch corrected by Jithesh Puthen (The University of Liverpool) as the microarrays were carried out across different days. ANOVA analysis was performed to generate p-values across the data sets. Gene lists were processed and a cut off value of $p<0.05$ and a fold change cut off of 1.6 was applied as an arbitrary value to filter the gene sets.

For single patient data, log fold changes were calculated for individual patients from intensity values and the averages from the serum free controls. A arbituary fold cut off of $\log_2(1.6)$ was applied and data was uploaded into various pathway analysis software packages.

6.2.8 Metacore™

Metacore™ (GeneGo Inc) is a commercial integrated software suite for network and pathway analysis. Metacore™ allows different data-types to be

uploaded, visualised and analysed with the use of its manually curated knowledge database of protein- protein interactions, transcription factors, drug targets, metabolic pathways and signaling pathways.

6.2.9 Ingenuity

Ingenuity is a commercially available integrated software suite for network and pathway analysis. The software allows for different data types to be uploaded, visualised and also analysed with the use of its knowledge database of signaling pathways. Gene lists were uploaded into ingenuity following normalisation and processing as described previously. A core analysis function was selected to process the data, and pathway, network and transcription analyses were generated.

6.2.10 Genevestigator

Genevestigator is a software platform that can be used to obtain information and insight into expression profiles of specific genes of interest, including; identifying cancers, diseases or conditions, which overexpress the target gene. The software can also cluster related genes or multiple genes of interest to look at co-expression and down-stream targets. To carry out Genevestigator analysis, probe database Human Affymetrix HG-U33 Plus was selected and uploaded into the software platform. Genes associated with neoplasms and cancer cell lines databases were also accessed and uploaded into the database in order to run gene search algorithms and co-expression analysis. Data was exported into ImageJ as a heatmap in order to visualise gene expression patterns across the datasets.

6.2.11 Mitotracker Staining

Cancer Associated Myofibroblast Cells and Normal Tissue Myofibroblast Cells between passages 5 and 10 were cultured on 35mm four chambered glass bottomed dishes to reach 80% confluency in DMEM full media. Cell media was removed and replaced with DMEM media containing 150nm Mitotracker CMXRos dye. Dishes were incubated in the dark at 37^{o}C, 5% Co^{2} for 25 minutes before cells were washed three times in 1 xPBS. Fresh DMEM full media was added to the dishes before live cell imaging at 560nm using the 63x oil emersion lens on the Multiphoton 2 microscope. Images were taken and analysed using ImageJ software. Images were imported into ImageJ software and then mitochondria intensity was quantified and recorded, before analysis in GraphPad Prism Software. GraphPad software was used to plot the data and a one-way ANOVA was carried out to determine statistical significance between data sets.

6.2.12 Preparation of Cell Dishes with Cell-Tak

Cell-Tak was prepared from stock solution, 20µl was added to sodium bicarbonate with 10µl of hydrochloric acid (1M). 50µl of Cell-Tak solution was then added to each well of the Seahorse XF Flux Analyser 24 well plates and left to coat the wells for 20 minutes. The Cell-Tak was then removed and 200µl of autoclaved water was then used to wash each well, plates were left to dry for an houbefore the cells were seeded.

6.2.13 XF Extracellular Flux Analyser

To investigate glycolytic capacity and oxygen consumption rate in cells, cells were split onto 24 well XF Seahorse Flux analyser cell dishes, which had been

pre-treated with BD Sciences Cell-Tak. Four wells were left free of cells, to be used as the background control for each condition. Ten wells were treated with metabolic drugs while control wells were left untreated. For all Seahorse experiments, cells were serum starved overnight and the following day media was replaced with 450ul of Seahorse Assay media. XF assays require a non-buffered medium to accurately measure extracellular acidification rate and proton production rate of cells growing in culture. The Seahorse Assay media is based on the formulation of DMEM, including 2 mM of L-glutamine (as L-alanyl-glutamine) but without sodium bicarbonate, glucose, or sodium pyruvate. 60 minutes prior to running the experiment, the XF24 cell culture plate was placed in a 37℃ incubator, without CO2 to allow cells to equilibrate to the new media. 1.0 ml of Seahorse Bioscience XF24 Calibrant pH 7.4 was added to each well of a Seahorse Bioscience 24-well sensor cartridge plate, this was stored at 37oC without CO2 overnight. The sensor cartridge plate contains wells that have ports that are used to inject the cell media with compounds; port A contains 50ul 10mM glucose, port B 55ul oligomycin (1ug/ul) and port C 100uM deoxyglucose. Real-time measurements of OCR and ECAR are made by probes isolating a small volume of cell media above the cells on the seahorse plate. Cellular oxygen consumption (respiration) and proton excretion (glycolysis) cause changes to the concentrations of dissolved oxygen and free protons, which are measured at second intervals by the probes. Results for each set of measurements were recorded using the Seahorse XF Flux Analyser software. Data was imported into Graph pad prism software and analysed following normilisation to DNA (see below) data was expressed as averages of each substrate injection and one-way ANOVA analysis was performed to determine differences between cell subsets and

conditions.

6.2.14 DNA Normalisation

Seahorse results were normalised to DNA concentration to account for any potential variability in cell seeding number. To prepare plates for the DNA assay all liquid was removed from each well. Quant-iT PicoGreen ds DNA kit was used to measure DNA concentration. Cell lysis buffer was prepared; 0.5M EDTA, 180 mM NaCl and 0.5 ml of 20x TE lysis buffer, 200ul of RNase A was also added to the lysis buffer to remove any RNA contaminates. 50ul of lysis buffer was added per well and plates were incubated at room temperature for one hour, rocking gently. 40ul of the samples were incubated in a 96 well plate and mixed with 40ul Quant-iT PicoGreen dsDNA reagent dye. DNA standards were also set up in triplicate from lambda DNA standard stock solution ranging from 1ug/ml to 1ng/ml. Samples were excited at 480 nm and the fluorescence emission intensity was measured at 520 nm. Fluorescence emission intensity was then plotted versus DNA concentration to create a standard curve using Graph Pad Prism Software from the DNA standards. DNA concentration from the cell samples was extrapolated from the standard curve and then used for normalisation.

6.2.15 Cell Fixation for IF Using Paraformaldehyde

Cells were grown on glass coverslips in DMEM full media at a density of 1,000 cells / ml for 24 hours to obtain 80% confluency. Cells were washed three times in 1xDPBS before being fixed for 15 minutes in 4% PFA. After fixation, cells were washed three times in 1xPBS then quenched in 50mM ammonia

chloride for 10 minutes. After further washing with 1xPBS, the cells were then permeabilised in 0.2% triton-X for 10 minutes. The coverslips were then blocked for one hour in 3% BSA. Following blocking the cells were then incubated for one hour in primary antibody [table 20] then washed three times in 1xPBS, before being incubated in secondary antibody for one hour [table 20] then were washed again three times in 1xPBS. Coverslips were left to air dry on whatman 3mm paper for 10 minutes before being mounted onto slides with ProLong Gold plus DAPI.

6.2.16 Cell Imaging and Analysis

Fixed coverslips were imaged using the Zeiss fixed cell microscope. Images were captured then analysed using ImageJ. Images were imported into ImageJ and then image intensity was quantified.

6.2.17 RNA Extraction for Real Time PCR

AGS cells between passages 20 to 25 were grown at in 10cm dishes in 37^{o}C, 5 % C02, until they reached 60-70 % confluency. AGS cells were then washed three times in 1xPBS before 10ml conditioned media from CAMs was added to these cells for 24 hours. After 24 hours the cells were washed again three times in 1xDPBS before being trypsinised for 5 minutes and then centrifuged at 1000 rpm. Cells were then washed again three times in 1xPBS and centrifuged at 1000 rpm to remove excess media, then RNA was extracted according to the Qiagen RNAeasy Kit manufacturers protocol. RNA concentration and purity was measured using the nanodrop 2000. 2µg of RNA was used per reverse transcriptase reaction. cDNA reverse transcription was carried out using AMV reverse transcriptase, DEPEC treated water,

oligo(dT) 15 primer, 10mM deoxynucleotides and recombinant RNasin® ribonuclease inhibitor, according to manufacturers instructions. Reverse Transcription reactions were aliquoted in 10ul volumes to prevent cDNA degradation due to freeze thaw cycles.

qPCR primers were designed using Vector NTI software; mRNA sequences were imported into the Vector NTI database, and the parameters for primer design were set; the melting temperature was established between 55°C and 65°C, the GC content between 40-60% and the amplicons were set to 70-100 base pairs. Using these parameters, primer sequences were generated and ordered. For all primer sets ordered, primers were optimised first and checked for efficiency and for melt curve formation (in case of primer dimers).

Primers for qPCR		
	Forward	**Reverse**
Mct1	5'-CTT-TTG-TTG-ACA-TGG-TAG-CCC-GAC-3'	5'-ATT-TGC-ACC-CAT-GTC-TGC-TT-3'
GLUT1	5'-CGC-TGG-ACC-CAT-GTC-TGG-TT-3'	5'-CAG-TGC-TTG-GCT-CCC-TGC-AGTT-3'
GAPDH	5'-CCG-CTT-CGC-TCT-CTG-CTC-CTC-3'	5'-TGC-TGA-CCA-GGC-GCC-CAA-3'
CEACAM5	5'-TCA-GCA-GGG-ATG-CAT-TGG-GG-3'	5'-CGT-TGG-GGG-GAG-AGA-AA-3'
IGFBP5	5'-CGT-TGG-GGG-GAG-AGA-AA-3'	5'-TGC-GTT-CCC-TGC-TTG-TCC-CA-3'
BETA-ACTIN	5'-AGG-CTG-TGC-TAT-CCC-TGT-ACG-C-3'	5'-ATG-GGC-ACA-GTG-TGG-GTG-AC-3'

Table 26. Table to show lists of primers used for qPCR experiments.

6.2.18 EdU Proliferation Assay for Flow Cytometry

AGS cells between passages 20 to 25 were used for flow cytometry proliferation assays. Cells seeded at 1,000 cells per ml and were grown for 24 hours in 10 cm dishes to reach 80% confluency. Cells were serum starved for 24 hours before being treated with conditioned media from CAM and NTM cells for 24 hours. 16 hours prior to cell harvesting, the dishes were treated with 10uM of EdU. Cells were washed three times in 1x PBS before being trypsinised and spun at 1,000 rpm. Cell pellets were washed in 3mls of 1%BSA before spinning again at 1,000 rpm. Click-iT fixative was added to cell pellets, and pellets were left for 15 mins in the dark, after washing once with 3mls of 1% BSA, cells were spun again at 1,000 rpm. Pellets were re-suspended in 100ul of 1 x click-iT saponin-based permeabilisation and wash reagent. The Click-iT® reaction cocktail was prepared according the manufacturers instructions. Cells were treated with 500ul of reaction cocktail for 30 minutes in the dark before washing in 3mls Click-iT saponin-based permeabilisation and wash reagent. Cells were again spun at 1,000 rpm to form a pellet, and resuspended in 500ul Click-iT saponin-based permeabilisation and wash reagent. Flow cytometric analysis was then performed at a low flow rate.

6.2.19 EdU Proliferation Assay for Immunoflurescence

AGS cells between passages 20 to 25 were cultured onto coverslips in 24 well plates to reach 80% confluence. Cells were serum starved for 24 hours before being treated with conditioned media from myofibroblast cells for 24 hours. 16 hours prior to cell harvesting, the dishes were treated with 10uM of EdU. Following incubation, coverslips were washed three times in 1x PBS before being fixed in 4% PFA for 15 minutes at room temperature. Coverslips were then washed twice with 1 mL of 3% BSA in PBS. After removal of BSA solution, 1 mL of 0.5% Triton® X-100 in PBS was added to each well for 20 minutes at room temperature to permeablise the cells. Following permeablisation, cells were washed twice with 1 mL of 3% BSA in PBS. The Click-iT® reaction cocktail was prepared according the manufacturers instructions. 0.5 mL of Click-iT® reaction cocktail was added to each well containing a coverslip and coverslips were incubated for 30 minutes at room temperature, protected from light, gently rocking to ensure the coverslips didn't dry out**.** The reaction cocktail was removed and then the cells were washed once with 1 mL of 3% BSA in PBS. Following this, each well was washed with 1 mL of PBS then cells were stained with Hoechst 33342 dye. Hoechst 33342 was diluted 1:2000 in 1xPBS to obtain a 1X solution of 5 μg/mL. 1 mL of 1X Hoechst 33342 solution was added per well, and plates were then incubated for 30 minutes at room temperature, protected from light and gently rocking**.** The coverslips were washed twice with 1 mL of PBS and coverslips were left out to dry on whatman 3mm paper before being mounted onto slides using Prolong Gold reagent.

6.2.20 Preparation of Cell Lysates

Cells were washed in 1X PBS then lysed in 1x RIPA buffer containing 1% protease and phosphatase inhibitors for 30 minutes on ice, samples were then centrifuged for 15 minutes at 13,000 rpm to pellet any debris. BCA assays were carried out in 96 well plates according to the manufacturers instructions, to determine the protein concentration in each sample. Lysates were mixed 1:1 with 3x SDS sample buffer [table 22] before boiling at 98 °C for 15 minutes; samples were then centrifuged at 13,000 rpm for 5 minutes. For all western blots, a final concentration of 20μg of protein was loaded per well.

6.2.21 Western Blotting

Proteins were resolved by SDS-PAGE using either 10% polyacrylamide gels as described in table 22 or 4-12 % pre-cast gels. Samples were heated at 98°C for 5 minutes before loading onto the gel. Gels were run for 1 hour 30 minutes, at 90 volts for 30 minutes, then one hour at 150 volts. Proteins were transferred from SDS gels to nitrocellulose membranes by a wet transfer method; whatman 3mm paper and nitrocellulose membrane were pre-soaked in transfer buffer for 10 minutes before the transfer was set up. The transfer was run for 1 hour at 300 mA and kept on ice. Membranes were stained with Ponceau-S [table 22] for 5 minutes, to check the transfer efficiency and then washed with distilled water until all stain was removed. The membranes were then incubated in 5% blocking buffer [table 22] to block unoccupied protein binding sites for one hour. After blocking, membranes were incubated in primary antibody [table 20] diluted in 5% blocking buffer for 1 hour at room temperature. The membrane was then washed three times for ten minutes in wash buffer [table 22]. Membranes were incubated with peroxidase-coupled

secondary antibody diluted in blocking buffer [table 20] for 1 hour at room temperature, then washed three times for ten minutes in wash buffer [table 22], before a final wash for ten minutes in 1 xPBS. Bound antibodies were detected by chemilluminescence using ECL Western blot detection reagents for 5 minutes according to manufacturers instructions. Membranes were placed protein side face up on cling film before being taped to the inside of an X-ray cassette. Kodak X-Omat XAR-5 film was placed over the membrane and films were exposed between 2 seconds to 10 minutes before being processed in developing reagent for two minutes, and then fixed in reagent for 5 minutes. Films were left to dry overnight. Films were scanned and images processed using Image J and Adobe Illustrator.

6.2.22 Boydon Chamber Migration Assays

Using an 80% confluent flask of AGS cells, cells were split and counted as previously described. Cells were centrifuged at 1,000 rpm for five minutes to form a pellet, and then re-suspended in 10 ml of media (9ml serum free DMEM media plus 1 ml DMEM plus 10% FBS media) to obtain a final cell concentration of 20,000 cells/ml. 10,000 AGS cells were seeded into each top insert in a final volume of 500ul serum free medium**.** In the lower compartment of the boydon chamber, 750ul of serum free, CAM and NTM conditioned media were added into the wells. The chambers were incubated overnight at 37°C, 5% Co2. The following day 24 well plates were prepared with quick diff kit solutions according to manufacturers instructions, to stain cells which had migrated through the membrane. Briefly, the inserts were placed in fixative for 8 minutes to fix cells to the membrane, then red cellular

stain for 5 minutes, then finally blue counterstain for 4 minutes. Inserts were then washed in distilled water before being left to dry. After drying, the membrane was removed from the inserts using a scalpel before being mounted onto a coverslip using a drop of immersion oil. Migrated cells were counted in 5 different fields at 10x on a light microscope, and then results were expressed as an average.

6.2.23 Gene Set Enrichment Analysis and array quality metrics report (Dr Helen Jones, Manchester University)

Array quality metrics reports were carried out using Bioconductor in R by Dr Helen Jones, Manchester University. Gene Set Enrichment Analysis was carried out using the GSEA software suit by Dr Helen Jones, Manchester University.

6.2.24 Statistical Methods and Analysis

For all immunofluorescence analyses ImageJ software was used to quantify intensity of fluorescence before being exported to Microsoft excel. Statistical analyses were carried out using Graphpad Prism software.

References

Abdulghani, J. *et al.* Stat3 promotes metastatic progression of prostate cancer. *Am. J. Pathol.* 172, 1717–1728 (2008).

Acharyya, S. *et al.* A CXCL1 paracrine network links cancer chemoresistance and metastasis. *Cell* 150, 165–178 (2012).

Akkiprik, M., Hu, L., Sahin, A., Hao, X. & Zhang, W. The subcellular localization of IGFBP5 affects its cell growth and migration functions in breast cancer. *BMC Cancer* 9, 103 (2009).

Al Jumah, M. A. & Abumaree, M. H. The immunomodulatory and neuroprotective effects of mesenchymal stem cells (MSCs) in experimental autoimmune encephalomyelitis (EAE): A model of multiple sclerosis (MS). *International Journal of Molecular Sciences* 13, 9298–9331 (2012).

Albini, A. & Sporn, M. B. The tumour microenvironment as a target for chemoprevention. *Nat. Rev. Cancer* 7, 139–147 (2007).

Allaman, I., Bélanger, M. & Magistretti, P. J. Astrocyte-neuron metabolic relationships: For better and for worse. *Trends in Neurosciences* 34, 76–87 (2011).

Almeida, R. *et al.* Expression of intestine-specific transcription factors, CDX1 and CDX2, in intestinal metaplasia and gastric carcinomas. *J. Pathol.* 199, 36–40 (2003).

Amann, T. *et al.* GLUT1 expression is increased in hepatocellular carcinoma and promotes tumorigenesis. *Am. J. Pathol.* 174, 1544–1552 (2009).

Anton, K., Banerjee, D. & Glod, J. Macrophage-associated mesenchymal stem cells assume an activated, migratory, pro-inflammatory phenotype with increased IL-6 and CXCL10 secretion. *PLoS One* 7, (2012).

Archer, M. C. Role of sp transcription factors in the regulation of cancer cell metabolism. *Genes Cancer* 2, 712–9 (2011).

Ashizawa, T. *et al.* Clinical significance of interleukin-6 (IL-6) in the spread of gastric cancer: Role of IL-6 as a prognostic factor. *Gastric Cancer* 8, 124–131 (2005).

Alkasalias *et al.,* Inhibition of tumor cell proliferation and motility by fibroblasts is both contact and soluble factor dependent. *PNAS* (2014).

Babu, S. D., Jayanthi, V., Devaraj, N., Reis, C. A. & Devaraj, H. Expression profile of mucins (MUC2, MUC5AC and MUC6) in Helicobacter pylori infected pre-neoplastic and neoplastic human gastric epithelium. *Mol. Cancer* 5, 10 (2006).

Banchereau, J., Pascual, V. & O'Garra, A. From IL-2 to IL-37: the expanding spectrum of anti-inflammatory cytokines. *Nature Immunology* 13, 925–931 (2012).

Barron, D. A. & Rowley, D. R. The reactive stroma microenvironment and prostate cancer progression. *Endocrine-Related Cancer* 19, (2012).

Baughman, J., Nilsson, R. & Gohil, V. A computational screen for regulators of oxidative phosphorylation implicates SLIRP in mitochondrial RNA homeostasis. *PLoS Genet.* 5, (2009).

Bélanger, M., Allaman, I. & Magistretti, P. J. Brain energy metabolism: Focus on Astrocyte-neuron metabolic cooperation. *Cell Metabolism* 14, 724–738 (2011).

Ben-Baruch, A. Inflammation-associated immune suppression in cancer: The roles played by cytokines, chemokines and additional mediators. *Seminars in Cancer Biology* 16, 38–52 (2006).

Bennett, G., Sadlier, D., Doran, P. P., Macmathuna, P. & Murray, D. W. A functional and transcriptomic analysis of NET1 bioactivity in gastric cancer. *BMC Cancer* 11, 50 (2011).

Bernstein, A. M., Twining, S. S., Warejcka, D. J., Tall, E. & Masur, S. K. Urokinase receptor cleavage: a crucial step in fibroblast-to-myofibroblast differentiation. *Mol. Biol. Cell* 18, 2716–2727 (2007).

Bhowmick, N. A., Neilson, E. G. & Moses, H. L. Stromal fibroblasts in cancer initiation and progression. *Nature* 432, 332–337 (2004).

Bianchini, F., Giannoni, E., Serni, S., Chiarugi, P. & Calorini, L. 22 : 6n-3 DHA inhibits differentiation of prostate fibroblasts into myofibroblasts and tumorigenesis. *British Journal of Nutrition* 1–9 (2012). doi:10.1017/S0007114512000359

Bissell, M. J. & Hines, W. C. Why don't we get more cancer? A proposed role of the microenvironment in restraining cancer progression. *Nat. Med.* 17, 320–329 (2011).

Biswas, S., Lunec, J. & Bartlett, K. Non-glucose metabolism in cancer cells--is it all in the fat? *Cancer Metastasis Rev.* 31, 689–98 (2012).

Blumenthal, R. D., Hansen, H. J. & Goldenberg, D. M. Inhibition of adhesion, invasion, and metastasis by antibodies targeting CEACAM6 (NCA-90) and CEACAM5 (carcinoembryonic antigen). *Cancer Res.* 65, 8809–8817 (2005).

Blumenthal, R. D., Leon, E., Hansen, H. J. & Goldenberg, D. M. Expression patterns of CEACAM5 and CEACAM6 in primary and metastatic cancers. *BMC Cancer* 7, 2 (2007).

Bonuccelli, G. *et al.* Ketones and lactate "fuel" tumor growth and metastasis: Evidence that epithelial cancer cells use oxidative mitochondrial metabolism. *Cell Cycle* 9, 3506–3514 (2010).

Borish, L. C. & Steinke, J. W. 2. Cytokines and chemokines. *J. Allergy Clin. Immunol.* 111, S460–S475 (2003).

Bornschein, J., Kandulski, A., Selgrad, M. & Malfertheiner, P. From gastric inflammation to gastric cancer. in *Digestive Diseases* 28, 609–614 (2010).

Bose, R. *et al.* Activating HER2 mutations in HER2 gene amplification negative breast cancer. *Cancer Discov.* 3, 224–237 (2013).

Branco-Price, C. *et al.* Endothelial cell HIF-1α and HIF-2α differentially regulate metastatic success. *Cancer Cell* 21, 52–65 (2012).

Brentnall, T., *et al.* Arousal of cancer-associated stroma: overexpression of palladin activates fibroblasts to promote tumor invasion. *PLoS One* 7, (2012).

Buck, M. B. & Knabbe, C. TGF-beta signaling in breast cancer. in *Annals of the New York Academy of Sciences* 1089, 119–126 (2006).

Buganim, Y. *et al.* Transcriptional activity of ATF3 in the stromal compartment of tumors promotes cancer progression. *Carcinogenesis* 32, 1749–1757 (2011).

Burke, W. M. *et al.* Inhibition of constitutively active Stat3 suppresses growth of human ovarian and breast cancer cells. *Oncogene* 20, 7925–7934 (2001).

Burkitt, M. D., Varro, A. & Pritchard, D. M. Importance of gastrin in the pathogenesis and treament of gastric tumors. *World Journal of Gastroenterology* 15, 1–16 (2009).

Cai, Z. *et al.* A combined proteomics and metabolomics profiling of gastric cardia cancer reveals characteristic dysregulations in glucose metabolism. *Mol. Cell. Proteomics* 9, 2617–28 (2010).

Calvo, F. & Sahai, E. Cell communication networks in cancer invasion. *Curr. Opin. Cell Biol.* 23, 621–9 (2011).

Calvo, F. *et al.* RasGRF suppresses Cdc42-mediated tumour cell movement, cytoskeletal dynamics and transformation. *Nat. Cell Biol.* 13, 819–26 (2011).

Cancer Research UK,. 'Cancer Research UK'. N.p., 2015. Web. 26 Feb. 2015.

Cao, D. *et al.* Expression of HIF-1alpha and VEGF in colorectal cancer: association with clinical outcomes and prognostic implications. *BMC Cancer* 9, 432 (2009).

Capparelli, C. *et al.* Autophagy and senescence in cancer-associated fibroblasts metabolically supports tumor growth and metastasis , via glycolysis and ketone production. *Landes Bioscience*. 2285–2302 (2012).

Catalano, V. *et al.* Gastric cancer. *Critical Reviews in Oncology/Hematology* 71, 127–164 (2009).

Cavallo, F., De Giovanni, C., Nanni, P., Forni, G. & Lollini, P. L. 2011: The immune hallmarks of cancer. *Cancer Immunology, Immunotherapy* 60, 319–326 (2011).

Cave, D. R. How is Helicobacter pylori transmitted? *Gastroenterology* 113, S9–S14 (1997).

Cell, N. The Role of Tumour Stroma in Cancer Progression and. 6, 209–217 (2011).

Chan, I. S. *et al.* Paracrine Hedgehog signalling drives metabolic changes in hepatocellular carcinoma. *Cancer Res.* 72, 6344–50 (2012).

Chandler, J. D., Williams, E. D., Slavin, J. L., Best, J. D. & Rogers, S. Expression and localization of GLUT1 and GLUT12 in prostate carcinoma. *Cancer* 97, 2035–2042 (2003).

Chang, W.-J., Du, Y., Zhao, X., Ma, L.-Y. & Cao, G.-W. Inflammation-related factors predicting prognosis of gastric cancer. *World J. Gastroenterol.* 20, 4586–4596 (2014).

Chauhan, H. *et al.* There is more than one kind of myofibroblast: analysis of CD34 expression in benign, in situ, and invasive breast lesions. *J. Clin. Pathol.* 56, 271–276 (2003).

Chen, C.-L., Chu, J.-S., Su, W.-C., Huang, S.-C. & Lee, W.-Y. Hypoxia and metabolic phenotypes during breast carcinogenesis: expression of HIF-1alpha, GLUT1, and CAIX. *Virchows Arch.* 457, 53–61 (2010).

Chen, H. *et al.* CD147 is required for matrix metalloproteinases-2 production and germ cell migration during spermatogenesis. *Mol. Hum. Reprod.* 17, 405–414 (2011).

Chen, W. Y., Chen, N., Yun, J., Wagner, T. E. & Kopchick, J. J. In vitro and in vivo studies of the antagonistic effects of human growth hormone analogs. *J. Biol. Chem.* 269, 20806 (1994).

Cheung, E. C. & Vousden, K. H. The role of p53 in glucose metabolism. *Current Opinion in Cell Biology* 22, 186–191 (2010).

Chuang, J. Y., Wu, C. H., Lai, M. D., Chang, W. C. & Hung, J. J. Overexpression of Sp1 leads to p53-dependent apoptosis in cancer cells. *Int. J. Cancer* 125, 2066–2076 (2009).

Christofk H, *et al.,* The M2 splice isoform of pyruvate kinase is important for cancer metabolism and tumour growth. Nature (2008).

Colombo, M. P. & Piconese, S. Regulatory-T-cell inhibition versus depletion: the right choice in cancer immunotherapy. *Nat. Rev. Cancer* 7, 880–887 (2007).

Correa, P. & Piazuelo, M. B. The gastric precancerous cascade. *J. Dig. Dis.* 13, 2–9 (2012).

Correa, P. Gastric Cancer. Overview. *Gastroenterology Clinics of North America* 42, 211–217 (2013).

Correa, P. Human Gastric Carcinogenesis : A Multistep and Multifactorial Process First American Cancer Society Award Lecture on Cancer Epidemiology and Prevention 1 I Atrophic. *Gastric Cancer* 52, 6735–6740 (1992).

Costa, C. *et al.* Exposure of human skin to benzo[a]pyrene: Role of CYP1A1 and aryl hydrocarbon receptor in oxidative stress generation. *Toxicology* 271, 83–86 (2010).

Crew, K. D. & Neugut, A. I. Epidemiology of gastric cancer. *World Journal of Gastroenterology* 12, 354–362 (2006).

Cuff, M. A., Lambert, D. W. & Shirazi-Beechey, S. P. Substrate-induced regulation of the human colonic monocarboxylate transporter, MCT1. *J. Physiol.* 539, 361–371 (2002).

Cui, J. *et al.* An integrated transcriptomic and computational analysis for biomarker identification in gastric cancer. *Nucleic Acids Res.* 39, 1197–207 (2011).

Cunningham, D. *et al. Perioperative chemotherapy versus surgery alone for resectable gastroesophageal cancer. The New England journal of medicine* 355, 11–20 (2006).

Curry, J. M. *et al.* Cancer metabolism, stemness and tumour recurrence : MCT1 and MCT4 are functional biomarkers of metabolic symbiosis in head and neck cancer. *Cell Cycle* 12, 1371–1384 (2013).

Dai, C. & Gu, W. P53 post-translational modification: Deregulated in tumorigenesis. *Trends in Molecular Medicine* 16, 528–536 (2010).

Danielsen, T. & Rofstad, E. K. The constitutive level of vascular endothelial growth factor (VEGF) is more important than hypoxia-induced VEGF up-regulation in the angiogenesis of human melanoma xenografts. *Br. J. Cancer* 82, 1528–1534 (2000).

Darnell, J. E. Transcription factors as targets for cancer therapy. *Nat. Rev. Cancer* 2, 740–749 (2002).

De Heredia, F. P., Stuart Wood, I. & Trayhurn, P. Hypoxia stimulates lactate release and modulates monocarboxylate transporter (MCT1, MCT2, and MCT4) expression in human adipocytes. *Pflugers Arch. Eur. J. Physiol.* 459, 509–518 (2010).

De Vita, F. *et al.* Human epidermal growth factor receptor 2 (HER2) in gastric cancer: A new therapeutic target. *Cancer Treat. Rev.* 36, (2010).

De Wever, O., Demetter, P., Mareel, M. & Bracke, M. Stromal myofibroblasts are drivers of invasive cancer growth. *Int. J. Cancer* 123, 2229–38 (2008).

de-Assis, E.-M., Pimenta, L.-G.-G.-S., Costa-e-Silva, E., Souza, P.-E.-A. & Horta, M.-C.-R. Stromal myofibroblasts in oral leukoplakia and oral squamous cell carcinoma. *Med. Oral Patol. Oral Cir. Bucal* 17, e733–8 (2012).

DeClerck, Y. A. *et al.* Proteases, extracellular matrix, and cancer: a workshop of the path B study section. *Am. J. Pathol.* 164, 1131–1139 (2004).

Dicken, B. J. *et al.* Gastric adenocarcinoma: review and considerations for future directions.*Ann. Surg.* 241, 27–39 (2005).

Dimaline, R. & Varro, A. Attack and defence in the gastric epithelium - a delicate balance. *Exp. Physiol.* 92, 591–601 (2007).

Dockray, G. J. Clinical endocrinology and metabolism. Gastrin. *Best Pract. Res. Clin. Endocrinol. Metab.* 18, 555–568 (2004).

Du, J. *et al.* PI3K and ERK-induced Rac1 activation mediates hypoxia-induced HIF-1?? expression in MCF-7 breast cancer cells. *PLoS One* 6, (2011).

Dvorak, H. F. Tumors: wounds that do not heal. Similarities between tumor stroma generation and wound healing. *N. Engl. J. Med.* 315, 1650–1659 (1986).

Elsawa, S. F. *et al.* GLI2 transcription factor mediates cytokine cross-talk in the tumor microenvironment. *J. Biol. Chem.* 286, 21524–21534 (2011).

Elstrom, R. L. *et al.* Akt stimulates aerobic glycolysis in cancer cells. *Cancer Res.* 64, 3892–3899 (2004).

Eyden, B. The myofibroblast: a study of normal, reactive and neoplastic tissues, with an emphasis on ultrastructure. part 2 - tumours and tumour-like lesions. *J. Submicrosc. Cytol. Pathol.* 37, 231–296 (2005).

Fantin, V. R., St-Pierre, J. & Leder, P. Attenuation of LDH-A expression uncovers a link between glycolysis, mitochondrial physiology, and tumor maintenance. *Cancer Cell* 9, 425–434 (2006).

Favier, J. & Gimenez-Roqueplo, A. P. Pheochromocytomas: The (pseudo)-hypoxia hypothesis. *Best Practice and Research: Clinical Endocrinology and Metabolism* 24, 957–968 (2010).

Fiaschi, T. & Chiarugi, P. Metabolic Reprogramming : A Diabolic Liaison. 2012, (2012).

Fiaschi, T. & Chiarugi, P. Oxidative stress, tumor microenvironment, and metabolic reprogramming: a diabolic liaison. *Int. J. Cell Biol.* 2012, 762825 (2012).

Fine, E. J., Miller, A., Quadros, E. V, Sequeira, J. M. & Feinman, R. D. Acetoacetate reduces growth and ATP concentration in cancer cell lines which over-express uncoupling protein 2. *Cancer Cell Int.* 9, 14 (2009).

Fox, J. G. & Wang, T. C. Inflammation, atrophy, and gastric cancer. *Journal of Clinical Investigation* 117, 60–69 (2007).

Forman and Burley. Gastric cancer: global pattern of the disease and an overview of environmental risk factors. *Best Practice and Research: Clinical Gastroenterology* (2006).

Freeman, M. R., Li, Q. & Chung, L. W. K. Can stroma reaction predict cancer lethality? *Clin. Cancer Res.* 19, 4905–7 (2013).

Fuccio *et al.,* Systematic review: Helicobacter pylori eradication for the prevention of gastric Cancer. *Alimentary pharmacology & therapeutics.* (2007).

Fuyuhiro, Y. *et al.* Upregulation of cancer-associated myofibroblasts by TGF-β from scirrhous gastric carcinoma cells. *Br. J. Cancer* 105, 996–1001 (2011).

Gabbiani, G., Ryan, G. B. & Majno, G. Presence of modified fibroblasts in granulation tissue and their possible role in wound contraction. *Experientia* 27, 549–550 (1971).

Gabison, E. E., Hoang-Xuan, T., Mauviel, A. & Menashi, S. EMMPRIN/CD147, an MMP modulator in cancer, development and tissue repair. *Biochimie* 87, 361–368 (2005).

Gallagher, S. M., Castorino, J. J., Wang, D. & Philp, N. J. Monocarboxylate transporter 4 regulates maturation and trafficking of CD147 to the plasma membrane in the metastatic breast cancer cell line MDA-MB-231. *Cancer Res.* 67, 4182–4189 (2007).

Galluzzi, L., Kepp, O., Vander Heiden, M. G. & Kroemer, G. Metabolic targets for cancer therapy. *Nat. Rev. Drug Discov.* 12, 829–46 (2013).

Gan, Q., Yoshida, T., Li, J. & Owens, G. K. Smooth muscle cells and myofibroblasts use distinct transcriptional mechanisms for smooth muscle α-actin expression. *Circ. Res.* 101, 883–892 (2007).

Genc, S., Kurnaz, I. A. & Ozilgen, M. Astrocyte - neuron lactate shuttle may boost more ATP supply to the neuron under hypoxic conditions - in silico study supported by in vitro expression data. *BMC Systems Biology* 5, 162 (2011).

Giannoni, E. *et al.* EphA2-mediated mesenchymal-amoeboid transition induced by endothelial progenitor cells enhances metastatic spread due to cancer-associated fibroblasts. *J. Mol. Med.* 91, 103–115 (2013).

Giannoni, E. *et al.* Reciprocal activation of prostate cancer cells and cancer-associated fibroblasts stimulates epithelial-mesenchymal transition and cancer stemness. *Cancer Res.* 70, 6945–6956 (2010).

Govindan, S. V., Cardillo, T. M., Moon, S. J., Hansen, H. J. & Goldenberg, D. M. CEACAM5-targeted therapy of human colonic and pancreatic cancer xenografts with potent labetuzumab-SN-38 immunoconjugates. *Clin. Cancer Res.* 15, 6052–6061 (2009).

Grotendorst, G. R., Rahmanie, H. & Duncan, M. R. Combinatorial signaling pathways determine fibroblast proliferation and myofibroblast differentiation. *FASEB J.* 18, 469–479 (2004).

Guo, X., Oshima, H., Kitmura, T., Taketo, M. M. & Oshima, M. Stromal fibroblasts activated by tumor cells promote angiogenesis in mouse gastric cancer. *J. Biol. Chem.* 283, 19864–19871 (2008).

Guido C, *et al*. Metabolic reprogramming of cancer-associated fibroblasts by TGF-β drives tumor growth. *Cell Cycle*. (2012)

Habas, A., Hahn, J., Wang, X. & Margeta, M. Neuronal activity regulates astrocytic Nrf2 signaling. *Proc. Natl. Acad. Sci. U. S. A.* 110, 18291–6 (2013).

Hai, T., Wolford, C. C. & Chang, Y. S. ATF3, a hub of the cellular adaptive-response network, in the pathogenesis of diseases: Is modulation of inflammation a unifying component? *Gene Expression* 15, 1–11 (2010).

Han, S.-U. *et al.* CEACAM5 and CEACAM6 are major target genes for Smad3-mediated TGF-beta signaling. *Oncogene* 27, 675–683 (2008).

Hanahan, D. & Weinberg, R. a. Hallmarks of cancer: *Cell* 100, 646–74 (2000).

Hanahan, D. & Weinberg, R. A. Hallmarks of cancer: The next generation. *Cell* 144, 646–674 (2011).

Haniffa, M. A., Collin, M. P., Buckley, C. D. & Dazzi, F. Mesenchymal stem cells: The fibroblasts' new clothes? *Haematologica* 94, 258–263 (2009).

Harjes, U., Bensaad, K. & Harris, a L. Endothelial cell metabolism and implications for cancer therapy. *Br. J. Cancer* 107, 1207–12 (2012).

Hartgrink, H. H., Jansen, E. P. M., van Grieken, N. C. T. & van de Velde, C. J. H. Gastric cancer. *Lancet* 374, 477–490 (2009).

Hashimoto, T., Hussien, R. & Brooks, G. A. Colocalization of MCT1, CD147, and LDH in mitochondrial inner membrane of L6 muscle cells: evidence of a mitochondrial lactate oxidation complex. *Am. J. Physiol. Endocrinol. Metab.* 290, E1237–E1244 (2006).

Haskew-Layton, R. E., Ma, T. C. & Ratan, R. R. Reply to Bell et al.: Nrf2-dependent and -independent mechanisms of astrocytic neuroprotection. *Proc. Natl. Acad. Sci.* 108, E3–E4 (2010).

Haskew-layton, R. E., Payappilly, J. B., Smirnova, N. A., Ma, T. C. & Chan, K. K. Controlled enzymatic production of astrocytic hydrogen peroxide protects neurons from oxidative stress via an Nrf2-independent pathway. 1–6 (2010). doi:10.1073/pnas.1003996107

Hatiboglu, M. A. *et al.* The tumor microenvironment expression of p-STAT3 influences the efficacy of cyclophosphamide with WP1066 in murine melanoma models. *Int. J. Cancer* 131, 8–17 (2012).

Heldin, C. H., Vanlandewijck, M. & Moustakas, A. Regulation of EMT by TGF?? in cancer. *FEBS Letters* 586, 1959–1970 (2012).

Herrera, M. *et al.* Functional heterogeneity of cancer-associated fibroblasts from human colon tumors shows specific prognostic gene expression signature. *Clin. Cancer Res.* 19, 5914–26 (2013).

Hinsley, E. E., Hunt, S., Hunter, K. D., Whawell, S. A. & Lambert, D. W. Endothelin-1 stimulates motility of head and neck squamous carcinoma cells by promoting stromal-epithelial interactions. *Int. J. Cancer* 130, 40–47 (2012).

Hinz, B., Celetta, G., Tomasek, J. J., Gabbiani, G. & Chaponnier, C. Alpha-smooth muscle actin expression upregulates fibroblast contractile activity. *Mol. Biol. Cell* 12, 2730–2741 (2001).

Hinz, B., Dugina, V., Ballestrem, C., Wehrle-Haller, B. & Chaponnier, C. Alpha-smooth muscle actin is crucial for focal adhesion maturation in myofibroblasts. *Mol. Biol. Cell* 14, 2508–2519 (2003).

Hitosugi, T. & Chen, J. Post-translational modifications and the Warburg effect. *Oncogene* 1–7 (2013).

Hohenberger, P. *et al.* Neoadjuvant imatinib and organ preservation in locally advanced gastrointestinal stromal tumors (GIST). *J Clin Oncol (Meeting Abstracts)* 27: 10550 (2009).

Holmberg, C. *et al.* Release of TGF??ig-h3 by gastric myofibroblasts slows tumor growth and is decreased with cancer progression. *Carcinogenesis* 33, 1553–1562 (2012).

Holmes, S., Abbassi, B., Su, C., Singh, M. & Cunningham, R. L. Oxidative stress defines the neuroprotective or neurotoxic properties of androgens in immortalized female rat dopaminergic neuronal cells. *Endocrinology* 154, 4281–92 (2013).

Hong, K. H., Ryu, J. & Han, K. H. Monocyte chemoattractant protein-1-induced angiogenesis is mediated by vascular endothelial growth factor-A. *Blood* 105, 1405–1407 (2005).

Houthuijzen, J. M., Daenen, L. G. M., Roodhart, J. M. L. & Voest, E. E. The role of mesenchymal stem cells in anti-cancer drug resistance and tumour progression. *Br. J. Cancer* 106, 1901–6 (2012).

Hu, B., Wu, Z. & Phan, S. H. Smad3 mediates transforming growth factor-beta-induced alpha-smooth muscle actin expression. *Am. J. Respir. Cell Mol. Biol.* 29, 397–404 (2003).

Huang, S. *et al.* Inhibition of activated Stat3 reverses drug resistance to chemotherapeutic agents in gastric cancer cells. *Cancer Lett.* 315, 198–205 (2012).

Hudler, P. Genetic Aspects of Gastric Cancer Instability. *The Scientific World Journal* 2012, 1–10 (2012).

Hwang-Verslues, W. W. *et al.* Loss of corepressor PER2 under hypoxia up-regulates OCT1-mediated EMT gene expression and enhances tumor malignancy. *Proc. Natl. Acad. Sci. U. S. A.* 110, 12331–6 (2013).

Iacono, K. T., Brown, A. L., Greene, M. I. & Saouaf, S. J. CD147 immunoglobulin superfamily receptor function and role in pathology. *Experimental and Molecular Pathology* 83, 283–295 (2007).

Ishii, G. *et al.* Bone-marrow-derived myofibroblasts contribute to the cancer-induced stromal reaction. *Biochem. Biophys. Res. Commun.* 309, 232–240 (2003).

Ishii, G. *et al.* Fibroblasts associated with cancer cells keep enhanced migration activity after separation from cancer cells : A novel character of tumor educated fibroblasts. 317–325 (2010).

Ishii, G. *et al.* Fibroblasts associated with cancer cells keep enhanced migration activity after separation from cancer cells: A novel character of tumor educated fibroblasts. *Int. J. Oncol.* 37, 317–325 (2010).

Ishii, K. *et al.* Heterogenous induction of carcinoma-associated fibroblast-like differentiation in normal human prostatic fibroblasts by co-culturing with prostate cancer cells. *J. Cell. Biochem.* 112, 3604–11 (2011).

Izumi, H., Takahashi, M., Uramoto, H., Nakayama, Y., Oyama, T., Wang, K.Y., Sasaguri, Y., Nishizawa, S., and Kohno, K. Monocarboxylate transporters 1 and 4 are involved in the invasion activity of human lung cancer cells. *Cancer Sci 102*, 1007- 1013. (2011).

Jackson, C. B. & Giraud, A. S. STAT3 as a prognostic marker in human gastric cancer. *J. Gastroenterol. Hepatol.* 24, 505–7 (2009).

Jedrychowski, W. *et al.* Vodka consumption, tobacco smoking and risk of gastric cancer in Poland. *Int. J. Epidemiol.* 22, 606–613 (1993).

Jiang, J., Wu, C. & Lu, B. Cytokine-induced killer cells promote antitumor immunity. *J. Transl. Med.* 11, 83 (2013).

Jiang, L. & DeBerardinis, R. J. Cancer metabolism: When more is less. *Nature* 489, 511–512 (2012).

Jørgensen, J. T. Targeted HER2 treatment in advanced gastric cancer. *Oncology* 78, 26–33 (2010).

Jouneau, S. *et al.* EMMPRIN (CD147) regulation of MMP-9 in bronchial epithelial cells in COPD. *Respirology* 16, 705–712 (2011).

Junttila, M. R. & de Sauvage, F. J. Influence of tumour micro-environment heterogeneity on therapeutic response. *Nature* 501, 346–54 (2013).

Jumah and Abumaree. The immunomodulatory and neuroprotective effects of mesenchymal stem cells (MSCs) in experimental autoimmune encephalomyelitis (EAE): A model of multiple sclerosis (MS). *International Journal of Molecular Science.* (2012).

Kajanne, R., Miettinen, P., Tenhunen, M. & Leppä, S. Transcription factor AP-1 promotes growth and radioresistance in prostate cancer cells. 1175–1182 (2009). doi:10.3892/ijo

Kang, Y. & Massagué, J. Epithelial-mesenchymal transitions: Twist in development and metastasis. *Cell* 118, 277–279 (2004).

Karen F. Bella, Bashayer Al-Mubaraka, Jill H. Fowlerb, Paul S. Baxtera, Kunal Guptaa, Tadayuki Tsujitac, Sudhir Chowdhryc, Rickie Patanid, Siddharthan Chandrand, Karen Horsburghb, J. & D. Hayesc, and G. E. H. Mild oxidative stress activates Nrf2 in astrocytes, which contributes to neuroprotective ischemic preconditioning. *Proc.*108, 4–5 (2011).

Ke, Q. & Costa, M. Hypoxia-inducible factor-1 (HIF-1). *Mol. Pharmacol.* 70, 1469–1480 (2006).

Kersten, S. *et al.* The peroxisome proliferator-activated receptor alpha regulates amino acid metabolism. *FASEB J* 15, 1971–1978 (2001).

Kim, D. Y. *et al.* Clinicopathological characteristics of signet ring cell carcinoma of the stomach. *ANZ J. Surg.* 74, 1060–1064 (2004).

Kim, Y., Wallace, J., Li, F., Ostrowski, M. & Friedman, A. Transformed epithelial cells and fibroblasts/myofibroblasts interaction in breast tumor: A mathematical model and experiments. *J. Math. Biol.* 61, 401–421 (2010).

Kirk, P. *et al.* CD147 is tightly associated with lactate transporters MCT1 and MCT4 and facilitates their cell surface expression. *EMBO J.* 19, 3896–3904 (2000).

Klosek, S. K., Nakashiro, K. & Hara, S. Stat3 as a molecular target in RNA interference-based treatment of oral squamous cell carcinoma. 873–878 (2008). doi:10.3892/or

Koh, M. Y., Lemos, R., Liu, X. & Powis, G. The hypoxia-associated factor switches cells from HIF-1α- to HIF-2α-dependent signaling promoting stem cell characteristics, aggressive tumor growth and invasion. *Cancer Res.* 71, 4015–4027 (2011).

Kong, L. M. *et al.* Transcription factor Sp1 regulates expression of cancer-associated molecule CD147 in human lung cancer. *Cancer Sci.* 101, 1463–1470 (2010).

König, B. *et al.* Monocarboxylate transporter (MCT)-1 is up-regulated by PPARalpha. *Biochim. Biophys. Acta* 1780, 899–904 (2008).

König, B. *et al.* Monocarboxylate transporter 1 and CD147 are up-regulated by natural and synthetic peroxisome proliferator-activated receptor α agonists in livers of rodents and pigs. *Mol. Nutr. Food Res.* 54, 1248–1256 (2010).

Koppenol, W. H., Bounds, P. L. & Dang, C. V. Otto Warburg's contributions to current concepts of cancer metabolism. *Nat. Rev. Cancer* 11, 325–337 (2011).

Kosinski, C. *et al.* Indian hedgehog regulates intestinal stem cell fate through epithelial-mesenchymal interactions during development. *Gastroenterology* 139, 893–903 (2010).

Koukourakis, M. I., Giatromanolaki, A., Harris, A. L. & Sivridis, E. Comparison of metabolic pathways between cancer cells and stromal cells in colorectal carcinomas: A metabolic survival role for tumor-associated stroma. *Cancer Res.* 66, 632–637 (2006).

Kroemer, G. & Pouyssegur, J. Tumor Cell Metabolism: Cancer's Achilles' Heel. *Cancer Cell* 13, 472–482 (2008).

Kroemer, G. Mitochondria in cancer. *Oncogene* 25, 4630–2 (2006).

Kunz, P. L. *et al.* HER2 expression in gastric and gastroesophageal junction adenocarcinoma in a US population: clinicopathologic analysis with proposed approach to HER2 assessment. *Appl. Immunohistochem. Mol. Morphol.* 20, 13–24 (2012).

Kuphal, S. & Bosserhoff, A. K. Influence of the cytoplasmic domain of E-cadherin on endogenous N-cadherin expression in malignant melanoma. *Oncogene* 25, 248–259 (2006).

Landskron, G., De La Fuente, M., Thuwajit, P., Thuwajit, C. & Hermoso, M. A. Chronic inflammation and cytokines in the tumor microenvironment. *Journal of Immunology Research* 2014, (2014).

Larsson, O. *et al.* Fibrotic Myofibroblasts Manifest Genome-Wide Derangements of Translational Control. 3, (2008).

Le Floch, R. *et al.* CD147 subunit of lactate/H+ symporters MCT1 and hypoxia-inducible MCT4 is critical for energetics and growth of glycolytic tumors. *Proceedings of the National Academy of Sciences* 108, 16663–16668 (2011).

Lee, J. K., Park, B. J., Yoo, K. Y. & Ahn, Y. O. Dietary factors and stomach cancer: a case-control study in Korea. *Int. J. Epidemiol.* 24, 33–41 (1995).

Lee, S. L. C. *et al.* Hypoxia-induced pathological angiogenesis mediates tumor cell dissemination, invasion, and metastasis in a zebrafish tumor model. *Proc. Natl. Acad. Sci. U. S. A.* 106, 19485–19490 (2009).

Lee, Y. S. *et al.* Hypothalamic ATF3 is involved in regulating glucose and energy metabolism in mice. *Diabetologia* 56, 1383–1393 (2013).

Lee, Y. S. *et al.* Isolation of mesenchymal stromal cells (MSCs) from human adenoid tissue. *Cell. Physiol. Biochem.* 31, 513–524 (2013).

Leung, W. K. *et al.* Screening for gastric cancer in Asia: current evidence and practice. *The Lancet Oncology* 9, 279–287 (2008).

Li, B. & Wang, J. H. C. Fibroblasts and myofibroblasts in wound healing: Force generation and measurement. *J. Tissue Viability* 20, 108–120 (2011).

Li, C. *et al.* Advanced gastric carcinoma with signet ring cell histology. *Oncology* 72, 64–68 (2007).

Li, Z. *et al.* Hypoxia-Inducible Factors Regulate Tumorigenic Capacity of Glioma Stem Cells. *Cancer Cell* 15, 501–513 (2009).

Libermann, T. A. & Zerbini, L. F. Targeting transcription factors for cancer gene therapy. *Curr. Gene Ther.* 6, 17–33 (2006).

Liekens, S., De Clercq, E. & Neyts, J. Angiogenesis: regulators and clinical applications. *Biochem. Pharmacol.* 61, 253–70 (2001).

Lisanti, M. P. *et al.* Understanding the "lethal" drivers of tumor-stroma co-evolution: emerging role(s) for hypoxia, oxidative stress and autophagy/mitophagy in the tumor micro-environment. *Cancer Biol. Ther.* 10, 537–42 (2010).

Liu, J. *et al.* Targeting Wnt-driven cancer through the inhibition of Porcupine by LGK974. *Proc. Natl. Acad. Sci. U. S. A.* 110, 20224–9 (2013).

Liu, Y. Fatty acid oxidation is a dominant bioenergetic pathway in prostate cancer. *Prostate Cancer Prostatic Dis.* 9, 230–234 (2006).

Liu, C. Diet and Gastric Cancer. *The Biology of Gastric Cancers.* (2009)

Locasale, J. W. & Cantley, L. C. Altered metabolism in cancer. *BMC Biol.* 8, 88 (2010).

Lu, H., Forbes, R. A. & Verma, A. Hypoxia-inducible factor 1 activation by aerobic glycolysis implicates the Warburg effect in carcinogenesis. *J. Biol. Chem.* 277, 23111–23115 (2002).

Lyssiotis, C. A. & Cantley, L. C. SIRT6 puts cancer metabolism in the driver's seat. *Cell* 151, 1155–1156 (2012).

Madar, S., Goldstein, I. & Rotter, V. "Cancer associated fibroblasts"--more than meets the eye. *Trends Mol. Med.* 19, 447–53 (2013).

Manalo, D. J. *et al.* Transcriptional regulation of vascular endothelial cell responses to hypoxia by HIF-1. *Blood* 105, 659–669 (2005).

Mantovani, A., Porta, C., Rubino, L., Allavena, P. & Sica, A. Tumor-associated macrophages (TAMs) as new target in anticancer therapy. *Drug Discovery Today: Therapeutic Strategies* 3, 361–366 (2006).

Marshall, B. J. & Warren, J. R. Unidentified curved bacilli in the stomach of patients with gastritis and peptic ulceration. *Lancet* 1, 1311–1315 (1984).

Martin, F. T. *et al.* Potential role of mesenchymal stem cells (MSCs) in the breast tumour microenvironment: Stimulation of epithelial to mesenchymal transition (EMT). *Breast Cancer Res. Treat.* 124, 317–326 (2010).

Martinez-Outschoorn, U. E. *et al.* Stromal-epithelial metabolic coupling in cancer: Integrating autophagy and metabolism in the tumor microenvironment. *Int. J. Biochem. Cell Biol.* 43, 1045–1051 (2011).

Martinez-Outschoorn, U. E., Lisanti, M. P. & Sotgia, F. Catabolic cancer-associated fibroblasts transfer energy and biomass to anabolic cancer cells, fueling tumor growth. *Semin. Cancer Biol.* 25, 47–60 (2014).

Matsubara, D. *et al.* Subepithelial myofibroblast in lung adenocarcinoma: a histological indicator of excellent prognosis. *Mod. Pathol.* 22, 776–785 (2009).

McIlwain, H. Substances which support respiration and meta- bolic response to electrical impulses in human cerebral tissue. *J. Neurol. Neurosurg. Psychiat* 257–266 (1953).

Metzker, M. L. Sequencing technologies - the next generation. *Nat. Rev. Genet.* 11, 31–46 (2010).

Meyer, H.-J. & Wilke, H. Treatment strategies in gastric cancer. *Dtsch. Arztebl. Int.* 108, 698–705; quiz 706 (2011).

Micallef, L. *et al.* The myofibroblast, multiple origins for major roles in normal and pathological tissue repair. *Fibrogenesis Tissue Repair* 5 (2012).

Ming, S. C. Gastric carcinoma. A pathobiological classification. *Cancer* 39, 2475–2485 (1977).

Misra, A., Pandey, C., Sze, S. K. & Thanabalu, T. Hypoxia Activated EGFR Signaling Induces Epithelial to Mesenchymal Transition (EMT). *PLoS One* 7, (2012).

Moreno-Sánchez, R., Rodríguez-Enríquez, S., Marín-Hernández, A. & Saavedra, E. Energy metabolism in tumor cells. *FEBS J.* 274, 1393–1418 (2007).

Mogi C., Tobo M., Tomura H., Murata N., He X. D., Sato K., *et al.* Involvement of proton-sensing TDAG8 in extracellular acidification-induced inhibition of proinflammatory cytokine production in peritoneal macrophages. *J. Immunol*. 182, 3243–3251 (2009)

Navarro Silvera, S. A. *et al.* Food group intake and risk of subtypes of esophageal and gastric cancer. *Int. J. Cancer* 123, 852–860 (2008).

Nishikori, M. Classical and Alternative NF-.KAPPA.B Activation Pathways and Their Roles in Lymphoid Malignancies. *J. Clin. Exp. Hematop.* 45, 15–24 (2005).

Nishio, K., Qiao, S. & Yamashita, H. Characterization of the differential expression of uncoupling protein 2 and ROS production in differentiated mouse macrophage-cells (Mm1) and the progenitor cells (M1). *J. Mol. Histol.* 36, 35–44 (2005).

Oberringer, M. & Meins, C. In vitro wounding: effects of hypoxia and transforming growth factor β1 on proliferation, migration and myofibroblastic differentiation in an endothelial cell-fibroblast co-. *J. Mol. ...* 37–47 (2008). doi:10.1007/s10735-007-9124-3

Oguma, K., Oshima, H. & Oshima, M. Inflammation, tumor necrosis factor and Wnt promotion in gastric cancer development. *Future Oncol.* 6, 515–526 (2010).

Otsuji, E., Yamaguchi, T., Sawai, K. & Takahashi, T. Characterization of signet ring cell carcinoma of the stomach. *J. Surg. Oncol.* 67, 216–220 (1998).

Papandreou, I., Cairns, R. A., Fontana, L., Lim, A. L. & Denko, N. C. HIF-1 mediates adaptation to hypoxia by actively downregulating mitochondrial oxygen consumption. *Cell Metab.* 3, 187–197 (2006).

Park, S. Y. *et al.* Hypoxia enhances LPA-induced HIF-1α and VEGF expression: Their inhibition by resveratrol. *Cancer Lett.* 258, 63–69 (2007).

Pavlides, S. *et al.* The reverse Warburg effect: Aerobic glycolysis in cancer associated fibroblasts and the tumor stroma. *Cell Cycle* 8, 3984–4001 (2009).

Pavlides, S. *et al.* Warburg meets autophagy: cancer-associated fibroblasts accelerate tumor growth and metastasis via oxidative stress, mitophagy, and aerobic glycolysis. *Antioxid. Redox Signal.* 16, 1264–84 (2012).

Pellerin, L. *et al.* Evidence supporting the existence of an activity-dependent astrocyte-neuron lactate shuttle. *Developmental Neuroscience* 20, 291–299 (1998).

Phan *et al.,* Smad3 mediates transforming growth factor-beta-induced alpha-smooth muscle actin expression. *American journal of respiratory cell and molecular biology. (*2003)

Pinheiro, C. *et al.* GLUT1 and CAIX expression profiles in breast cancer correlate with adverse prognostic factors and MCT1 overexpression. *Histol. Histopathol.* 26, 1279–1286 (2011).

Polanska, U. M. & Orimo, A. Carcinoma-associated fibroblasts: non-neoplastic tumour-promoting mesenchymal cells. *J. Cell. Physiol.* 228, 1651–7 (2013).

Prockop, D. J. & Youn Oh, J. Mesenchymal Stem/Stromal Cells (MSCs): Role as Guardians of Inflammation. *Molecular Therapy* 20, 14–20 (2012).

Randle PJ, Garland PB, Hales CN, Newsholme EA. The glucose fatty-acid cycle. Its role in insulin sensitivity and the metabolic disturbances of diabetes mellitus. *Lancet 1*: 785–789, (1963.)

Ranganathan, P. *et al.* Expression profiling of genes regulated by TGF-beta: differential regulation in normal and tumour cells. *BMC Genomics* 8, 98 (2007).

Rofstad, E. K. & Danielsen, T. Hypoxia-induced metastasis of human melanoma cells: involvement of vascular endothelial growth factor-mediated angiogenesis. *Br. J. Cancer* 80, 1697–1707 (1999).

Rosanò, L., Spinella, F. & Bagnato, A. Endothelin 1 in cancer: biological implications and therapeutic opportunities. *Nat. Rev. Cancer* 13, 637–51 (2013).

Rossignol, R. *et al.* Energy Substrate Modulates Mitochondrial Structure and Oxidative Capacity in Cancer Cells. *Cancer Res.* 64, 985–993 (2004).

Rutkowski, P. *et al.* Neoadjuvant imatinib in locally advanced gastrointestinal stromal tumors (GIST): the EORTC STBSG experience. *Ann. Surg. Oncol.* 20, 2937–43 (2013).

Saeki *et al.,* Genetic factors related to gastric cancer susceptibility identified using a genome-wide association study. *Cancer Science.* (2013)

Sahar, S. & Sassone-Corsi, P. Metabolism and cancer: the circadian clock connection. *Nat. Rev. Cancer* 9, 886–896 (2009).

Salminen, A. & Kaarniranta, K. Glycolysis links p53 function with NF-kappaB signaling: impact on cancer and aging process. *J. Cell. Physiol.* 224, 1–6 (2010).

Sanchez-Alvarez, R. *et al.* Ethanol exposure induces the cancer-associated fibroblast phenotype and lethal tumor metabolism: implications for breast cancer prevention. *Cell Cycle* 12, 289–301 (2013).

Sanchez-Alvarez, R. *et al.* Mitochondrial dysfunction in breast cancer cells prevents tumor growth: understanding chemoprevention with metformin. *Cell Cycle* 12, 172–82 (2013).

Sanz-Moreno, V. *et al.* ROCK and JAK1 signaling cooperate to control actomyosin contractility in tumor cells and stroma. *Cancer Cell* 20, 229–45 (2011).

Satoh, H. *et al.* Nrf2-deficiency creates a responsive microenvironment for metastasis to the lung. *Carcinogenesis* 31, 1833–1843 (2010).

Schulze, A. & Downward, J. Flicking the Warburg Switch-Tyrosine Phosphorylation of Pyruvate Dehydrogenase Kinase Regulates Mitochondrial Activity in Cancer Cells. *Molecular Cell* 44, 846–848 (2011).

Shanmugam, M. *et al.* Targeting glucose consumption and autophagy in myeloma with the novel nucleoside analogue 8-aminoadenosine. *J. Biol. Chem.* 284, 26816–30 (2009).

Shao, X. D. *et al.* Expression and significance of HERG protein in gastric cancer. *Cancer Biol. Ther.* 7, 45–50 (2008).

Sharon, Y., Alon, L., Glanz, S., Servais, C. & Erez, N. Isolation of normal and cancer-associated fibroblasts from fresh tissues by Fluorescence Activated Cell Sorting (FACS). *J. Vis. Exp.* e4425 (2013). doi:10.3791/4425

Shaw, A., Gipp, J. & Bushman, W. The Sonic Hedgehog pathway stimulates prostate tumor growth by paracrine signaling and recapitulates embryonic gene expression in tumor myofibroblasts. *Oncogene* 28, 4480–4490 (2009).

Shimasaki, N. *et al.* Distribution and role of myofibroblasts in human normal seminal vesicle stroma. *Med. Mol. Morphol.* 40, 208–211 (2007).

Shweiki, D., Itin, A., Soffer, D. & Keshet, E. Vascular endothelial growth factor induced by hypoxia may mediate hypoxia-initiated angiogenesis. *Nature* 359, 843–845 (1992).

Slattery, M. L., Herrick, J. S., Lundgreen, A. & Wolff, R. K. Genetic variation in the TGF-β-signaling pathway and colon and rectal cancer risk. *Cancer Epidemiol Biomarkers Prev* 1–25 (2011). doi:10.1158/1055-9965.EPI-10-0843.Genetic

Slomiany, M. G. *et al.* Hyaluronan, CD44, and emmprin regulate lactate efflux and membrane localization of monocarboxylate transporters in human breast carcinoma cells. *Cancer Res.* 69, 1293–301 (2009).

Smith, J. P. & Drewes, L. R. Modulation of monocarboxylic acid transporter-1 kinetic function by the cAMP signaling pathway in rat brain endothelial cells. *J. Biol. Chem.* 281, 2053–2060 (2006).

Sobral, L. M. *et al.* Myofibroblasts in the stroma of oral cancer promote tumorigenesis via secretion of activin A. *Oral Oncol.* 47, 840–846 (2011).

Sonveaux, P. *et al.* Targeting the lactate transporter MCT1 in endothelial cells inhibits lactate-induced HIF-1 activation and tumor angiogenesis. *PLoS One*, (2012).

Sotiga, F., *et al.* Mitochondrial metabolism in cancer metastasis: visualizing tumor cell mitochondria and the "reverse Warburg effect" in positive lymph node tissue. *Cell Cycle* (2012)

Spaeth, E. L. *et al.* Mesenchymal CD44 expression contributes to the acquisition of an activated fibroblast phenotype via TWIST activation in the tumor microenvironment. *Cancer Res.* 73, 5347–5359 (2013).

State, O. Cross-family dimerization of transcription factors Fos / Jun and ATF / CREB alters DNA binding specificity. 88, 3720–3724 (1991).

Stephens, P. J. *et al.* The landscape of cancer genes and mutational processes in breast cancer. *Nature* 486, 400–4 (2012).

Stewart, T. J. & Smyth, M. J. Improving cancer immunotherapy by targeting tumor-induced immune suppression. *Cancer Metastasis Rev.* 30, 125–140 (2011).

Stock, P., DeKruyff, R. H. & Umetsu, D. T. Inhibition of the allergic response by regulatory T cells. *Curr. Opin. Allergy Clin. Immunol.* 6, 12–16 (2006).

Stojdl, D. F. *et al.* Exploiting tumor-specific defects in the interferon pathway with a previously unknown oncolytic virus. *Nat. Med.* 6, 821–825 (2000).

Subarsky, P. & Hill, R. P. The hypoxic tumour microenvironment and metastatic progression. *Clinical and Experimental Metastasis* 20, 237–250 (2003).

Sun, J., Hemler, M. E. & Interactions, M. I. Regulation of MMP-1 and MMP-2 Production through CD147 / Extracellular Matrix Metalloproteinase Inducer Interactions Regulation of MMP-1 and MMP-2 Production through CD147 / Extracellular Matrix. *Cancer Res.* 61, 2276–2281 (2001).

Surowiak, P. *et al.* Stromal myofibroblasts in breast cancer: Relations between their occurrence, tumor grade and expression of some tumour markers. *Folia Histochem. Cytobiol.* 44, 111–116 (2006).

Symersky, J., Osowski, D., Walters, D. E. & Mueller, D. M. Oligomycin frames a common drug-binding site in the ATP synthase. *Proceedings of the National Academy of Sciences* 109, 13961–13965 (2012).

Tamura, K. *et al.* Insulin-like growth factor binding protein-7 (IGFBP7) blocks vascular endothelial cell growth factor (VEGF)-induced angiogenesis in human vascular endothelial cells. *Eur. J. Pharmacol.* 610, 61–67 (2009).

Tang, N. *et al.* Loss of HIF-1 in endothelial cells disrupts a hypoxia-driven VEGF autocrine loop necessary for tumorigenesis. *Cancer Cell* 6, 485–495 (2004).

Tetzlaff *et al.,* Review of docetaxel in the treatment of gastric cancer. Therapeutics and clinical risk management. (2008)

Tomasek, J. J., Gabbiani, G., Hinz, B., Chaponnier, C. & Brown, R. A. Myofibroblasts and mechano-regulation of connective tissue remodelling. *Nat. Rev. Mol. Cell Biol.* 3, 349–363 (2002).

Tsugane, S., Tei, Y., Takahashi, T., Watanabe, S. & Sugano, K. Salty food intake and risk of Helicobacter pylori infection. *Japanese J. Cancer Res.* 85, 474–478 (1994).

Tsujino, T. *et al.* Stromal myofibroblasts predict disease recurrence for colorectal cancer. *Clin. Cancer Res.* 13, 2082–2090 (2007).

Turner, N. *et al.* FGFR1 amplification drives endocrine therapy resistance and is a therapeutic target in breast cancer. *Cancer Res.* 70, 2085–2094 (2010).

Tyan, S., Hsu, C., Peng, K. & Chen, C. Breast cancer cells induce stromal fibroblasts to secrete ADAMTS1 for cancer invasion through an epigenetic change. *PLoS One* 7, (2012).

Tyan, S., Kuo, W., Huang, C. & Pan, C. Breast cancer cells induce cancer-associated fibroblasts to secrete hepatocyte growth factor to enhance breast tumorigenesis. *PLoS One* 6, 1–9 (2011).

Ullah, M. S., Davies, A. J. & Halestrap, A. P. The plasma membrane lactate transporter MCT4, but not MCT1, is up-regulated by hypoxia through a HIF-1??-dependent mechanism. *J. Biol. Chem.* 281, 9030–9037 (2006).

Uemura *et al.,* Helicobacter pylori infection and the development of gastric cancer. *The New England journal of medicine.* (2001)

Van Cutsem E *et al.* Efficacy results from the ToGA trial: a phase III study of trastuzu- mab added to standard chemotherapy in first-line human epidermal growth factor receptor 2 (HER2)-positive advanced gastric cancer. *J Clin Oncol* 27, 798 (2009).

van Zijl, F. *et al.* Hepatic tumor-stroma crosstalk guides epithelial to mesenchymal transition at the tumor edge. *Oncogene* 28, 4022–4033 (2009).

Vauhkonen, M., Vauhkonen, H. & Sipponen, P. Pathology and molecular biology of gastric cancer. *Best Pract. Res. Clin. Gastroenterol.* 20, 651–674 (2006).

Vigani, G. Does a similar metabolic reprogramming occur in Fe-deficient plant cells and animal tumor cells? *Plant Sci* (2012).

Wallach-Dayan, S. B., Golan-Gerstl, R. & Breuer, R. Evasion of myofibroblasts from immune surveillance: a mechanism for tissue fibrosis. *Proc. Natl. Acad. Sci. U. S. A.* 104, 20460–5 (2007).

Walters, D. K., Arendt, B. K. & Jelinek, D. F. CD147 regulates the expression of MCT1 and lactate export in multiple myeloma cells. *Cell Cycle* 12, 3175–3183 (2013).

Wang, H. & Chen, L. Tumor microenviroment and hepatocellular carcinoma metastasis. *J. Gastroenterol. Hepatol.* 28 Suppl 1, 43–8 (2013).

Wang, H. *et al.* Epithelial-mesenchymal transition (EMT) induced by TNF-alpha requires AKT/GSK-3beta-mediated stabilization of snail in colorectal cancer. *PLoS One* 8, e56664 (2013).

Wang, Z., Gerstein, M. & Snyder, M. RNA-Seq: a revolutionary tool for transcriptomics. *Nat. Rev. Genet.* 10, 57–63 (2009).

Warburg, O. Origin of cancer cells. *Oncol.* 9, 75–83 (1956).

Warburg, O., Wind, F. & Negelein, E. The metabolism of tumors in the body. *J. Gen. Physiol.* 8, 519–530 (1927).

Warren and Marshall. Unidentified curved bacilli in the stomach of patients with gastritis and peptic ulceration. *Lancet*. (1984).

Wcrf.org,. 'World Cancer Research Fund International'. N.p., 2015. Web. 26 Nov. 2014.

Witkiewicz AK, *et al.* Loss of stromal caveolin-1 expression predicts poor clinical outcome in triple negative and basal-like breast cancers**.** *Cancer Biol Ther*. 2010

Whitaker-Menezes, D. *et al.* Evidence for a stromal-epithelial "lactate shuttle" in human tumors: MCT4 is a marker of oxidative stress in cancer-associated fibroblasts. *Cell Cycle* 10, 1772–1783 (2011).

Wilson, J. & Balkwill, F. The role of cytokines in the epithelial cancer microenvironment. *Semin. Cancer Biol.* 12, 113–120 (2002).

Wolford, C. C. *et al.* Transcription factor ATF3 links host adaptive response to breast cancer metastasis. *J. Clin. Invest.* 123, 2893–906 (2013).

Wroblewski, L. E., Peek, R. M. & Wilson, K. T. Helicobacter pylori and gastric cancer: Factors that modulate disease risk. *Clinical Microbiology Reviews* 23, 713–739 (2010).

Yamashita, M. *et al.* Role of stromal myofibroblasts in invasive breast cancer: Stromal expression of alpha-smooth muscle actin correlates with worse clinical outcome. *Breast Cancer* 19, 170–176 (2012).

Yashiro, M. & Hirakawa, K. Cancer-stromal interactions in scirrhous gastric carcinoma. in *Cancer Microenvironment* 3, 127–135 (2010).

Yauch, R. L. *et al.* A paracrine requirement for hedgehog signalling in cancer. *Nature* 455, 406–410 (2008).

Yazhou,C., Wenlv, S., Weidong, Z. & and Licun, W. Clinicopathological significance of stromal myofibroblasts in invasive ductal carcinoma of the breast. *Tumour. Biol* 290–295. (2004).

Ye, J. *et al.* The GCN2-ATF4 pathway is critical for tumour cell survival and proliferation in response to nutrient deprivation. *EMBO J.* 29, 2082–2096 (2010).

Yeung, T.-L. *et al.* TGF-β modulates ovarian cancer invasion by upregulating CAF-derived versican in the tumor microenvironment. *Cancer Res.* 73, 5016–28 (2013).

Yi, W. *et al.* Phosphofructokinase 1 Glycosylation Regulates Cell Growth and Metabolism. *Science* 337, 975–980 (2012).

Yin, C., Evason, K. J., Asahina, K. & Stainier, D. Y. R. Hepatic stellate cells in liver development, regeneration, and cancer. *J. Clin. Invest.* 123, 1902–10 (2013).

Yin, X., Dewille, J. W. & Hai, T. A potential dichotomous role of ATF3, an adaptive-response gene, in cancer development. *Oncogene* 27, 2118–2127 (2008).

Young, C. D. *et al.* Modulation of glucose transporter 1 (GLUT1) expression levels alters mouse mammary tumor cell growth in vitro and in vivo. *PLoS One* 6, (2011).

Yu, H., Kortylewski, M. & Pardoll, D. Crosstalk between cancer and immune cells: role of STAT3 in the tumour microenvironment. *Nat. Rev. Immunol.* 7, 41–51 (2007).

Yu, Y. *et al.* Cancer-associated fibroblasts induce epithelial-mesenchymal transition of breast cancer cells through paracrine TGF-β signalling. *Br. J. Cancer* 110, 724–32 (2014).

Yuan, X. *et al.* ATF3 suppresses metastasis of bladder cancer by regulating gelsolin-mediated remodeling of the actin cytoskeleton. *Cancer Res.* 73, 3625–3637 (2013).

Yue, P. & Turkson, J. Targeting STAT3 in cancer: how successful are we? *Expert Opin. Investig. Drugs* 18, 45–56 (2009).

Zhang, C. *et al.* Tumour-associated mutant p53 drives the Warburg effect. *Nat. Commun.* 4, 2935 (2013).

Zhang, M., Zhu, G., Zhang, H., Gao, H. & Xue, Y. Clinicopathologic features of gastric carcinoma with signet ring cell histology. *J. Gastrointest. Surg.* 14, 601–606 (2010).

Zhao, Z. *et al.* Downregulation of MCT1 inhibits tumor growth, metastasis and enhances chemotherapeutic efficacy in osteosarcoma through regulation of the NF-κB pathway. *Cancer Lett.* 342, 150–158 (2014).

Zheng, C. *et al.* A novel Anti-CEACAM5 Monoclonal antibody, CC4, suppresses colorectal tumor growth and enhances NK cells-mediated tumor immunity. *PLoS One* 6, (2011).

Zheng, R. & Blobel, G. A. GATA Transcription Factors and Cancer. *Genes Cancer* 1, 1178–1188 (2010).

Zhou, P. *et al.* In vivo discovery of immunotherapy targets in the tumour microenvironment. *Nature* 506, 52–7 (2014).

Zhu, C.-Q. *et al.* Integrin alpha 11 regulates IGF2 expression in fibroblasts to enhance tumorigenicity of human non-small-cell lung cancer cells. *Proc. Natl. Acad. Sci. U. S. A.* 104, 11754–11759 (2007).

Zitvogel, L., Tesniere, A. & Kroemer, G. Cancer despite immunosurveillance: immunoselection and immunosubversion. *Nat. Rev. Immunol.* 6, 715–727 (2006).